UNIVERSITY OF CALGARY

Entamoeba histolytica-Induced Caspase-4 Activation Regulates IL-1β Secretion Through Caspase-1

by

Jeanie Quach

A THESIS

SUBMITTED TO THE FACULTY OF GRADUATE STUDIES

IN PARTIAL FULFILMENT OF THE REQUIREMENTS FOR THE

DEGREE OF DOCTOR OF PHILOSOPHY

GRADUATE PROGRAM IN MICROBIOLOGY AND INFECTIOUS DISEASES

CALGARY, ALBERTA

APRIL, 2018

Abstract

Entamoeba histolytica (*Eh*) is the causative agent of amebiasis, one of the top four parasitic causes of mortality worldwide. In 90% of infected individuals, *Eh* harmlessly colonizes the large intestine and results in a non-invasive and asymptomatic infection. In the remaining 10% of infected individuals, the parasite breaches the intestinal barrier causing amebic colitis and in rare cases, it can cause extra-intestinal lesions, mainly liver abscesses. During invasion, *Eh* encounter macrophages in the lamina propria and this intricate host-parasite interaction is critical in eliciting a tissue damaging raging pro-inflammatory response. When *Eh* binds macrophages via the Gal-lectin, surface *Eh*CP-A5 ligates $\alpha_5\beta_1$ integrin to activate caspase-1 in a complex known as the NLRP3 inflammasome. In this study, we investigated the parasite requirements underlying macrophage caspase-4 and -1 activation and the role caspase-4 play in augmenting pro-inflammatory cytokine responses. Surprisingly, caspase-4 activation was similar to caspase-1 requiring live *Eh* attachment via the Gal-lectin, *Eh*CP-A5 and cellular stresses such as K^+ efflux and ROS. However, unlike caspase-1, caspase-4 activation was independent of ASC and NLRP3. Using CRISPR/Cas9 gene editing of caspase-4 and caspase-1 in human macrophages, we determined that caspase-1 and bioactive IL-1β release was highly dependent on caspase-4 activation in response to *Eh*. Formaldehyde cross-linking to stabilize protein-protein interactions in transfected COS-7 cells stimulated with *Eh* revealed that caspase-4 specifically interacted with caspase-1 in a protein complex that enhanced the cleavage of caspase-1 CARD domains to augment IL-1β release. The mouse ortholog caspase-11, displayed similar requirements for its

activation, however, it was not involved in regulating caspase-1 activation in the same way as caspase-4. These findings reveal a novel role for human caspase-4 as a critical sensor molecule to amplify downstream pro-inflammatory responses when macrophage encounters live *Eh*.

Preface

This thesis consists of a literature review, material and methods section, experimental results, and a discussion and conclusions section.

CHAPTER 1 is an extensive literature review on innate host defense against *Entamoeba histolytica* and the role of caspases and inflammasomes in inflammation. Included is a book chapter that has been published in the *Encyclopedia of Immunobiology* in collaboration with Dr. Kris Chadee. I wrote the section on innate immunity against *Entamoeba histolytica*. Included is also a review that has been published in *Human Vaccines & Immunotherapeutics* in collaboration with Dr. Joëlle St-Pierre and Dr. Kris Chadee.

CHAPTER 2 is the materials and methods section that I wrote and Dr. Kris Chadee reviewed and edited the writing.

CHAPTER 3 consists of the results of my PhD that have components of a research manuscript submitted to *PLoS Pathogens* for publication. I designed and conducted experiments, analyzed data and prepared the manuscript for publication. Christina Sandall designed the NLPRP3 CRISPR/Cas9 KO cells. France Moreau, my laboratory manager, provided technical expertise and assisted with the study.

CHAPTER 4 provides a general discussion on the findings during my PhD research and future directions in the field of amebiasis and inflammasomes. I wrote this section and Kris Chadee reviewed and edited the writing.

Acknowledgements

First and foremost, I would like to thank my supervisor, Dr. Kris Chadee for providing me with direction in my project and allowing me to develop my own scientific reasoning skills. Thank you for helping me realize my strengths and weaknesses and encouraging me to improve upon them. Thank you to my lab manager, France Moreau for your patience, support, and encouragement. You have assisted me with some of the most difficult technical aspects of my project and I am truly grateful to work with you as a team.

I thank my supervisory committee, Dr. Donna Marie McCafferty and Dr. Robin Yates, for giving of their time and effort to oversee my project in the program. Thank you, Dr. Leanne Mortimer, Dr. Joëlle St-Pierre, and Dr. Steve Cornick for being great mentors and helping me improve on my critical thinking and writing skills. Many thanks to the Chadee laboratory members (Aralia León Coria, Sharmin Begum, Dr. Preeti Shahi, Dr. Manish Kumar, Dr. Sameer Tiwari, and Hayley Gorman) for creating a fun and supportive environment. I will not forget our annual lab hikes and yoga poses in the mountains.

I would like to offer my sincerest thanks to my funding provided by NSERC CREATE HPI and the tremendous number of workshops and activities hosted by HPI to enhance my professional development. Thank you, Teresa Emmett, for all the opportunities that

you have offered me and the things that you have taught me when I was on the Trainee Operations Committee.

Thank you for the Queen Elizabeth II scholarships (University of Calgary), William Davies Scholarship (University of Calgary), Graduate Citizenship Awards (University of Calgary), and 2016 Outstanding Contribution to HPI Award (University of Calgary), for acknowledging my accomplishments during my PhD program. Thank you for the ICPI Trainee Travel Award (ASIP), Faculty of Graduate Studies Travel Award (University of Calgary), and the University of Calgary Professional Development Grant Awards for providing the funding to attend conferences.

Finally, thank you to my family for your guidance and encouragement to learn and to stay persistent. Thank you to my sister, Kimberly Quach; my fiancée, Henry Gee; and my best friend, Yingjie Liu for being there by my side and supporting me every step of the way.

Thank you for believing in me and inspiring me to do my personal best!

Dedication

I would like to dedicate this thesis to my parents.

Thank you for being the best parents, supporting me in whatever I do and loving me unconditionally.

Table of Contents

List of Tables

List of Figures and Illustrations

List of Symbols, Abbreviations, Nomenclatures

Abbreviation	Definition
AIM-2	absent in melanoma-2
ALA	amebic liver abscess
Aa	amino acids
Ab	antibody
ASC	apoptosis-associated spec-like protein containing CARD
BMDM	bone marrow-derived macrophages
CARD	caspase activation and recruitment domain
COX	cyclooxygenase
CP	cysteine proteinases
CRD	carbohydrate recognition domain
DPI	diphenyliodium chloride
Eh	*Entamoeba histolytica*
*Eh*APA-	*E. histolytica* that have *Eh*APA (amebapore A) gene silenced
*Eh*CP5/*Eh*CP-A5	*E. histolytica* cysteine protease 5
*Eh*CP-A5-	*E. histolytica* that have *Eh*CP5 gene silenced
Eh Gal-lectin	*E. histolytica* galactose/N-acetylgalactosamine-inhibitable lectin
FCAS	Familial cold auto-inflammatory syndrome
Hgl	*Eh* Gal-lectin heavy subunit

IFN	Interferon
IL	Interleukin
iNOS	inducible nitric oxide synthase
KCl	potassium chloride
LN	LPS + nigericin
LPS	Lipopolysaccharide
LRR	leucine rich repeats
LYS	cell lysates
Mϕ	macrophages
MSU	monosodium urate
MW	Muckle Wells Syndrome
NF-κB	nuclear-factor κB
NLR	Nod-like receptor
NLRC4	Nod-like receptor containing a CARD 4
NLRP1	Nod-like receptor containing a pyrin domain 1
NLRP3	Nod-like receptor containing a pyrin domain 3
NO	nitric oxide
$P2X_7$	ATP-gated $P2X_7$ receptor
PAMP	pathogen-associated molecular pattern
PI3K	phosphatidylinositol 3-kinase
PMA	phorbol-12-myristate-13-acetate
ROS	reactive oxygen species
SEAP	secreted embryonic alkaline phosphatase

SN	supernatants
siRNA	single nucleotide RNA
TLR	toll-like receptor
TNF-α	tumor necrosis factor-α
Eh+E-64	*Eh* cultured overnight in cysteine protease inhibitor E-64

Chapter One: **Introduction**

This section includes excerpts from

Book chapter:

***Entamoeba histolytica*: pathogenesis and innate host defense – Immunity to Intestinal Protozoa**

Quach J, Chadee K. *Encyclopedia of Immunobiology*, Edited by Michael JH Ratcliffe. Academic Press. Pages 133 -141.

Jeanie Quach wrote the original draft and reviewed and edited the writing. Kris Chadee reviewed and edited the writing.

Review article:

The future for vaccine development against *Entamoeba histolytica*

Quach J, St-Pierre J, Chadee K. 2014. *Human Vaccines & Immunotherapeutics*. 10: 1514-1521.

Jeanie Quach wrote the original draft and reviewed and edited the writing. Kris Chadee and Joëlle St-Pierre reviewed and edited the writing.

All figures were drawn by Jeanie Quach.

1.1 Entamoeba histolytica

1.1.1 *Entamoeba histolytica Biology and Life Cycle*

Entamoeba histolytica (*E. histolytica*) is an enteric protozoan parasite that infects humans and is the etiologic agent of amebiasis. Its name in Greek "histo" and "lytic" translates into tissue and to dissolve, describing the parasite's ability to dissolve tissue. Amebiasis remains a worldwide health problem, accounting for 11,300 global deaths in the year 2013, making it the fourth leading cause of parasitic diseases [1]. *Eh* has a relatively simple life cycle compared to other parasites, transitioning between the disease-inducing trophozoite (10-60 μM in diameter) stage and the infectious cyst (10-15 μM in diameter) stage [2]. When amebic cysts are ingested, they bypass the stomach, and the nucleus in each cyst divides, which then gives rise to eight uninucleated trophozoites in the terminal ileum [3] (**Figure 1.1**). Trophozoites then migrate to the colon and colonize the mucus layer, where they feed on resident microbiota and mucin sugars. In most forms of infection, individuals are asymptomatic and trophozoites remain in the lumen or they re-encyst in the descending colon and are passed out with the stool as infective cysts. The cyst contains a chitin wall allowing them to survive outside of the host for days to weeks and can infect another individual that comes into contact with contaminated food or water. However, in a small number of infected people, aberrant host response and trophozoite virulence factors can contribute to the breakdown of the mucosal barrier, leading to acute invasive amebiasis [3].

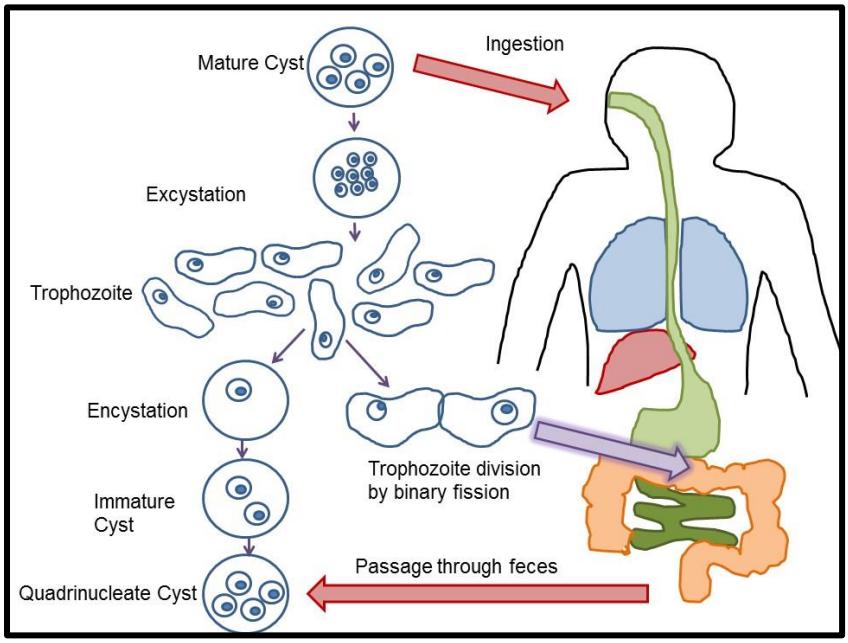

Figure 1.1 *E. histolytica* life cycle.

Infection begins with the ingestion of mature cysts that enter the stomach and travel to the terminal ileum where they excyst. The mature trophozoites migrate to the colon and establish themselves in the mucus layer. In the colon, the trophozoite can take two routes, either encysting back into a cyst that is passed through the feces or it can divide via binary fission and continue to survive in the host. In some cases, trophozoites can invade the colonic mucosa to cause amebic ulcers or can disseminate via the bloodstream and cause liver abscesses.

1.1.2 *Clinical Features*

Invading trophozoites enter the interglandular epithelium and form early superficial ulcerations [4]. Some of the common clinical manifestations include acute diarrhea and dysentery [3]. Symptoms associated with *Eh* colitis or dysentery includes abdominal pain, tenderness, diarrhea and weight loss. Fulminant colitis, ameboma, cutaneous amebiasis, and rectovaginal fistulas are associated with intestinal amebiasis as well. Furthermore, in rare cases, the parasite can disseminate to extra-intestinal sites such as the liver, brain, genitourinary tract, and the heart via the bloodstream. Liver abscess is the most common complication of extra-intestinal amebiasis and it is associated with fever and abdominal pain and tenderness [3].

1.1.3 *Epidemiology*

There are no recent reports on the prevalence of *Eh* because it was confused with its morphologically identical non-pathogenic species, *E. dispar* [5]. *E. dispar* is non-invasive and results in asymptomatic infection. Amebiasis is found worldwide, however, there are many factors that increase the risk of infection with *Eh*. Since the main route of transmission is via ingestion of infectious cysts, areas with poor sanitation and lack of clean water are found to have the highest prevalence of this disease. These areas include tropical and subtropical areas of Mexico, South and West Africa, Western South America, and South Asia [6]. Several factors are involved in the establishment of invasive amebiasis including: host factors including mutations in the leptin receptor and

being malnutritioned [7,8]. Travelers and migrants from endemic areas can also contract the disease.

1.1.4 *Diagnosis and Management*

Some methods of diagnosis of *Eh* infection include identification of cysts or trophozoites by microscopy, fecal antigen detection, DNA detection by PCR and serologic antibody, but all pose disadvantages. It is important that methods for diagnosis are quick and accurate to allow early interventions for treatment and to halt further progression to invasive disease. A third generation rapid fecal antigen detection test (*E. HISTOLYTICA* QUIK *CHEK*^{TM}), targeting *Eh* galactose/N-acetylgalactosamine (Gal/GalNac) adherence lectin (Gal-lectin) was found to be 100% specific and sensitive [9].

In non-invasive *Eh* infections, oral drugs including paromomycin (7 days), diloxanide furoate (10 days), or iodoquinol (20 days) are used to treat luminal parasites [10]. No treatment is required for *E. dispar* infections. In invasive infections, nitroimidazole derivates including metronidizaole (also known as Flagyl, 10 days) or tinidazole (3 days) are used for the treatment of trophozoites followed by a luminal drug, such as paromomycin [10]. In cases of liver abscess, chloroquine and/or drainage of the abscess is performed in addition to metronidazole treatment [10]. The ideal treatment for amebiasis would be a vaccine, since humans are the only hosts for this parasite. However, to date, there is no successful vaccine against *Eh* and the most potential vaccine candidates appear to be the Gal-lectin.

1.1.5 *Virulence Factors*

1.1.5.1 Gal-lectin

Galactose-*N*-acetyl-*D*-galactosamine inhibitable lectin (Gal-lectin) is a 260-kDa heterodimer localized on the surface of *Eh* that acts as an adhesin molecule to attach to cell surfaces [11]. Gal-lectin consists of a heavy subunit (170-kDa, HgL) that is disulfide-linked to a light subunit (31/35-kDa, LgL) which is non-covalently associated with a 150-kDa intermediate subunit (**Figure 1.2**) [12]. The heavy chain consists a cysteine rich site in the carbohydrate binding region (CRD) and is responsible for the high affinity binding of Gal-lectin [13]. *Eh* normally resides on the surface of the colonic mucosal layer by binding via Gal-lectin to galactose and *N*-acetyl galactosamine residues of colonic mucins [14]. This adherence is a prerequisite for colonization, cytolytic activity, and invasion. *Eh* can also bind to bacteria [15], epithelial cells, and inflammatory cells [16].

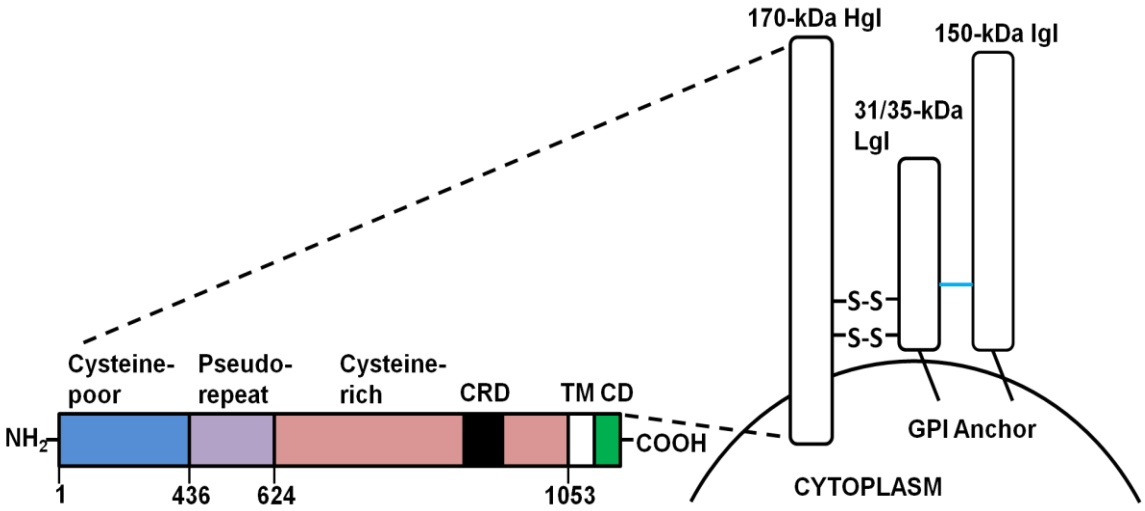

Figure 1.2 Structure of *E. histolytica* Gal-lectin.

The Gal-lectin adhesin is composed of three subunits. The heavy subunit (Hgl) is linked by disulfide bonds to the light subunit (Lgl), which is non-covalently associated with the intermediate subunit (Igl). The heavy subunit has a short cytoplasmic tail and both the light and intermediate subunits are GPI anchored. TM=transmembrane, CD=cytoplasmic domain, CRD=carbohydrate rich domain, GPI= glycosylphophatidylinositol (Adapted from Quach *et al* (2014), *Human Vaccines & Immunotherapeutics* 10: 1514-1521.)

Mucosal anti-Gal-lectin IgA responses are critical for resistance to amebic colonization and invasion [17,18]. Several studies showed that a susceptible population of children from Bangladesh had stool IgA Gal-lectin-specific antibodies that correlated with reduced re-infection rates with *Eh* [19,20]. Increases in anti-Gal-lectin IgA antibodies were associated with clearance of subsequent amebic infections, demonstrating that amebic liver abscess (ALA) subjects developed a heightened immune responsiveness and have retained memory of the parasite [17]. Interestingly, using the gerbil model of ALA, purified native Gal-lectin protected 86% of animals from abscesses [21]. The recombinant form of aa 758–1134 on the cysteine-rich region of the Gal-lectin 170-kDa subunit, termed LC3, was found to be efficacious as a subunit vaccine against *Eh* [22]. Moreover, several studies that looked at the serum IgA antibodies of ALA patients found that these antibodies bound with high affinity to the LC3 regions aa 868–944 and aa 1114–1134 [23]. Altogether, these studies show that Gal-lectin is the best candidate for vaccine development.

Gal-lectin was shown to induce dendritic cell maturation and promote the production of the Th1 cytokines IL-12 and interferon (IFN)-γ *in vitro* and *in vivo* [24]. Additionally, the cysteine rich region of Gal-lectin can also induce murine macrophages to produce tumour necrosis factor (TNF)-α [25] and human macrophages to produce IL-12 [26]. Gal-lectin activates mitogen-activated protein kinases (MAPK) and nuclear-factor κB (NF-κB) signalling pathways to up regulate mRNA and cytokine and receptor genes involved in pro-inflammatory responses including TLR2 mRNA and surface expression [27]. Despite the ongoing research efforts, there is no host receptor identified for Gal-lectin.

1.1.5.2 Cysteine Proteases

Eh possesses a number of cysteine proteases (CP) that are critical for disease pathogenesis and it is also one of the major differences seen from its similar counterpart, *E. dispar*. *Eh* has 10- to 1,000 fold more cysteine proteases compared to *E. dispar* [28]. *Eh* express cysteine proteinases: *Eh*CP-A1, *Eh*CP-A2, *Eh*CP-A3, *Eh*CP-A5, *Eh*CP-A8, *Eh*CP-A9 and *Eh*CP-A112 [29]. *Eh*CP-A1, *Eh*CP-A2 and *Eh*CP-A5 make up 90% of all the *Eh*CP transcripts [29]. The major cysteine proteinase is *Eh*CP-A5, which is both membrane bound and secreted. *Eh*CP-A5 cleaves MUC2 mucin at the C-terminus causing it to depolymerise [30], thus allowing the parasite to overcome the first line of innate immune defense. *Eh*CP-A5 can also disrupt tight junction proteins between epithelial cells that may aid *Eh* access to the lamina propria where there are patrolling resident macrophages and infiltrating neutrophils [4]. Moreover, *Eh* pro-mature CP5 contains an RGD motif that engages the αvβ3 integrin on colonic cells to trigger phosphatidylinositol-4,5-bisphosphate 3-kinase (PI3K) phosphorylation [31]. The integrin-linked kinase (ILK) phosphorylation activates Akt and causes ubiquitination of NF-κB essential modulator (NEMO) and subsequent activation of NF-κB [31]. *Eh*CP-A5 is also important for mediating mucin exocytosis from colonic goblet cells via αvβ3 integrin and activation of PI3K, protein kinase C (PKC)δ, and myristoylated alanine-rich C-kinase substrate (MARCKS) [32]. It was only recently that *Eh*CP-A1 and *Eh*CP-A4 were found to be important in initiating pro-inflammatory signalling pathways as well [33]. Even secretory IgA (s-IgA) and IgG which are important in the first line of defense against pathogens, can easily be degraded by *Eh*CPs [34,35]. In *in vivo* studies, *Eh*CP-A5

deficient parasites inflicted less damage to the intestinal barrier and failed to induce IL-1β production [36]. Interestingly, *Eh*CPs can act like an interleukin-converting enzyme and activate pro-IL-1β [36].

1.1.5.3 Amebapores

Eh produce amebapores, which are small amphipathic peptides that are 8 kDa with an α-helical structure stabilized by three disulphide bonds. There are three amebapores A, B, and C [37]. They are inserted into the plasma membranes of target cells and induce cell lysis [37]. It is one of the major pathogenicity factors and it has been shown to be involved in amebic liver abscess formation [38,39]. Interestingly, amebapore deficient *Eh* were still able to induce inflammation and tissue damage in colonic cells, indicating that different virulence factors are at play in different organs [39].

1.1.5.4 Prostaglandin E_2

Prostaglandin E_2 (PGE_2) is an important pro-inflammatory lipid mediator. PGE_2 has been found to be increased 10 fold in *Eh* infected colons [40]. Interestingly, *Eh* expresses a cyclooxygenase (COX)-like enzyme and synthesizes PGE_2 in the presence of arachidonic acid [41]. *Eh* PGE_2 dissociates claudin-4 from the tight junction complex via signalling through the EP4 receptor, resulting in increased sodium permeability toward the lumen [42]. This early event is what triggers watery diarrhea seen with *Eh* infection. Among all the virulence factors in *Eh*, PGE_2 released by parasite was the first study to show that *Eh* could elicit disease in a contact-independent manner. Moreover, PGE_2 coupling through

EP4 receptors induced IL-8 secretion from colonic epithelial cells [43]. The IL-8 chemokine is a neutrophil chemoattractant that could be associated with the early acute inflammatory response to *Eh* infection.

1.1.5.5 Phagocytosis

Interestingly, phagocytosis is considered an important virulence factor for *Eh* as parasites deficient in phagocytosis were shown to be less virulent [44,45]. *Eh* has the ability to induce host cell apoptosis and phagocytose apoptotic cells. Phagocytosis of apoptotic cells serves to limit inflammation as a mode of evasion and to allow *Eh* to survive. There were 121 genes identified that are involved in ameba phagocytosis, particularly cytoskeleton and actin-binding genes [46]. Exposure to a phagocytic stimulus led to increased phagocytic ability during another stimulus encounter, suggesting this unique feed-forward regulation of phagocytosis [46]. The defining feature of cells undergoing apoptosis is the exposure of phosphatidylserine on the outside of the plasma membrane [47]. This was observed with *Eh* and Jurkat T cells, where contact led to caspase-3 activation, DNA fragmentation, and phosphatidylserine exposure and finally its fate ends with amebic phagocytosis [47–49]. Not surprisingly, phagocytosis was mediated by the Gal-lectin as addition of D-galactose blocked cytotoxicity and abrogated phagocytosis [47]. Erythrophagocytosis is a characteristic feature of *Eh* infection, but is not seen with *E. dispar* [50]. *Eh* also recognize erythrocytes by phosphatidylserine exposure, but the receptor is unknown [51]. Remarkably, *Eh* can kill cells directly by chewing off fragments of host cells known as “amebic trogocytosis”. This process was characterized

by increased intracellular calcium levels, eventual loss of plasma membrane integrity, nuclear DNA degradation, and mitochondrial potential loss [52]. Once cells die, *Eh* cease trogocytosis and detach from the corpses [52]. Similar to phagocytosis, *Eh* requires Gal-lectin mediated contact, actin recruitment, amebic C2 domain-containing protein kinase (EhCP2K), and PI3K signalling [52].

1.2 Innate Host Defense Against *E. histolytica* and Immunopathogenesis

The gastrointestinal tract is comprised of a thick mucosal barrier that separates the external environment from the immune system and the mucosal layer is home to an enormous number of microorganisms. While on the one hand there are commensal microorganisms that are important in health and homeostasis, there are also pathogenic microorganisms that can invade the mucosal layer to cause diseases.

1.2.1 *Mucus Bilayer*

The colonic mucus bilayer serves to act as a physical barrier separating the sterile internal environment from insults found from the external environment and allows for easy elimination of adherent pathogens through peristalsis [53]. Moreover, it provides a site for gas and nutrient exchange [54]. The mucus bilayer consists of a dense inner layer that is devoid of bacteria and an outer loose layer colonized with the host microbiota [54]. The major component of the mucus layer is the gel-forming mucin, MUC2, which is produced by goblet cells [53]. MUC2 is a large glycoprotein made up of 5179 amino

acids, and contains a large central O-glycosylated domain and N- and C-terminal cysteine-rich domains [55].

My laboratory has been extensively studying the role of the mucus layer in *Eh* pathogenesis. In a majority of infections, *E. histolytica* resides in or on the mucus layer and feeds on bacteria and cellular debris and it is able to do this by binding to colonic mucins via the Gal-lectin adhesin to galactose and *N*-acetylgalactosamine residues on the O-linked sugar side chains [14]. During invasive infection, *Eh* overcomes the mucus layer using cysteine proteases and glycosidases that disrupt the mucin network [30,56,57]. The degradation of mucin is driven by *Eh*CP-A5 as it was shown to specifically cleave the C-terminal cysteine rich domain of MUC2, leading to the loss of protective function of the mucus layer [30]. Moreover, ameba deficient in *Eh*CP-A5 were also unable to overcome the protective mucus barrier [58]. The mucus layer is critical for protective against *Eh* infection as Muc2-deficient mice were shown to have increased gross pathology scores with observed dilated colons, expanded colonic loops, and brown and bloody mucosal exudates [59]. There was also increased pro-inflammatory cytokine secretion including TNF-α, IFN-γ, and IL-13 in Muc2-deficient as compared to WT mice treated with *Eh* [59]. *Eh* also induces hypersecretion of mucin from goblet cells [32]. This mucus hypersecretion is mediated by *Eh*CP-A5 ligation of αvβ3 integrin on goblet cells and induction of SRC family kinase, PI3K and PKCδ signalling pathways [32]. The breakdown of the mucosal bilayer is detrimental as it creates a gap, facilitating *Eh* penetration further down the submucosa and causing the development of flask-shaped ulcers and inflammation [3].

1.2.2 *Epithelial Cells*

Epithelial cell-initiated inflammation also plays a crucial role in early tissue damage in *Eh* infection of the human intestine. Interestingly, it was shown that *Eh* promature-CP5 RGD motif can bind the αvβ3 integrin on colonic epithelial cells to trigger activation of NF-κB [31]. NF-κB is the transcriptional regulator of cytokine gene expression including TNF-α, IL-1β, and IL-12p40 [60]. The ubiquitination of NF-κB essential modulator (NEMO) led to the activation of IKK and IKB ubiquitin-mediated degradation [60]. Subsequently, this releases NF-κB into the nucleus where it induced expression of TNF-α and IL-1β in colonic cells [31]. These cytokines are important for recruiting more immune cells to help at the site of invasion. *Eh* can also induce secretion of monocyte chemotactic protein (MCP)-1 from epithelial cells, which is chemotactic for monocytes [61]. This occurs via activation of PI3K and posttranslational modification of the NF-κB p65 subunit [61].

Tight junction proteins serve as an integral part of epithelial cells to regulate ions through the paracellular pathway and to prevent luminal microbes from translocating to the basal side. Another complex known as *Eh*CPADH112, composed of *Eh*CP112 and *Eh*ADH112 adhesin was shown to degrade tight junction proteins including occludin, claudin-1, ZO1, and ZO2 [62]. This led to the breakdown of tight epithelial cell-cell interaction, loss of transepithelial resistance (TER) and subsequently, increases in paracellular permeability [62]. *Eh* also expresses a 55 kDa occludin-like protein that is capable of displacing the

human occludin protein, and reducing trans-epithelial resistance and disrupting colonic barrier integrity [63]. The changes in tight junctions were also assessed using the ameba colonic loop model in the presence or absence of a mucus barrier. Interestingly, WT mice infected with *Eh* displayed increased occludin, but Muc2-deficient mice had increased claudin-2 and decreased occludin and ZO1 [59]. Additionally, *Eh* was shown to cause decreases in Na^+ and Cl^- absorption attributed to serotonin, thus driving diarrhea [61].

1.2.3 *Neutrophils*

The recognition of the parasite by intestinal epithelial cells induces the secretion of IL-8, which results in immediate immune cell recruitment and infiltration into the lamina propria [4,64]. Neutrophils are one of the first immune cells recruited to the site of infection. While neutrophils are armed with cytotoxic granules (neutral proteases, lysozyme, and acid hydrolases) that are targeted to kill *Eh*, one trophozoite has been shown to kill up to 3,000 neutrophils [65]. The process by which host cells are killed by *Eh* occurs in three steps: 1) adherence 2) cytolysis and 3) phagocytosis [66]. *Eh* killing of neutrophils leads to increased tissue destruction due to the release of harmful neutrophilic constituents into the environment [67]. In the reverse, i*n vitro* studies have shown that neutrophils activated by both IFN-γ and TNF-α can kill *Eh* up to 67% after 6 hours of incubation via reactive oxygen species (ROS), most notably H_2O_2 [65,68].

1.2.4 *Macrophages*

The healthy intestinal mucosa is comprised of the largest reservoir of macrophages in the body, which is beneficial to the host as the gut is constantly exposed to a variety of bacteria and antigens. Under homeostasis, resident intestinal macrophages possess high phagocytic and bactericidal activity, enabling them to readily clear microorganisms in the absence of inducing an inflammatory cascade [69]. They do not express LPS co-receptor CD14 or the IgA (CD89) and IgG (CD16, 32, and 64) receptors [69], which means that they do not initiate inflammatory signalling pathways.

The release of chemokine (C-C motif) ligand 2 and 4 (CCL2 and CCL4) leads to the recruitment of circulating blood monocytes into the lamina propria where they can differentiate into mature macrophages [69]. These macrophages are highly responsive to inflammatory stimuli and they can produce reactive oxygen and nitrogen species [69]. In order to distinguish between self and microorganisms, macrophages express a plethora of pattern recognition receptors (PRRs) including toll-like receptors (TLR) and nod-like receptors (NLR). These receptors are important for recognizing pathogen-associated molecular patterns (PAMPs) and danger-associated molecular patterns (DAMPs). When challenged with lipopolysaccharide (LPS) or IFN-γ, macrophages produce a variety of cytokines including IL-1, IL-18 [70], and TNF-α [71] to elicit a proper immune response against invading pathogens. The uncontrolled production of these cytokines, however, leads to the development of inflammatory diseases [72]. Present evidence support the idea that central to host defense against *Eh* invasion are macrophage-mediated effector

mechanisms. Macrophages are major producers of TNF-α, an autocrine mediator that enhances inducible nitric oxide synthase (iNOS) gene expression and nitric oxide (NO) production [73]. Several experiments have shown that addition of combinations of recombinant cytokines activated macrophages *in vitro* for amebicidal activity. *In vitro* studies indicated that IFN-γ and TNF-α act synergistically to stimulate macrophages to release NO and they are able to efficiently kill up to 87% of amoebic trophozoites [74]. NO release has been shown to be effective against killing of *Eh* by inhibiting cysteine proteinases and alcohol dehydrogenase [74,75]. A combination of both IFN-γ and *Eh* extract also triggered the production of TNF-α for ameba killing [76]. Of critical importance is that macrophage-ameba contact is necessary for amebicidal activity [77]. *Eh* DNA can also increase iNOS mRNA expression and activate toll-like receptor (TLR) 9 signalling to trigger TNF-α levels [78]. Another molecule, a macrophage migration inhibitory factor (MIF) was identified in *Eh* genome to be an immunomodulator of macrophage activity [79]. MIF was shown to be capable of binding to CD74 and it augmented TNF-α secretion by LPS-stimulated macrophages, another dominant cytokine characterizing the pro-inflammatory responses [79].

1.2.5 *Entamoeba histolytica Immune Evasion Mechanisms*

Parasites have evolved evasion strategies or they can exploit the immune responses of their host to enable them to be successful survivors. For each step of the inflammatory process aimed at eliminating the parasite, *Eh* have built-in mechanisms that allow it to counter the attack (**Figure 1.3**). While heat shock proteins serve to protect cells exposed

to stress, they are utilized by *Eh* as a means to modulate inflammation [31]. *Eh* dampened colonic inflammation by phosphorylation of the heat shock protein 27, which leads to suppression of NF-κB activity [31]. Though it is not entirely clear how this contributes to disease pathogenesis, it may be an explanation for why a majority of individuals infected with *Eh* are asymptomatic.

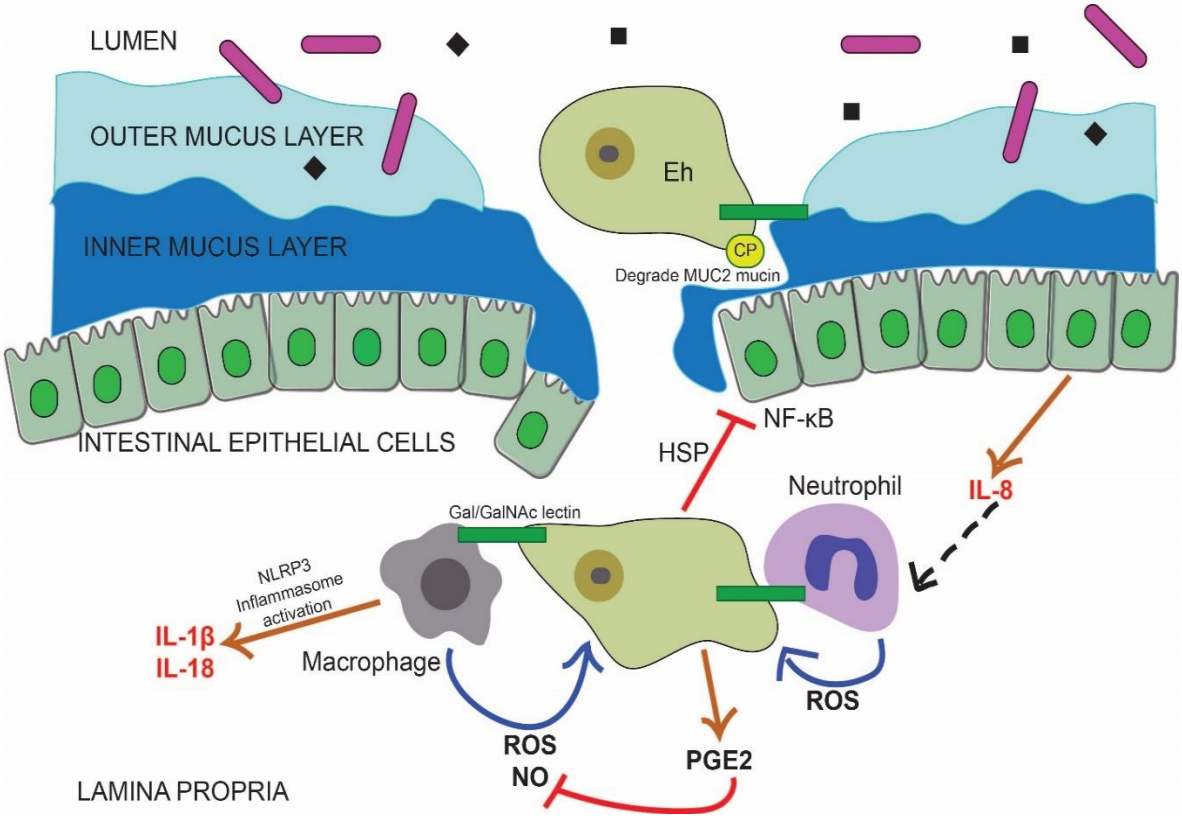

Figure 1.3 *E. histolytica* invasion of intestinal mucosal barrier.

The first lines of defense that *Eh* overcomes are the outer and inner mucus layers by using glycosidases and cysteine proteinases to cleave MUC2 mucins. The main adhesin, Gal-lectin found on *Eh*, binds to host cells and is required for cytolytic activity. Upon traversing the mucus layer, *Eh* can also disrupt tight junctions that hold epithelial cells together as a sheet. *Eh* can inhibit NF-κB activity in epithelial cells by regulating heat shock proteins. Furthermore, epithelial cells release IL-8 that attracts neutrophils to the site of infection. Neutrophils release ROS in an attempt to kill the parasite. Similarly, *Eh* in direct contact with macrophages leads to the activation of the NLRP3 inflammasome, subsequently releasing active IL-1β and IL-18. Macrophages also produce ROS and NO as products to destroy *Eh*. Despite these effector mechanisms to get rid of the parasite, *Eh* also has counter mechanisms including the synthesis of PGE_2 to inhibit NO synthesis. (Adapted from Quach & Chadee. 2016, *Encyclopedia of Immunobiology* 133-141.)

Normally residing in the luminal side of the intestine in an anaerobic environment, during tissue invasion, *Eh* is exposed to a higher oxygen environment that is rich in ROS such as superoxide radical anions (O_2^-) and H_2O_2 [80]. There are three key antioxidant enzymes that serve to protect *Eh* against oxygen toxicity: an iron-containing superoxide dismutase (Fe-SOD)[80] and a flavin reductase (NADPH: Flavin oxidoreductase) [81] which both function to reduce O_2 to H_2O_2. A thiol-rich 29-kDa surface antigen or known as peroxiredoxin functions in concert with the other two enzymes of *Eh*, aiding in the degradation of H_2O_2 [82].

Eh can also impair macrophage responses by inhibiting iNOS mRNA and NO production as well as TNF-α production via PGE_2 [83]. More specifically, *Eh* does this by utilizing arginase to convert L-arginine into L-ornithine, thus preventing synthesis of NO which is a potent effector molecule against *Eh* [84]. The role of macrophages in immune defenses is not limited to the innate arm, as it has also been shown to be critical in antigen presentation to T cells via class II molecules [85]. *Eh* can also inhibit IFN-γ-induced class II molecule expression due in part by stimulating the production of PGE_2, which has been reported to inhibit class II MHC genes [85].

In addition to being faced with effector cells of the immune system, *Eh* encounters the complement system, which is made up of distinct plasma proteins that react with one another in a cascade of events. This leads to the recognition of cells, opsonisation followed by intracellular killing by phagocytes or direct cell lysis. While complement proteins are essential for eliminating the pathogen, bacteria and parasites have developed

mechanisms that allow them to evade this system. *Eh* extracellular cysteine proteinase has been shown to degrade anaphylatoxins C3a and C5a, thereby inhibiting the complement pathway [86]. The consequences of inhibiting C3a and C5a proteins extend beyond the pathway as they are also important for regulating vasodilation and attracting macrophages, neutrophils, and mast cells [87]. Moreover, *Eh* Gal-lectin and a 21 kDa protein was found to exhibit epitope similarities to the complement inhibitory protein, CD59, which functions to protect cells from lysis by C5b-9 proteins [88,89]. In a similar manner, *Eh* binds to C8 and C9 via its Gal-lectin in order to avoid the formation of the membrane attack complex [89].

Another unique mechanism that *Eh* uses to avoid the immune system is called receptor capping. In this process, the parasite surface receptors are clustered together and moved to the posterior end of the cell where they are released as membrane vesicles to avoid being recognized [90]. Interestingly, *Eh* encodes for *Eh*ROM1, an active intramembrane protease localized at the base of the cap with *Eh* Gal-lectin [91]. This suggests that *Eh*ROM1 is responsible for cleaving Gal-lectin, specifically facilitating the release of these caps once they are formed [91]. Taken together, all of these evasion strategies essentially allow the parasite to successfully colonize and in rare cases, establish chronic infection in organs such as the liver.

1.3 Animal models for Studying Amebiasis

There are limited animal models for studying *Eh* infection simply because none are able to replicate the entire life cycle of *Eh*. The Mongolian gerbil (*Meriones unguiculatus*) has

been used as the standard model for amebiasis to look at both intestinal and hepatic complications [92,93]. Cecal infections of *Eh* were characterized by destruction of the interglandular epithelium, amebic ulcers, cecal hypertrophy and crypt hyperplasia [92]. Hepatic infections resemble that of human hepatic amebiasis, with the formation of granulomas and the development of fluid-filled cavitary lesions at later stages [92]. *Eh* infections in mice were attempted to reproduce intestinal and hepatic lesions, however, they proved to be unsuccessful. The strains of mice that were found to be susceptible to intestinal amebiasis included C3H/HeCr, BALB/c, NZB/B1N, B10.A, DBA/2 and C57Bl/6 [94]. The strains A/J, CE, DBA/1 and CD-1 were resistant to amebiasis [94]. An interesting model that was also explored was implantation of human intestine into the subcapsular region of severe combined immunodeficient (SCID) mice (SCID-HU-INT) [95]. When the human xenografts were stimulated with *Eh*, there was the production of pro-inflammatory cytokines IL-1β and IL-8 from intestinal epithelial cells [95]. Furthermore, there was amebic invasion into submucosal tissues, formation of amebic ulcers, neutrophilic inflammatory responses and the formation of micro abscesses [95]. An *ex vivo* human intestinal model was also used to study the early steps in ameba pathogenesis [96]. During the first 2 hours of infection, *Eh* depleted the mucosal layer and penetrated into the lamina propria. There was significant cell lysis and an increase in pro-inflammatory markers including IL-1β, IFN-γ, IL-6, IL-8, and TNF-α [96]. Currently, ameba colonic loop models are widely used as a model for early acute pro-inflammatory responses and has been the major model used in the Chadee lab [97].

1.4 Pattern Recognition Receptors (PRRs)

Inflammation is a double-edged sword because while inflammation is crucial for protecting against invasive pathogens, it can simultaneously lead to severe host tissue damage. For this reason, inflammation is tightly regulated. Pattern recognition receptors (PPRs) are germline-encoded receptors involved in recognizing danger associated molecular patterns (DAMPS) and pathogen associated molecular patterns (PAMPs) [98]. DAMPS include intracellular proteins that are released as a result of sterile injury. PAMPs are nucleic acids and proteins unique to bacteria and viruses including LPS, ssRNA, and flagellin. There are three groups of receptors: 1) extracellular receptors, 2) cell surface receptors, and 3) intracellular receptors. The extracellular receptors include mannan binding lectin and C-reactive protein. The cell surface receptors include toll-like receptors (TLRs) and C-type lectin receptors (CLRs). The majority of receptors are intracellular and they include TLRs, NOD-like receptors (NLRs), and retinoic acid-inducible gene-1 (RIG)-like receptors (RLRs).

1.4.1 *Nucleotide-Binding Oligomerization Domain (NOD)-Like Receptors (NLRs)*

There are four subfamilies in the NLRs including: 1) NLRA which consists of the acidic transactivating domain, 2) NLRC which consists of the CARD, 3) NLRB which consists of the BIR, and 4) NLRP which consists of a PYD that is crucial for inflammasome organization. They all contain a variable N-terminal interaction domain, a central NACHT domain, and C-terminal leucine-rich repeat domain (LRR). NLRs are found on

macrophages, dendritic cells, neutrophils, and epithelial cells [99]. Some NLRs are able to form large multimeric complexes known as inflammasomes.

1.5 Caspases

Caspases are a family of highly conserved **c**ysteine-dependent **asp**artate specific prote**ases** that mediate a cascade of events leading to the transduction of signalling pathways that culminate in the desired biological response such as apoptosis or inflammation. Caspase-1 was the first mammalian caspase to be described and was identified to be important for the processing of IL-1β [100]. Caspases share a common structure, consisting of a 3-24 kDa N-terminal pro-domain, a 17-21 kDa central large domain and a 10-13 kDa small C-terminal subunit domain [101]. All caspases consist of an active cysteine residue in the large domain that specifically cleaves after the aspartate residue in substrates [101] (**Figure 1.4**). Caspases are regulated post-translationally. Specifically, they are synthesized as "procaspases", zymogens that are inactive until they are cleaved at two sites: one site is between the pro-domain and large subunit, and another site between the large subunit and small subunit [101]. There are three major groups of caspases: Group I: inflammatory caspases; Group II: apoptosis initiator caspases, and Group III: apoptosis effector caspases [102,103], totalling 13 caspases (**Table 1.1**). The pro-domains contain either death effector domains (DEDs) or caspase recruitment domains (CARDS). Caspases are either activated by upstream caspases or undergo scaffold-mediated transactivation [101]. Caspases need to be tightly regulated as hyper activation can promote auto-inflammatory conditions, while insufficient activation

of caspases can lead to susceptibility to infection and sepsis [104]. The activation and activity of caspases are distinct processes, as a caspase can become activated, but have its activity suppressed. It is still unclear what specific functions each of these caspases have and if there is redundancy among them.

Table 1.1 Categories of Caspases

Type of Caspase	Human Caspase	Mouse Caspase
Initiator Apoptotic	2, 8, 9, 10	2, 8, 9
Effector Apoptotic	3, 6, 7	3, 6, 7
Inflammatory	1, 4, 5	11, 12

1.5.1 *Inflammatory Caspases*

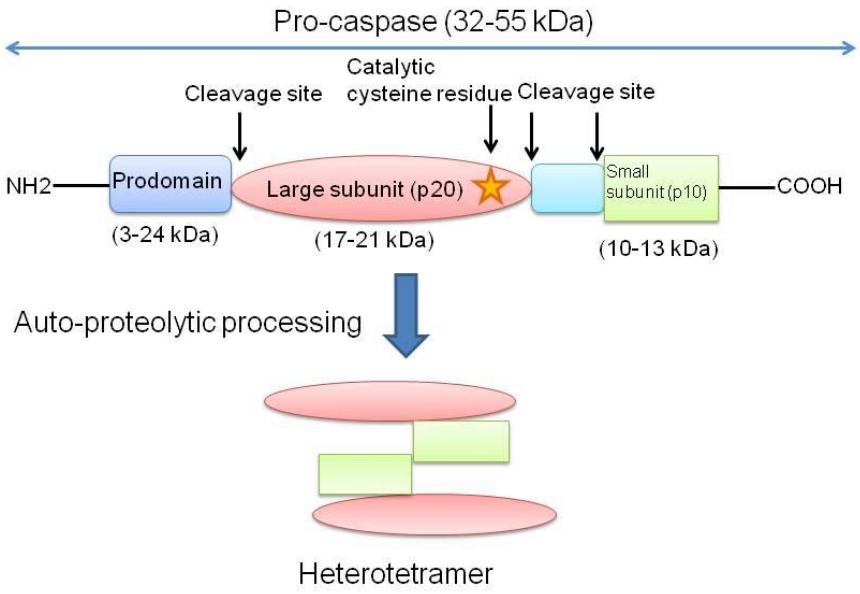

Figure 1.4 Caspase activation.

Caspases share a common structure, consisting of a 3-24 kDa N-terminal pro-domain, a 17-21 kDa central large domain and a 10-13 kDa small C-terminal subunit domain. All caspases consist of an active cysteine residue in the large domain that specifically cleaves after the aspartate residue in substrates. Following autoproteolytic cleavage of pro-caspase generates the active caspase heterotetramer.

Caspase-1, -4, -5, and -12 comprise the inflammatory subset in humans, and caspase-1, -11, and -12 comprise the inflammatory subset in mice [105]. The role of this group of caspases in the inflammatory response is cytokine maturation. It is now appreciated that there are other functions for these caspases, one of which is pyroptosis, an inflammatory form of programmed cell death [106]. Multiple lines of research demonstrate that caspase-1 has multifaceted roles in host defense. Chromosomal mapping revealed that the human caspase-4 gene is colocalized within a cluster of functionally related genes including caspase-1, -5, and -12 and caspase-1 pseudogenes ICE-BERG, COP, and INCA in human chromosome 11q22–23 [106]. These pseudogenes are inhibitors of caspases. It has been suggested that caspase-4 and caspase-5 may have originated from caspase-11 [106], and caspase-11 share 60% amino acid identity to caspase-4 [107]. Caspase-5 recruitment was shown to act as a co-activator of the NLRP1 inflammasome, while caspase-12 acted as a negative regulator of caspase-1 activity [106]. In light of recent studies on the role of the apoptotic initiator caspase-8, its ability to cleave the inflammatory cytokine pro-IL-1β suggests that the roles of caspases are not so clear-cut [108]. Hence, there is a degree of cross talk between the apoptotic and inflammatory caspases that determine the fate of the cell, and influence the outcome of host response to infections.

1.5.2 *Caspase-1*

Caspase-1 (also known as interleukin-1β-converting enzyme (ICE), interleukin-1β-convertase (IL-1BC), or p45) was the first discovered caspase and it has a strict

requirement for an Asp residue at position P1 and has a preferred cleavage sequence of YEVD [109]. It is present as an inactive zymogen and upon assembly into a high multimeric complex called the inflammasome, pro-caspase-1 is cleaved into caspase-1 and caspase-1 is well known as an activator of IL-1β. Caspase-1 also mediates pyroptosis, which is a form of inflammatory cell death characterized by cell swelling and plasma membrane rupture [110]. Pyroptosis has been shown to be important for bacterial clearance [110]. When cells are lysed, the cytosolic protein called lactate dehydrogenase (LDH) is released into the extracellular space and this is used as a readout for cell death.

1.5.3 *Caspase-11*

Caspase-11 has a strict requirement for Asp at the P1 position and has a preferred cleavage sequence of LEHD [111]. Its expression is strictly regulated as there is very little detection of caspase-11 in unstimulated cells [112]. Furthermore, it has also been pointed out that elevated expression of caspase-11 protein allows for auto-activation [112]. The caspase-11 locus encodes for two proteins 38 and 43 kDa [113]. The 43 kDa protein was hypothesized to be the major protein to undergo auto-activation, whereas the 38 kDa protein may require activation by other proteins [113]. It is possible that cleavage products, especially those of the smaller subunit (p10) are not always observed due to its instability, therefore the reported cleavage products of caspase-11 is on the activation and processing of the intermediate forms and larger subunits (p20) [113].

What is particularly interesting is that inflammatory caspases have diverse pleiotropic functions other than their proteolytic activity. Another interesting role ascribed to caspase-11 is in regulating the cytoskeleton machinery [114]. One report showed that caspase-11 is involved in phagolysosomal formation for restricting *Legionella pneumophila* infections within murine macrophages [115]. This occurs by the modulation of actin polymerization through cofilin [115]. In parallel, the use of human THP-1 macrophages transfected with caspase-4 and caspase-5 plasmids demonstrated that both caspases are required for cofilin dephosphorylation and therefore the promotion of the phagosome-lysosome fusion [115]. Moreover, the expression of both caspase-4 and -5 triggered caspase-1 cleavage [115], suggesting interactions amongst the inflammatory caspase family members.

The relevance of caspase-11 indicated in *in vivo* models has been explored in the context of sepsis. Caspase-11 knockout mice were more resistant to lethal doses of LPS compared to wild-type mice [116,117]. Cholera toxin B is the known caspase-11 activating toxin that enables the movement of LPS into the cytosol via the ganglioside receptor GM1 [118]. Several studies have also been done in dextran sodium sulphate (DSS)-induced colitis. Due to the discovery of caspase-1 knockout mice being deficient in caspase-11 as well, reported hyper-susceptibility to infection with caspase-1 could also be explained by the absence of caspase-11 [118]. Caspase-11 has been reported to be expressed constitutively in the colon and mediates protection against DSS-induced colitis independently of inflammasome activation [119]. Compared to WT counterparts,

Caspase-11$^{-/-}$ and *Caspase-1*$^{-/-}$*Caspase-11*$^{-/-}$ mice had increased tissue damage and inflammatory cell infiltration [119].

1.5.4 *Caspase-4*

Caspase-4 (also known as ICE_{rel}II, ICH-2, protease TX) is constitutively expressed and is highly expressed in the spleen and lungs [120]. It has a preferred cleavage sequence of LEVD [109]. Since it is believed that human caspase-4 arose from a duplication of the ancestral gene caspase-11, it could play similar roles as caspase-11 in regulating caspase-1 activation [118].

1.5.4.1 Caspase-4 and Caspase-1 Interactions

One study has shown that macrophages deficient in caspase-4 had decreased caspase-1 activation and reduced IL-1β secretion when stimulated with ATP and MSU [121], suggesting that similar to caspase-11, it can regulate caspase-1 activation. Caspase-4 was also implicated in dengue virus infection where it was discovered to be important in regulating caspase-1 activity and subsequent IL-1β activation [122]. However, no further studies have been addressed to indicate that caspase-4 and -1 directly interact. Furthermore, caspase-4 does not cleave pro-IL-1β suggesting that although there is high sequence conservation with caspase-1, there is also a degree of non-redundancy [107]. A fascinating study by one group explored the role of caspase-4 *in vivo*. Caspase-4 transgenic mice that were exposed to LPS led to 50% lethality within 24 hours [120]. When the BMDMs from the caspase-4 transgenic mice were isolated and stimulated with

LPS, there were increased levels of IL-1β and IL-18 [120]. Caspase-4 and caspase-1 plasmids were also transfected to determine if the proteins interacted and it was evident that caspase-4 supported processing of caspase-1 [120].

1.5.4.2 Caspase-4 Activation Mechanisms and Protein Interactions

Interestingly, using enzymatic assays, caspase-1 activation was shown to require dimerization, while caspase-4 required both dimerization and interdomain cleavage [123]. Caspase-4 was shown to bind TNF receptor-associated factor 6 (TRAF6) to mediate LPS-induced NF-κB-dependent production of IL-8 and CC chemokine ligand 4 (macrophage-inflammatory protein-1) [124]. As well, caspase-4 along with other inflammatory caspases including caspase-5 and caspase-11 were shown to bind LPS via the CARD domain of caspases, leading to oligomerization and activation [125].

1.5.4.3 Caspase-4 in Epithelial Cells

Currently, there is emerging evidence for the role of caspase-4 in intestinal epithelial cell (IECs) host defense. This is supported by data showing that caspase-4 expression is high in IECs [126]. In response to *Salmonella enterica* serovar Typhimurium, caspase-4 was critical for IL-18 secretion, but not IL-1β secretion [126]. Similarly, murine caspase-11 was found to also govern IL-18 secretion [126]. In parallel with macrophages, caspase-4 was able to sense LPS intracellularly. Both caspase-4 and caspase-11 also drive pyroptotic cell death of epithelial cells infected with *S. typhimurium* in order to restrict bacterial growth [126]. Interestingly, *Shigella flexneri* was shown to counteract host

caspase-4-induced cell death by utilizing a type III effector, OspC3 [127]. *S. flexneri* deposited the OspC3 at the putative catalytic pocket of caspase-4 to prevent caspase-4-p19 and caspase-4-p10 heterodimerization [127]. This was then shown to inhibit IL-18 release and delayed epithelial cell death [127]. Caspase-4 driven cell death was also important for enteropathogenic *Escherichia coli* (EPEC) infection [127].

1.5.4.4 Caspase-4 in Other Cell Types

One study has characterized caspase-4 as being required for the maturation of pro-IL-1β and for unconventional secretion in keratinocytes [121]. Moreover, pro-inflammatory cytokine stimulation of human retinal pigment epithelial cells was reported to increase caspase-4 mRNA and protein expression [128]. Not only is caspase-4 important for inflammatory signaling processes, it is also involved in endoplasmic reticulum stress-induced apoptosis [129]. These studies show that caspase-4 activation can occur throughout many cells, displaying diverse functions. Although there are studies that have addressed both caspase-4 and caspase-11, it is still unclear whether they are functional orthologues. More studies are warranted to decipher their functions in inflammation.

1.6 Inflammasomes

To date, there are four types of inflammasomes characterized: 1) NLRP1: recognizes anthrax lethal toxin, 2) NLRP3: a variety of PAMPs and DAMPs, 3) NLRC4: cytosolic flagellin, and 4) AIM2: cytosolic dsDNA [130]. Inflammasomes are large molecular complexes that assemble upon activation by sterile stimuli or pathogens and are critical

for host defenses. They are highly expressed in myeloid cells, namely macrophages [131]. The inflammasome consists of three major components: 1) a NOD-like receptor (NLR) which acts as the intracellular sensor, 2) an adaptor protein such as ASC (apoptosis speck-like protein containing a CARD) which recruits pro-caspase-1 to the complex through CARD domain interactions, and 3) pro-caspase-1 [106] (**Figure 1.5**). NLRP contains a central NACHT nucleotide-binding domain and carboxy-terminal leucine-rich repeats (LRRs) [132]. The NACHT domain has ATPase activity and allows for oligomerization to occur, while the LRRs could be involved in ligand association [132]. ASC consists of two death-fold domains: a pyrin domain and a caspase activation and recruitment domain (CARD). Upon engagement of the sensor molecular via the pyrin domain, this leads to ASC oligomerization which we call "protein speck". ASC brings together pro-caspase-1 into close proximity via the CARD domain and this leads to caspase-1 cleavage and formation of the heterotetramer. This is termed the "canonical inflammasome" consisting of these three components.

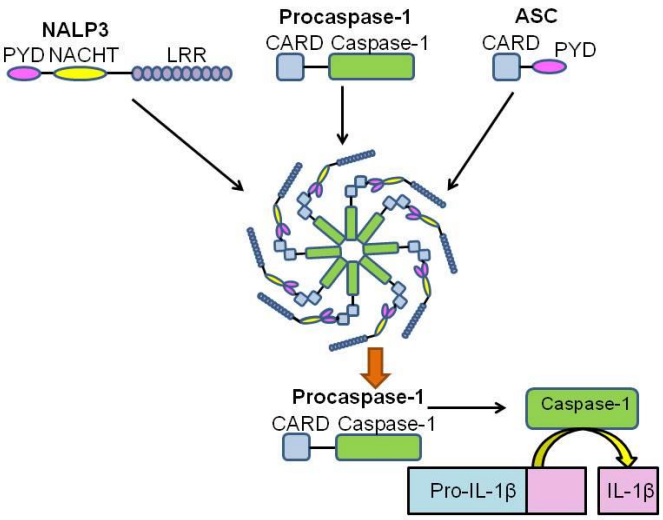

Figure 1.5 Structural organization of the inflammasomes.

The inflammasome complex is comprised of a sensor (NLRP3) that consists of a pyrin domain (PYD), NACHT and leucine rich repeat (LRR), which allows it to recruit ASC. The ASC adaptor consists of CARD and PYD that allows the recruitment of pro-caspase-1 by binding to CARD. This forms a multimeric complex that leads to the maturation of pro-caspase-1 into caspase-1 and cleavage of pro-forms of IL-1β into its active form.

The domains come together to auto-proteolytically cleave pro-caspase-1 into its active form. Caspase-1 is constitutively expressed in the cytosol as inactive zymogens and activated caspase-1 leads to the cleavage of precursors of IL-1β into the 17 kDa active form [133]. In addition to IL-1β, caspase-1 also cleaves other cytokines from the IL-1 family including IL-18 and IL-33 [134]. These pro-inflammatory cytokines are have been proposed to be secreted via unconventional secretion pathways including: exocytosis of the secretory lysosomes [135], shedding of plasma membrane microvesicles, direct release via transporters [136] or release via multivesicular bodies containing exosomes [137,138]. The activation of the inflammasome is a tightly regulated process and occurs via two steps: 1) transcriptional upregulation of pro-IL-1β and NLRP3, and 2) cleavage of pro-caspase-1 and maturation of IL-1β [139]. The two-step process is intuitively a safeguard mechanism to prevent unintentional inflammasome activation. Discovered more than two decades ago, IL-1β is a potent mediator of inflammatory responses, playing a myriad of roles including recruiting leukocytes (i.e. neutrophils, macrophages) and inducing tissue remodelling [139].

1.6.1 *NLRP3 Inflammasome*

The NLRP3 inflammasome is a well-characterized inflammasome that is activated by a wide variety of PAMPs, including Influenza virus, *Citrobacter rodentium*, bacterial pore-forming toxins such as nigericin and DAMPs, including ATP, monosodium urate crystals (MSU), and aluminium hydroxide [140]. To date, there is no evidence to suggest that a ligand directly binds to NLRP3, but there are common mechanisms elicited by all NLRP3

activators. Three mechanisms that have been proposed include: 1) potassium efflux [141], 2) lysosomal leakage and release of lysosomal protease cathepsin B into the cytosol [142], and 3) reactive oxygen species [130].

1.6.2 *Non-canonical Inflammasome*

The term "non-canonical inflammasome" describes the inflammasome that consists of other components outside of the conventional inflammasome components that was discovered later. The caspase-11 non-canonical inflammasome is made up of caspase-11, caspase-1, NLRP3, and ASC. Recent studies indicate that caspase-11 activation occurs particularly upon sensing bacterial molecules within the cytosol of macrophages. Similar to the two-signal model for inflammasome activation, caspase-11 activation also seems to follow the same pattern. Caspase-11 has been shown to mediate several pathways including NLRP3/ASC and NAIP5/NLRC4 inflammasomes, as well as caspase-1-independent cell death and IL-1α release [143]. In contrast to caspase-1 which is absolutely required for IL-1β secretion, caspase-11 is not required, however it does enhance caspase-1-dependent IL-1β secretion [143]. Caspase-11 has been shown to trigger caspase-1-independent macrophage death and caspase-1-dependent IL-1β and IL-18 production in response to several inflammasome activators [118,144].

Another non-canonical caspase-8 inflammasome consists of dectin-1, mucosa-associated lymphoid tissue lymphoma translocation protein 1 (MALT1), ASC, and caspase-8. Dectin-1 recognizes fungal components that allow it to signal kinase SYK for the

formation of the non-canonical inflammasome complex [145]. This MALT1-ASC-caspase-8 complex can activate IL-1β in dendritic cells [145]. Interestingly, caspase-8 was shown to be required for caspase-1 and IL-18 activation in response to *Yersinia* infection [146] and caspase-8 can itself also process IL-1β [146].

1.7 Inflammasomes and Disease

Inflammasomes and particularly IL-1β are involved in the pathogenesis of many inflammatory diseases. For instance, gain-of-function mutations in the NLRP3 have been shown to be associated to susceptibility to autoinflammatory diseases termed cryopyrin-associated periodic syndromes (CAPs). The spectrum of diseases associated with this include familial cold auto-inflammatory syndrome (FCAS), Muckle Wells syndrome (MW) and neonatal onset multisystem inflammatory disorder (NOMID) characterized by systemic inflammation involving the skin, joints, central nervous system, and eyes and presents with symptoms including fever and urticarial rash [147]. THP-1 cells expressing the Q705K polymorphism in the NLRP3 led to an overactive inflammasome and increased IL-1β levels [148]. To further support the critical role of IL-1β in the pathogenesis of these inflammatory diseases, treatment with IL-1R blockade using Anakinra improved symptoms dramatically [149,150]. Moreover, NLRP3 inflammasome has also been implicated in metabolic disorders such as atherosclerosis and type II diabetes [151].

Although a lot is known about the various signals that activate NLRP3 inflammasome, how it gets turned off is not well characterized. This tight regulation of turning on and off the NLRP3 inflammasome is a critical determining factor for the development of chronic diseases. PGE_2 was shown to signal via the EP4 receptor to inhibit NLRP3 inflammasome activation in response to nigericin and ATP [152]. This phenomenon occurred via activation of adenylyl cyclase, followed by an increase in cyclic AMP, thereby increased PKA and phosphorylation of NLRP3, resulting in inhibition of NLRP3 ATPase function [152]. For the translatability of these results, CAPs mutations make the NLRP3 unresponsive to cAMP inhibition [152], leading to uncontrolled activation of the inflammasome, IL-1β release, and therefore inflammation. Interestingly though, PGE_2 enhanced caspase-11 activation and IL-1α release [152], indicating that PGE_2 exerts different functions on different proteins.

1.8 Rationale for Study

Research on *Eh* began in the late 19^{th} century, but there are still gaps in our knowledge concerning key aspects in disease pathogenesis and host defence. *Eh* is an extracellular protozoan parasite that colonizes the large intestine of humans. In 90% of cases the parasite causes asymptomatic infection, while in 10% of individuals *Eh* invades the colonic mucosal barrier and triggers an acute pro-inflammatory response. In 2013, there were 11,300 global deaths from amebiasis, making it the fourth leading cause of parasitic diseases [1]. Manifestations of the disease include amebic colitis and the potential to cause fatality due to liver, lung, or brain abscesses [3]. While there are more cases of

amebiasis in developing countries with poor sanitation and lack of clean water, host factors also contribute to the susceptibility of disease. These factors include host genetics and malnutrition [7,8]. When *Eh* breaches innate host defenses and is sensed by the immune system, an appropriate pro-inflammatory response is triggered to eliminate the parasite, but at the same time it can be damaging to innocent bystander cells. Hence, the inflammatory response is tightly regulated. One of the first cells that *Eh* encounters within the innate immune compartment is resident macrophage, which is highly phagocytic and bactericidal. Macrophages are major producers of IL-1β and TNF-α, the hallmark cytokines in amebiasis known to be important in recruiting immune cells to the site of infection. This response can be protective as IFN-γ and TNF-α act synergistically to activate macrophages to release NO that can kill up to 87% of *Eh in vitro* [74]. This dynamic *Eh*-macrophage interaction is therefore critical for understanding host defence and disease pathogenesis.

Another important determinant of disease outcome are the virulence factors expressed by *Eh*. One of the most well-characterized virulence factor of *Eh* is the Gal-lectin, which is important for mediating attachment to host cells via galactose and *N*-acetyl-galactosamine residues [153,154]. We recently showed that both *Eh*CP-A1 and *Eh*CP-A4 activate caspase-6-dependent cleavage of the cytoskeletal proteins talin, Pyk2 and paxillin in macrophages to trigger downstream inflammatory signaling pathways [33] (**Figure 1.6**).

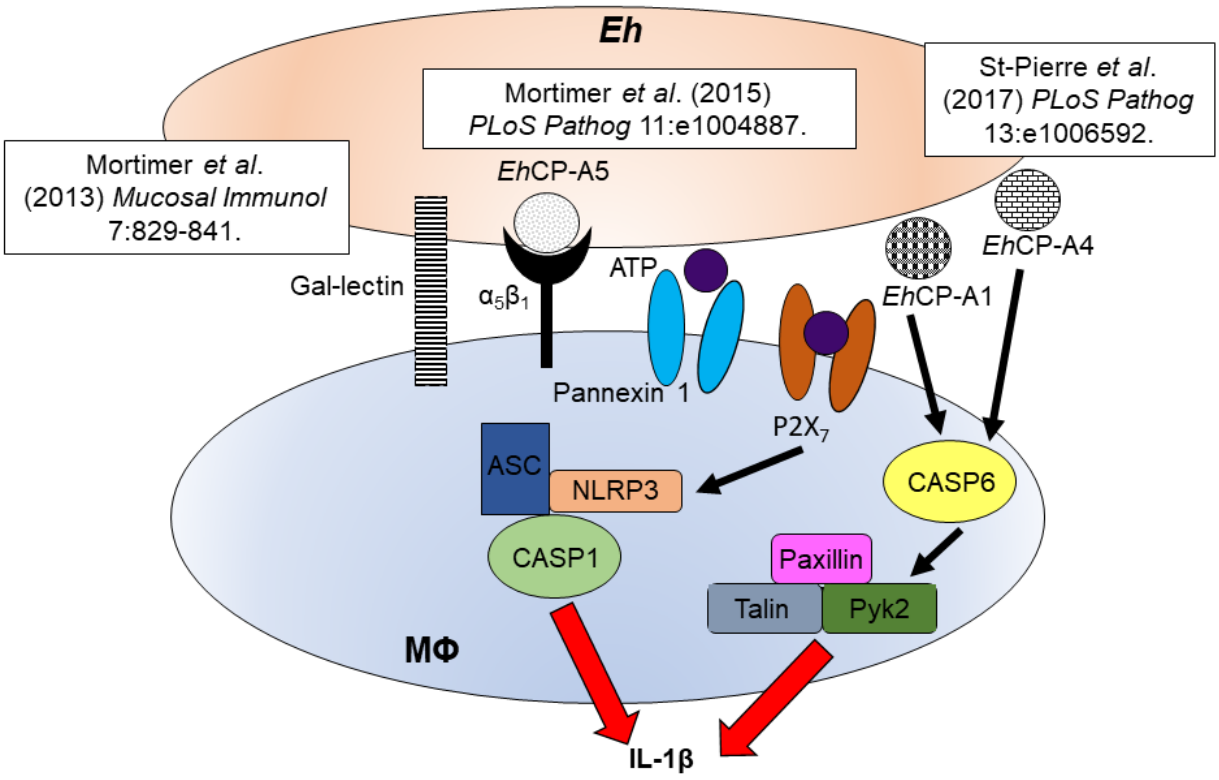

Figure 1.6 *E. histolytica*-macrophage interactions characterized in the Chadee Lab

The *E. histolytica*-macrophage interactions have been characterized to involve several different signaling pathways from the binding of Gal-lectin and the delivery of the *Eh*CP-A5 to ligation of the $\alpha_5\beta_1$ integrin. This is followed by the activation of SRC family kinases and the release of ATP through pannexin 1 channel and subsequent signaling onto the $P2X_7$ receptor. Another pathway, independent of the *Eh*CP-A5 involves *Eh*CP-A1 and *Eh*CP-A4 mediated caspase-6 activation and degradation of cytoskeletal proteins, paxillin, talin, and pyk2.

Innate sensing of *Eh* also occurs through proteins known as inflammasomes, which are intracellular sensors made up of domains including the NLRP3 sensor, ASC adaptor, and caspase-1. When *Eh* contacts macrophages with the Gal-lectin it forms an intercellular bridge allowing *Eh*CP-A5 RGD sequence to bind $\alpha_5\beta_1$ integrin to activate the NLRP3 inflammasome [155,156]. While it is known that caspase-1 activation is important in regulating the secretion of IL-1β and IL-18 [130], the role caspase-4 play to the overall pro-inflammatory response is less characterized. Almost nothing is known to suggest cross talk occur among the caspases or if there are compensatory mechanisms for the loss or dysfunction of a particular caspase. Caspase-4 falls into the category of inflammatory caspases along with others including caspase-5 and caspase-12 strictly in humans, and caspase-11 in mouse [107,157,158]. Caspase-11 is believed to be the ortholog of human caspase-4 because they both share 60% homology and was reported to activate caspase-1 [116,117]. Studying the function of caspase-4 is important because it has been shown to be involved in inflammation by regulating IL-1α, IL-18, IL-8, and MIP-1 secretions and cell death [124,126,159], but the molecular mechanisms that regulate these are largely unknown. Therefore, we wanted to determine the role of caspase-4 in *Eh* infections and how it differs from caspase-1. Interestingly when *Eh* invades tissues there is a raging pro-inflammatory response with augmented IL-1β levels, however, an understanding of the cellular mechanisms that drives this is lacking. It is believed that macrophages have several intracellular sensors to distinguish between threatening and non-threatening stimuli and are able to induce activation of various signalling pathways to respond appropriately. Human inflammatory caspase-4 was found to act as another sensor molecule like the NLRP3 inflammasome to orchestrate pro-inflammatory responses. This

study unravels new concepts on how *Eh*-induced activation of inflammatory caspases in macrophages can converge onto one role to shape the magnitude of the host pro-inflammatory responses in disease pathogenesis. The aim of my research was to investigate the molecular mechanisms by which *Eh* trigger caspase-4 activation and the functional role of caspase-4 in macrophage pro-inflammatory responses.

1.9 Hypothesis

Human caspase-4 and the murine, caspase-11 ortholog, are upstream regulators of inflammasome signalling and activation is required for *Eh*-elicited pro-inflammatory responses in macrophages.

1.10 Specific Aims

Aim 1: To characterize the parasite-host interactions that lead to the activation of caspase-4.

a) To identify the parasite molecules required for the activation of caspase-4.
b) To identify the macrophage cell receptors or molecular mechanisms required for the activation of caspase-4.

Aim 2: To define the role of caspase-4 activation in macrophage inflammatory response to *E. histolytica*.

a) To determine if caspase-4 is required for caspase-1 regulation.

b) To identify caspase-4 binding partners or substrates.

c) To characterize the macrophage cellular responses triggered by caspase-4 activation.

My studies have elucidated that live parasite, resembling that of tissue-invading *Eh*, is sensed by both caspase-4 and -1. The two *Eh* proteins that mediated inflammatory caspase activation were the Gal-lectin adhesin and *Eh*CP-A5, emphasizing the importance of "contact". Caspase-4 was shown to cleave at the CARD domain of caspase-1, resulting in increased IL-1β maturation. Although caspase-4 was not found to interact with inflammasome components including NLRP3 and ASC, it was able to sense similar cellular changes as the NLRP3 inflammasome. Using formaldehyde treatment to cross-link proteins, I have elucidated that both caspase-4 and -1 interacted into a protein complex to enhance IL-1β levels.

Chapter Two: **Materials and Methods**

Jeanie Quach wrote the original draft and reviewed and edited the writing. Kris Chadee reviewed and edited the writing. France Moreau maintained the *E. histolytica* and COS-7 cells and Jeanie Quach maintained the different THP-1 cell lines and mouse cells.

2.1 THP-1 defASC and NLRP3, CASP1, CASP4 CRISPR/Cas9 THP-1 KO cells

THP-1 defASC cells were purchased from Invivogen (thp-dasc). These cells were derived from THP-1 human monocytic cells that do not express ASC, but express native levels of NLRP3 and pro-caspase-1. NLRP3 CRISPR/Cas9 KO THP-1 cells were a gift from D. Muruve (Department of Immunology, University of Calgary, Canada). They used the gRNA TGCAAGCTGGCCAGGTACC**TGG** and GTCATAGCCCCGTAATCAA**CGG**. CASP1 and CASP4 CRISPR/Cas9 KO THP-1 cells were a gift from V. Hornung (Institute of Molecular Medicine, University Hospital, University of Bonn, Germany). They were verified for CASP1 and CASP4 KO prior to performing experiments. V. Hornung's group had used a plasmid encoding a CMV-mCherry-CAS9 expression cassette and a gRNA under the U6 promoter. The CRISPR target sites used were (PAM regions in bold): ATTGACTCCGTTATTCCGAA**AGG** (CASP1), GCTCATCCGAATATGGAGGC**TGG** (CASP4). Cells were maintained in complete RPMI media as described above.

2.1.1 *Cell Preparation and Stimulation*

THP-1 human monocytic cells (ATCC, Manassas, VA) were cultured in RPMI with 10% FBS, 10 mM HEPES, 50 μM 2-mercaptoethanol, 100 U/ml penicillin and 100 μg/ml streptomycin sulfate in a humidified incubator with 5% CO_2. They were passed at $1.5x10^6$ cells/mL for 4 days or $1.5x10^6$ cells/mL for 3 days. Cells were spun down at 300 x g for 5 min at 4°C. THP-1 cells were plated onto 24-well plates at $4x10^5$ cells/well with 50 ng/mL PMA (P1585, Sigma-Aldrich) in complete RPMI 1640 overnight. Cells were stimulated with *Eh*, *Eh*CP-A5$^-$, or *Eh*AP-A$^-$ in 250 μL serum-free RPMI for the indicated times (10, 30 and 60 min). For inhibitor studies, THP-1 cells were pre-treated at 37°C unless otherwise stated with the indicated concentrations of DPI (25–100 μM, 1h pre-treatment, 300260, Calbiochem), and KCl (90–200 mM, 1h pre-treatment, P5405, Sigma-Aldrich) before stimulation with *Eh*. All cells were changed to fresh serum-free RPMI prior to stimulation with *Eh*, LPS from *Escherichia coli* 0111:B4 (L3012, Sigma-Aldrich), nigericin (N7143, Sigma-Aldrich), MSU (Y. Shi, University of Calgary), or ATP (A7699, Sigma-Aldrich). Commonly used reagents for cell culture are listed in **Table 2.1**.

THP-1 macrophages were stimulated with 1:20 *Eh* per well in 250 μL serum-free RPMI for the indicated times. As a control for the silencing technology in *Eh*CP-A5$^-$ we tested a vector control strain that had the same silencing technology as *Eh*CP-A5 designated *Eh*AP-A$^-$.

Table 2.1 Commonly Used Reagents

Reagents	Catalog No., Source
Penicillin & Streptomycin	15140-122, Sigma-Aldrich
Zeocin	ant-zn-1, InvivoGen
Plasmocin	ant-mpt, InvivoGen
Hygrogold B	10687010, Fisher Scientific
RPMI	11875-119, Invitrogen
DPBS	14190-250, Invitrogen
PageRuler™ Prestained Protein Ladder 10X	PI26617, Fisher Scientific
DMEM	12430-062, Invitrogen
HEPES, Free Acid, High Purity	CA97061-824, VWR
Fetal Bovine Serum (FBS)	28310, Sigma-Aldrich
Gibco™ 2-mercaptoethanol	21985-023, Invitrogen

2.2 *E. histolytica* Culture

E. histolytica HM-1:IMSS were grown axenically in TYI-S-3 medium with 100 U/ml penicillin and 100 µg/mL streptomycin sulfate at 37°C in sealed 15 mL borosilicate glass tubes as described previously [160]. To maintain virulence, trophozoites were regularly passed through gerbil livers as described [77]. Ameba were harvested after 72h of growth (log phase) by centrifugation at 200 x g for 5 min at 4°C and suspended in serum-free RPMI prior to stimulating cells. *E. histolytica* cultures deficient in *Eh*CP-A5^{-} and *Eh*AP-A^{-} (vector control) were a gift from D. Mirelman (Weizmann Institute of Science). To irreversibly inhibit cysteine protease activity, *Eh* were cultured overnight in E-64 (100 µM, E3132, Sigma-Aldrich) as described previously [31].

2.3 COS-7 cells

COS-7 cells were a gift from R. Yates (Department of Comparative Biology and Experimental Medicine, University of Calgary, Canada). COS-7 cells were maintained using complete DMEM (10% FBS, 100 U/ml penicillin and 100 µg/ml streptomycin sulfate) in a humidified incubator with 5% CO_2. COS-7 cells were transfected with caspase-4 (100 ng), caspase-1 (10 ng), and IL-1β (1 µg) plasmids [152] using jetPRIME® transfection reagent (114-07, Polyplus) according to the manufacturer's protocol. Plasmid was diluted in jetPRIME® buffer, vortexed for 10 sec, and spun down at 200 x g for 5 min. jetPRIME® reagent was added to the plasmid and was vortexed for 10 sec, spun down at 200 x g for 5 min, and incubated for 10 min at room temperature.

The transfection mix was added to the cells in complete DMEM. The product information for the plasmids are in **Table 2.2.**

Table 2.2 Plasmids

Plasmids	Clone ID	NM	Source
pcDNA3.1(+), Ampicillin, 5431 bp Pro-IL-1β	OHu25334C	NM_000576	GenScript
pcDNA3.1(+), Ampicillin, 5431 bp Pro-Caspase-1	OHu21385C	NM_033292	GenScript
V51 pIRESpuro-GLUE-(pGLUE) Pro-Caspase-4	15100		Addgene

2.4 Nucleofection

Transfection of THP-1 cells was performed using the Nucleofector II® Device (AAD-1001S, Amaxa) according to the manufacturer's protocol with the Nucleofector V Kit (AMA-VCA1003). For each reaction, a ratio of 4.5:1 (82 µL:18 µL) Nucleofector® Solution to supplement is used to make a total reaction volume of 100 µL. 12-well plates were filled with 1 mL of complete RPMI and incubated at 37°C. Briefly, $1x10^6$ cells were counted and centrifuged at 90 x g for 10 min at room temperature. The supernatant was discarded. Next, the cells were resuspended carefully in 100 µL of Nucleofector® Solution and then with 1 µg caspase-4 plasmid. The cell/DNA suspension was transferred into a cuvette and capped on followed by applying the Nucleofector® Program U-001 (THP-1 high viability program). The cuvette was taken out of the device once the program was completed and 500 µL of pre-warmed complete RPMI was added to the cuvette. After gentle resuspension of the cells, it was transferred into the 12-well plate. Then, PMA (50 ng/mL) was added to differentiate the cells overnight prior to experimentation the next day. Cells were replaced with serum-free media and then stimulated with *Eh*.

2.5 Caspase-4 siRNA

Firstly, $4x10^5$ THP-1 cells were plated in an advanced tissue culture 12-well plate (665980, Greiner Bio-One) and differentiated overnight with PMA (50 ng/mL) prior to transfection the next day. Cells were transfected with SMARTpool: SiGENOME caspase-4 siRNA target sequence: GGACUAUAGUGUAGAUGUA (M-004404-01-

0005, Dharmacon), or scrambled siRNA (D-001206-14-05, Dharmacon) as a control, with the INTERFERin reagent (409-10, Polyplus), as per the manufacturer's protocol. siRNA was diluted in Opti-MEM with a total volume of 200 µL and mixed by pipetting up and down. A total of 10 µL of INTERFERin reagent was added to the diluted siRNA and homogenized by vortexing for 10 sec and sat at room temperature for 10 min. During this time, the growth medium was removed from the THP-1 macrophages and fresh pre-warmed 500 µL of complete RPMI was added into each well. The final siRNA concentration in each well was 50 nM for both the caspase-4 and scrambled siRNA. About 6 hours later, an additional 1 mL of complete media was added to each well. Media was replaced with fresh complete RPMI 24h later. *Eh* stimulation was performed 48h following siRNA transfection for 60 min and cells were harvested for western blot and the SEAP assay. Three wells were pooled for each treatment to obtain sufficient protein for western blot.

2.6 Plasmids

The cDNA coding region of caspase-4 alpha isoform (NP_001216.1) was amplified using the following primers, CASP4FNot1: GCCgcggccgcGGCAGAAGGCAACCACAGAA and CASP4RBAM: GCCggatccTCAATTGCCAGGAAAGAGGT. The CASP4 plasmid was generated using the V51 pIRESpuro-GLUE (#15100, Addgene) as the backbone vector [161]. Experiments using the CASP4 plasmid was abbreviated as pC-4.

2.7 Formaldehyde Cross-link and Pull-down Studies

Formaldehyde solution was obtained by dissolving 0.8% paraformaldehyde in PBS for 2h at ~80°C. The solution was filtered (0.22 μm) and stored in the dark at room temperature. THP-1 macrophages and COS-7 cells were stimulated with *Eh* for 20 min. Cells were washed with 1X PBS and spun down at 300 x g at 4°C. Next, 0.8% formaldehyde was added at $1x10^7$ cells/mL for 7 min at room temperature and immediately quenched with ice-cold glycine to a final concentration of 125 mM. Samples were pelleted at 1,800 x g at room temperature for 3 min and the supernatant was discarded. Cells were washed with glycine, transferred to a microtube, and spun down again at 300 x g in 4°C. Next, the cell pellets were lysed in RIPA buffer at $1x10^8$ cells/mL, along with the aid of a dounce homogenizer. Lysates were spun for 15 min at 18,000 x g at 4°C to remove insoluble debris. Caspase-4 or caspase-1 primary antibody was added at 1 μg and placed on a shaker in 4°C for 3h. Several different caspase-4 antibodies were screened for use including: anti-caspase-4 (M029-3, MBL International Corporation), anti-caspase-4 (NBP1-76602, Novus Biologicals), and anti-caspase-4 (#4450, Cell Signaling). The anti-caspase-4 (M029-3) was used for formaldehyde cross-linking studies. Several different caspase-1 antibodies were screened for use including: anti-caspase-1 (sc-2225, Santa Cruz), anti-caspase-1 (sc-56036, Santa Cruz), and anti-caspase-1 p20 (Bally-1, Adipogen). The anti-caspase-1 (sc-56036) was used for formaldehyde cross-linking studies. About 30 μL of protein A/G PLUS-agarose beads (sc-2003, Santa Cruz) were added overnight on a shaker in 4°C overnight. The next day, the beads were spun down at 300 x g at 4°C and washed 3 times with RIPA buffer and 10

times with Tris, NaCl, EDTA solution. The beads were then incubated with 50 µL of 1.5X sample buffer at 65°C for 5 min. Samples were run on SDS-PAGE and probed with antibodies or stained with Coomassie Blue.

2.8 Immunoblot

2.8.1 *Protein Extraction*

THP-1 macrophage cell supernatants from 4 wells were pooled and centrifuged at 2,000 x g for 5 min at 4°C. Pelleted debris was discarded and supernatants were concentrated by TCA precipitation. For cell lysates, plates were washed in cold 1X PBS before lysis buffer (100 mM NaCl, 20 mM Tris (pH 8), 0.1% SDS, 0.5% Triton X-100, 5 mM EDTA, 6.8X PMSF, 0.1mM E-64, 1 µg/L leupeptin, 1 µg/L aprotonin, and 0.02% protease inhibitor cocktail (Sigma-Aldrich)) was added and centrifuged at 14,000 x g for 15 mins at 4°C.

2.8.2 *Trichloroacetic Acid Precipitation of Cell Supernatant*

After cell supernatant has been centrifuged, 10% volume of 1% deoxycholic acid (Sigma-Aldrich, D2510) was added to supernatants. Then, 10% volume of 77% trichloroacetic acid (TCA, Fisher Scientific, SA433-500) was also added to supernatants. Each tube was inverted once and then incubated on ice for 30 mins. Following that, tubes were spun at 14,000 x g for 15 min at 4°C. The supernatant was discarded and the remaining pellet was washed with 400 µL of ice-cold acetone. Tubes were spun down at 14,000 × g for 2

mins at 4°C and the acetone was removed and discarded. Pellets were resuspended in 40 µL Laemmli buffer (25 mM Tris pH8 and 3µL NaOH) until well-dissolved. Samples were prepared with 10 µL 5X sample buffer and boiled for 5 mins for SDS-page gel. Equal volumes were resolved on 12% polyacrylamide gels.

2.8.3 *Protein Quantifications*

Protein concentrations were determined using the bicinchoninic acid (BCA) protein assay, using bovine serum albumin as a standard (Thermo Scientific, Catalog No. CAPI23225). Samples were diluted 1:5 in double distilled water (ddH2O) and 10 µL from each diluted sample was loaded in triplicate to a 96-well plate. A standard curve was prepared using a known concentration of the protein bovine serum albumin (BSA) with a serial dilution (0-2000 pg/mL), and loading 10 µL from each dilution in duplicate to the 96-well plate. Then, 200 µL of 1:50 (Reagent A: Reagent B) solution was added to each well and incubated for 30 min at 37°C. The absorbance was measured at 595 nm on a plate reader. About 30 µg of protein was prepared for lysates to run an SDS-PAGE.

2.8.4 *Gel Electrophoresis and Membrane Transfer*

Equal amounts of proteins were boiled for 5 mins in Laemmli buffer and were resolved on 10% (for Caspase-4) or 12% (for Caspase-1 and IL-1β) polyacrylamide gels and transferred to 0.22 µM nitrocellulose membranes (Fisher Scientific, Catalog No. WP2HY00010) using transfer buffer for about 1 h 20 mins. Ponceau S (Fisher Scientific,

Catalog No. BP10310) was added to membranes to visualize presence of proteins, followed by 3X ddH_2O washes.

2.8.5 *Blocking, Antibody Staining, and Detection*

Membranes were blocked in 5% skim milk, incubated overnight at 4°C in primary antibodies and visualized with secondary HRP-conjugated antibodies (**Table 2.3**). Supernatants were detected with SuperSignal West Femto Chemiluminescence Reagents (Pierce, Catalog No. CAPI34096), Clarity Max™ Western ECL Substrate (Biorad, Catalog No. 1705062) and lysates with Immobilon Western Chemiluminescent HRP Substrate (EMD Millipore, Catalog No. WBKLS0500).

Table 2.3 Primary and Secondary Antibodies

Antibody	Protein	Specificity	Dilution	Catalog No., Source
Primary	Caspase-1	Human	1:1000	sc-622, Santa Cruz
Primary	Caspase-1	Human	1:1000	Bally-1, Adipogen
Primary	Caspase-4	Human	1:1000	M-029-3, MBL International
Primary	Caspase-4	Human	1:1000	17D9, Novus Biologicals
Primary	Caspase-4	Human	1:1000	#4450, Cell Signaling
Primary	IL-1β	Human	1:1000	sc-7884, Santa Cruz
Primary	Caspase-1	Human	1:1000	sc-56036, Santa Cruz
Primary	NLRP3	Human, Mouse	1:1000	AG-20B-0014, Adipogen
Primary	ASC		1:1000	30153, Santa Cruz
Primary	IL-1β	Mouse	1:1000	AF-401, R&D
Primary	Caspase-11	Mouse	1:1000	17D9, Novus Biologicals
Primary	Caspase-1 p20	Human	1:1000	Casper 1, Adipogen
Secondary	GAPDH	Human	1:10000	CB1001, Millipore
Secondary	Anti-mouse IgG HRP	Goat	1:10000	115-035-146, Jackson Immunoresearch
Secondary	Anti-rabbit IgG HRP	Goat	1:10000	111-035-144, Jackson Immunoresearch
Secondary	Anti-goat IgG-HRP	Donkey	1:10000	705-035-147, Jackson Immunoresearch

2.8.6 *ChemiDoc and ImageLab Analysis*

Bioflex Blue Lite EC Films (Mandel, MED-CLEC810) and an image processor were used to visualize the majority of blots, however, for some blots the ChemiDoc™ Imaging System (Biorad, #17001401) was used as well. ImageLab Software Version 6.0 was used for western blot analysis and to measure densitometric values from 3 independent experiments. Results were reported as mean ± SEM.

2.9 IL-1β Assay in HEK-Blue™ Reporter cells

HEK-Blue™ IL1β cells were a gift from R. Yates (Department of Comparative Biology and Experimental Medicine, University of Calgary, Canada). HEK-Blue™ IL1β cells were cultured in complete DMEM containing 10% FBS, 100 U/ml penicillin and 100 µg/ml streptomycin sulfate, 2.5 µg/mL plasmocin, 0.1 mg/mL zeocin, and 0.1 mg/mL hygrogold in a humidified incubator with 5% CO2. They were passed two times a week to confluency. HEK-Blue™ IL1β cells specifically respond to bioactive IL-1β. Once IL-1β binds to its receptor, IL-1R on the surface of HEK-Blue™ IL-1β cells, this triggers a signalling cascade leading to the activation NF-κB and the subsequent production of secreted embryonic alkaline phosphatase (SEAP).

Following stimulation of THP-1 macrophages, supernatants were kept on ice for immediate processing or frozen at -80°C. In the morning, HEK-Blue™ IL1β cells were plated in a 96-well plate at $4x10^5$ cells/mL with a total of 150 µL in each well. Next, 50

µL of supernatants from THP-1 macrophages were added undiluted into each well containing HEK-Blue™ IL1β cells overnight at 37°C in an incubator with 5% CO_2. A standard curve using recombinant human IL-1β (200-01B, Peprotech) was made with serial dilutions (100 ng/µL to 0.01 ng/µL). A total of three replicates were performed for each treatment condition. The following day, 50 µL of supernatant was transferred into a black 96-well plate. Then 150 µL of the QUANTI-Blue™ (rep-qb1, Invivogen) was added into each well. The QUANTI-Blue™ is initially a pink colour and eventually turns into blue over time, indicative of SEAP levels. The intensity of the colour reaction is proportional to the amount of IL-1β in the supernatant from stimulated THP-1 macrophages. The plate was incubated at 37°C for 90 min and the SEAP levels were determined using a spectrophotometer at 655 nm.

2.10 Human IL-1β ELISA

THP-1 macrophages were stimulated with *Eh* and the supernatants were centrifuged to remove cellular components. The supernatants were frozen at -80°C or used fresh for enzyme-linked immunosorbent assay (ELISA, DY201, R&D) as per the manufacturer's protocol.

Plate Preparation

The Capture Antibody was diluted to the working concentration in DPBS and 100 µL was added into each well of a 96-well ELISA plate. The plate was sealed with an adhesive strip and incubated overnight at room temperature. The next day, the wells were

aspirated and washed with 400 µL of Wash Buffer for 3X by inverting the plate and blotting it against clean paper towels. The plate was then blocked by adding 300 µL Reagent Diluent (Blocking Buffer) to each well and incubated at room temperature for 1h. Next, the plates were washed with 400 µL of Wash Buffer for 3X.

Assay Procedure

100 µL of sample or standards were diluted in Reagent Diluent and added to each well. The plate was sealed with an adhesive strip and incubated for 2h at room temperature. Next, the plate was washed with 400 µL of Wash Buffer for 3X. Then, 100 µL of the Detection Antibody, diluted in Reagent Diluent, was added to each well. The plate was incubated for another 2h at room temperature. Next, the plate was washed with 400 µL of Wash Buffer for 3X. 100 µL of the working dilution of Streptavidin-HRP was added to each well and the plate was covered with an aluminum foil and incubated for 20 mins at room temperature. The samples were aspirated and the plate was washed with 400 µL Wash Buffer for 3X. 100 µL of Substrate Solution was added to each well and the plate was covered with aluminum foil, and incubated for 20 mins at room temperature. For the final step, 50 µL of Stop Solution was added to each well and the plate was gently tapped to ensure thorough mixing. The color changed from blue to yellow, indicative of IL-1β levels. Using a microplate reader (Bio-Rad iMark^{TM} Microplate Reader), a reading was obtained at 450 nm and 595 nm, and the 595 nm reading was subtracted from the 450 nm reading.

2.11 Human Focused 13-Plex Cytokine/Chemokine Array

Cell supernatants of *Eh*-stimulated THP-1 macrophages were also analyzed for the presence of other cytokines and chemokines. The cell supernatants were centrifuged at at 2,000 x g for 5 min 4°C. The supernatant was removed and sent for the luminex human focused 13-plex-discovery assay performed by Eve Technologies (Calgary, AB) that examined the following cytokines/chemokines: GM-CSF, IFN-γ, IL-1β, IL-2, IL-4, IL-6, IL-8, IL-10, IL-12, MCP-1, TNF-α, IL-13, IL-5.

2.12 Lactate Dehydrogenase Assay

LDH levels were measured using the Promega™ CytoTox-ONE homogeneous membrane integrity assay (G7890, Fisher Scientific) as per the manufacturer's protocol. Cell supernatants of stimulated THP-1 macrophages were centrifuged at 2,000 x g for 5 min at 4°C to remove cellular debris. 25 µL of supernatant of each treatment was added into a 96-well black plate in triplicates. This was incubated at room temperature for 30 mins. Then 25 µL of CytoTox-ONE™ Reagent was added into each well for 10 min at room temperature. Next, 12.5 µL of Stop Solution was added to each well to stop the reaction. The plate was set to shake for 10 secs prior to recording the fluorescence at an excitation wavelength of 550 nm and an emission wavelength of 595 nm. The provided Lysis Solution was added to generate a Maximum LDH Release Control, with 2 µl of Lysis Solution added per 100 µl original volume to the positive control wells. Serum-free RPMI media alone was the background reading. Relative LDH release was calculated using the equation: LDH (% release) = % of ((LDH released from stimulation-

background) /(maximum LDH released-background)). The LDH (% release from control) was calculated using the LDH (% release) of unstimulated cells subtracted from stimulated cells.

2.13 Animals

Male C57BL/6 mice 8-10 weeks old were from purchased from Charles River. *Casp1*$^{-/-}$ *Casp11*$^{-/-}$ mice, bred onto a C57BL/6 background, were obtained from Dr. Yan Shi (Department of Immunology, University of Calgary). *Nlrp3*$^{-/-}$ and *Asc*$^{-/-}$ mice bred onto a C57BL/6 background, were obtained from Dr. Dan Muruve (Department of Immunology, University of Calgary). *Casp11*$^{-/-}$ femurs and tibia were obtained from Dr. Bruce Vallance (Department of Pediatrics, University of British Columbia). The legs were removed from mice and femurs and tibia were used for the growth of bone-marrow-derived macrophages (BMDM). The bones were placed into a new Petri dish containing 70% ethanol for 3 min to sterilize. Then, they were placed into a new Petri dish with complete RPMI. The tips of the bones on both sides were cut and using a 27 ½ G needle, the bones were flushed with complete RPMI through a 100 µM cell strainer. The remaining cells were broken within the strainer using the pipette tip. The cells were spun down at 600 x g for 5 min at 4°C. Then, the cells were resuspended in 20 mL complete RPMI and counted. BMDMs were cultured and incubated for 6 days in complete RPMI supplemented with 30% L929-cell supernatant. Cells have become attached and confluent by day 6 and were removed by incubating in 1:1 Versene/TrypLE media for 10 min at 37°C, scraping, and then resuspended in complete RPMI. Cells were spun down

for 300 x g for 5 min at 4°C and resuspended in complete RPMI and plated at $5x10^5$ cells per well in 24-well plates. On the day of experiment, BMDM were treated with 1 μg/ml LPS for 3.5 hours prior to stimulation with *Eh* to act as the priming signal.

2.13.1 *L929 Cell Media Preparation*

L929 cells were thawed and then left to grow to confluency for around 7 days in 55 mL of complete RPMI. On day 7, media was spun down at 300 x g to remove cellular debris. Media was removed carefully and kept in a sterile container at 4°C until after several passages of L929 cells to pool media together. The entire batch of media was filter sterilized and aliquoted into 50 mL tubes and stored at -80°C. To count cells, they were first washed with DPBS and trypsinized (1 mL) for 5 min at 37°C to allow for cells to detach and then complete RPMI was added to neutralize the trypsin.

2.14 Mass Spectrometry

The protocol for preparing cells for mass spectrometry is the same as the formaldehyde cross-linking protocol. Stimulated cells were lysed in RIPA buffer and lysates were spun for at 18,000 x g for 15 min at 4°C to remove insoluble debris. The caspase-4 M-029-3 antibody was added for 1h (1 μg) on a shaker at 4°C. Protein A/G beads were washed in in RIPA buffer 2X and 30 μL of beads was added into each tube of sample overnight. The next day, beads were spun down and washed 3X with RIPA buffer. Then, they were washed 1X with Tris, NaCl, EDTA solution. The beads were resuspended in a final volume of 20 μL of Tris, NaCl, EDTA solution. The beads were analyzed by liquid

chromatography-mass spectrometry (LC-MS/MS) at the SAMS Centre by Laurent Brechenmacher at the Cumming School of Medicine. The contaminants were removed from our final analysis based on previously reported common contaminants [162]. Laurent Brechenmacher provided the protocol for mass spectrometry.

LC–MS/MS Analysis

Tryptic peptides were analyzed on an Orbitrap Fusion Lumos Tribrid mass spectrometer (Thermo Scientific) operated with Xcalibur (version 4.0.21.10) and coupled to a Thermo Scientific Easy-nLC (nanoflow Liquid Chromatography) 1200 system. Tryptic peptides (2 µL) were loaded directly onto an Easy Spray Column (ES803; Thermo Scientific) at a maximum of 700 bars (2µm particle column). Peptides were eluted using a 45 min gradient from 5 to 40% (5% to 28% in 40 min followed by an increase to 40% B in 5min) of solvent B (0.1% formic acid in 80% LC-MS grade acetonitrile) at a flow rate of 0.3 µL/min and separated on a C18 analytical column (ES803). Solvent A was composed of 0.1% formic acid and 3% acetonitrile in LC-MS grade water. Peptides were then electrosprayed using 2.0 kV voltage into the ion transfer tube (300°C) of the Orbitrap Lumos operating in positive mode. The Orbitrap first performed a full MS scan at a resolution of 120000 FWHM to detect the precursor ion having a *m*/*z*between 375 and 1575 and a +2 to +7 charge. The Orbitrap AGC (Auto Gain control) and the maximum injection time were set at 4e5 and 50 ms, respectively. The Orbitrap was operated using the top speed mode with a 3 sec cycle time for precursor selection. The most intense precursor ions presenting a peptidic isotopic profile and having an intensity threshold of at least 5000 were isolated using the quadrupole and fragmented with HCD (30%

collision energy) in the ion routing multipole. The fragment ions (MS^2) were analyzed in the ion trap at a rapid scan rate. For the ion trap, the AGC and the maximum injection time were set at 1e4 and 35 ms, respectively. Dynamic exclusion was enabled for 30 sec to avoid acquisition of same precursor ion having a similar m/z (plus or minus 10 ppm).

Database search

The Lumos raw data files (*.raw) were converted into Mascot Generic Format (MGF) using RawConverter (v1.1.0.18; The Scripps Research Institute) operating in a data dependent mode. Monoisotopic precursors having a charge state of +2 to +7 were selected for conversion. This mgf file was used to search an Homo sapiens database (NCBI; 99739 entries) using Mascot algorithm (Matrix Sciences; version 2.4). Search parameters for MS data included trypsin as enzyme, a maximum number of missed cleavage of 1, a peptide charge equal to 2 or higher, cysteine carbamidomethylation as fixed modification, methionine oxidation as variable modification and a mass error tolerance of 10 ppm. A mass error tolerance of 0.6 Da was selected for the fragment ions. Only peptides identified with a score having a confidence higher than 95% were kept for further analysis. The Mascot dat files were imported into Scaffold (v4.3.4, Proteome Software Inc) for comparison of different samples based on their mass spectral counting. Scaffold (version Scaffold_4.8.4, Proteome Software Inc., Portland, OR) was used to validate MS/MS based peptide and protein identifications. Peptide identifications were accepted if they could be established at greater than 95.0% probability by the Peptide Prophet algorithm [163] with Scaffold delta-mass correction. Protein identifications were accepted if they could be established at greater than 95.0%

probability and contained at least 1 identified peptide. Protein probabilities were assigned by the Protein Prophet algorithm [164]. Proteins that contained similar peptides and could not be differentiated based on MS/MS analysis alone were grouped to satisfy the principles of parsimony.

2.15 Ethics Statement

The Health Sciences Animal Care Committee from the University of Calgary, have examined the animal care and treatment protocol (AC14-0219) and approved the experimental procedures proposed and certifies with the applicant that the care and treatment of animals used was in accordance with the principles outlined in the most recent policies on the "Guide to the Care and Use of Experimental Animals" by The Canadian Council on Animal Care.

2.16 Statistics

All experiments shown are representative of three independent experiments unless otherwise indicated. GraphPad Prism 5 (Graph-Pad Software, San Diego, CA) was used for statistical analysis. Treatment groups were compared using the paired Student's *t*-test or analysis of variance (ANOVA) with a Bonferroni post-hoc test. Statistical significance was assumed at $p<0.05$. Results are displayed as mean +/- standard error of the mean (SEM).

2.17 Acknowledgments

We thank Y. Shi for the MSU, *Casp1/11*$^{-/-}$ mice, D. Muruve for the NLRP3 CRISPR KO cells, *Nlrp3*$^{-/-}$ and *Asc*$^{-/-}$ mice, V. Hornung for the CASP1 and CASP4 CRISPR KO cells, and R. Yates for the HEK-Blue™ IL-1β cells and COS-7 cells.

Jeanie Quach did the conceptualization, data curation, formal analysis, project administration, writing of the original draft and reviewed and edited the writing. France Moreau did the data curation, investigation, methodology, project administration, and provided the resources. Kris Chadee did the conceptualization, acquired funding, project administration, provided the resources and reviewed and edited the writing. Christina Sandall generated the NLRP3 CRISPR/Cas9 KO THP-1 cells. Contributions to specific experiments are indicated in the figure legends.

Human Caspase-4 Studies

3.1 *E. histolytica* induces the activation and secretion of caspase-4

We have recently shown that direct interaction between *Eh* and macrophages via the Gal-lectin and coupling of *Eh*CP-A5 RGD motif to $\alpha_5\beta_1$ integrin activates caspase-1 that subsequently cleaves pro-IL-1β into its active form [155,156]. As other inflammatory caspases are activated upon *Eh* contact [33] that can potentially regulate inflammasome activation and IL-1β, in this study we determined the kinetics of *Eh*-induced caspase-4 and -1 in human THP-1 macrophages. As predicted, *Eh* activated caspase-4 (by the appearance of the intermediate forms) in a dose- and time-dependent manner with 1:20 *Eh* to macrophage ratio being the sub-optimal dosage (**Figure 3.1A** and **3.1C**). For comparison, caspase-1 activation as indicated by the cleavage of the N-terminal CARD protein (p10 and p11 doublet bands) that reflects processing and activation is shown for

all studies (highlighted). Similarly, cleaved IL-1β (17 kDa) protein was also immunoblotted to demonstrate conversion to bioactive protein (highlighted). In control macrophages (-ve) basal levels of caspase-1 remained in its inactive form, however following *Eh* stimulation it was recruited into a complex that cleaved the N-terminal CARD domain, which resulted in the formation of a heterodimer of p10 and p20 subunits. *Eh* activated caspase-4 as indicated by the 43 kDa and 32-36 kDa triplet bands (**Figure 3.1A** and **3.1C**) in both the supernatants (SN) and the lysates (LYS). We originally thought that the appearance of a band around 20 kDa would be the large subunit of caspase-4 or a band of 10 kDa for the small subunit, but these did not appear consistently with the caspase-4 M029-3 antibody. Therefore, the intermediate forms were used as the main indicators of activation. The original blots of a select few experiments are shown in the Appendix. Bioactive IL-1β levels increased dose-dependently with an increase in *Eh* to macrophage ratio, as detected using HEK-Blue™ IL-1β reporter cells and the measurement of secreted embryonic alkaline phosphatase (SEAP) production (**Figure 3.1B)**. Interestingly, intracellular caspase-4 was activated as early as 10 min; however, secretion did not appear until 30 min, indicating that activation and secretion are two distinct events possibly regulated by different signals (**Figure 3.1C**). This suggested that between 10 to 30 min, caspase-4 was cleaved from its inactive form, performed its function, either acting on substrates and/or interacting with other proteins and was then immediately secreted outside. The caspase-4 active intermediate forms accumulated in the supernatants over 60 min. Only the secretions indicated an obvious difference among the treatment conditions, whereas the lysates displayed minimal differences. Hence, the majority of conclusions are based on the secretions of caspases.

Bioactive IL-1β levels increased time-dependently, showing robust levels at 60 min (p<0.001) with *Eh* stimulation, indicating that the caspases are activated first prior to IL-1β release (**Figure 3.1D**). The release of both inflammatory caspases and IL-1β were due to active secretion as lactate dehydrogenase (LDH) assays as early as 10 min showed less than 1% cell death (**Figure 3.1E**). Even with prolonged exposure to *Eh* up to 60 min, there was only 5% cell death compared to LPS and nigericin (LN) stimulation that resulted in significant cell death compared to controls (70%, p<0.001). As a positive control for these studies we used the well-described agonist for NLRP3 inflammasome activation, monosodium urate crystals (MSU). MSU is readily taken up by macrophages via phagocytosis that subsequently causes lysosomal damage and rupture [140], and via the non-canonical pathway requiring caspase-4 to activate caspase-1 and to secrete IL-1β and IL-18 [121]. As IL-1β in the immunoblots (**Figure 3.1A** and **3.1C**) was an excellent indicator of IL-1β release, the SEAP assay was not performed in subsequent studies involving characterizing of the parasite and host factors. These results show that both caspase-4 and -1 are activated simultaneously and are actively secreted upon *Eh* stimulation.

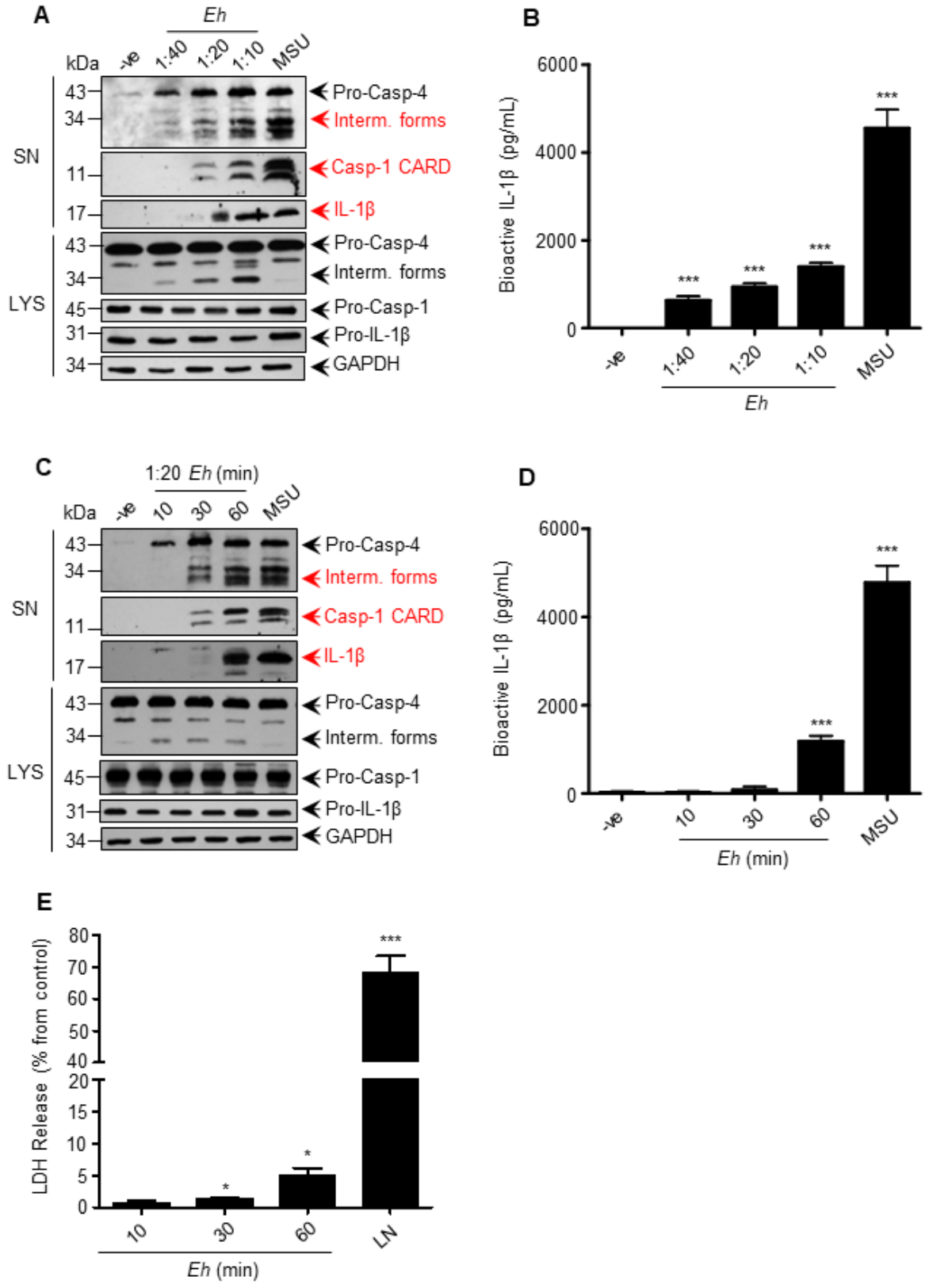
A
Eh
kDa
-ve
1:40
1:20
1:10
MSU
SN
LYS
43
34
11
17
45
31
Pro-Casp-4
Interm. forms
Casp-1 CARD
IL-1β
Pro-Casp-1
Pro-IL-1β
GAPDH
B
Bioactive IL-1β (pg/mL)
6000
4000
2000
0
***
Eh
C
1:20 Eh (min)
10
30
60
D
Eh (min)
E
LDH Release (% from control)
80
70
60
50
40
20
15
10
5
0
*
LN

Figure 3.1 *E. histolytica* activates caspase-4 and -1 in a dose and time-dependently manner.

THP-1 macrophages were incubated with (A, B) increasing ratios of *Eh* for 60 min and monosodium urate crystals (MSU) were added at 300 μg/mL for 6h as a positive control. Cells only were used as an internal control. Cell supernatant was TCA precipitated and cells were washed and lysed. Equal amounts of lysates were loaded onto SDS-PAGE gel and immunoblotted with the indicated antibodies. (B) Cell supernatant was added to HEK-Blue™ IL-1β reporter cells to detect bioactive IL-1β using the SEAP assay. (C-E) THP-1 macrophages were incubated for increasing amounts of time with 1:20 *Eh* to macrophage ratio. Immunoblot analysis was performed for caspase-4, caspase-1, IL-1β in both the supernatants (SN) and lysates (LYS), and blots were reprobed for GAPDH. (D) Cell supernatant was added to HEK-Blue™ IL-1β reporter cells to detect bioactive IL-1β using the SEAP assay. (E) Cell death was measured by lactate dehydrogenase (LDH) release into the culture supernatant and is shown as a percentage of LDH release from non-stimulated cells (control). LN is LPS (50 ng/mL) and nigericin (10 μM) stimulation for 60 min. Data are representative of three independent experiments and statistical significance was calculated with one-way analysis of variance (ANOVA) with a Bonferroni post-hoc test (*p<0.05, ***p<0.001). Bars represent ± SEM. Jeanie Quach performed the experiment from cell harvesting, SDS-PAGE, imaging, and data analysis.

3.2 Caspase-4 activation requires live *Eh*, contact with macrophage via the Gal-lectin and *Eh*CP-A5 and involves cellular perturbations

Eh is unique in that it is an extracellular parasite that requires Gal-lectin mediated contact with host cells to activate inflammatory signaling proteins to elicit cellular cytotoxicity [33,156]. Similarly, we also found that live *Eh* was critical for activating both caspase-4 and -1 in macrophages. Neither highly concentrated secreted protein from *Eh*, equivalent amounts of whole *Eh* lysates, cytoplasmic components or membrane components were able to activate the inflammatory caspases (**Figure 3.2A**). To determine the requirements for *Eh*-macrophage contact, 55 mM exogenous galactose was used to competitively block *Eh* from binding via Gal or GalNAc residues on the macrophage surface. Galactose treatment completely inhibited caspase-4 activation and secretion as compared to glucose, the osmotic control, which was the same as *Eh* treatment alone (**Figure 3.2B**). IL-1β secretion also corresponded to caspase-1 activation where there was complete abrogation with galactose treatment. These results support the notion that inflammatory caspase activation is tightly regulated and only while sensing live *Eh* does the host see it as a danger signal that requires immediate attention. Among *Eh* virulent factors, cysteine proteases have been shown to play major roles in *Eh* pathogenesis [36]. *Eh*CP-A5 is a major protease that is membrane-bound and secreted by *Eh*, which is involved in cleaving the N-terminus of MUC2 mucin to dissolve the protective mucus barrier [30,57]. To determine if *Eh*CP-A5 played a role in caspase-4 activation, *Eh* was incubated overnight with the irreversible cysteine protease inhibitor, E-64 and there was no difference in both caspase-4 and -1 activation and IL-1β protein secretion (**Figure 3.2C**). Complete

inhibition was seen with *Eh*CP-A5^{-} with no detectable caspase-4 activation and secretion compared to parasites carrying the empty vector *Eh*AP-A^{-}. These results show that both *Eh*CP-A5 and its enzymatic activity are important for activating caspase-4.

Since the triggers that result in caspase-1 activation were reported previously to involve K^+ efflux and ROS production [155], we were curious to know whether the same phenomenon occurred during the activation of caspase-4. Predictably, using increasing concentrations of K^+ added to macrophages for 1h prior to *Eh* stimulation to block K^+ efflux led to a dose-dependent inhibition of caspase-4 and -1 activation and IL-1β release (**Figure 3.2D**). Furthermore, using increasing concentrations of diphenyleneiodonium chloride (DPI) dose-dependently inhibited caspase-4 and -1 activation and IL-1β release indicating that ROS is also a cellular event that triggers caspase activation (**Figure 3.2E**). These results indicate that cellular stresses converge both to trigger caspase-4 and -1 activation, which suggests that they are upstream of the pathway.

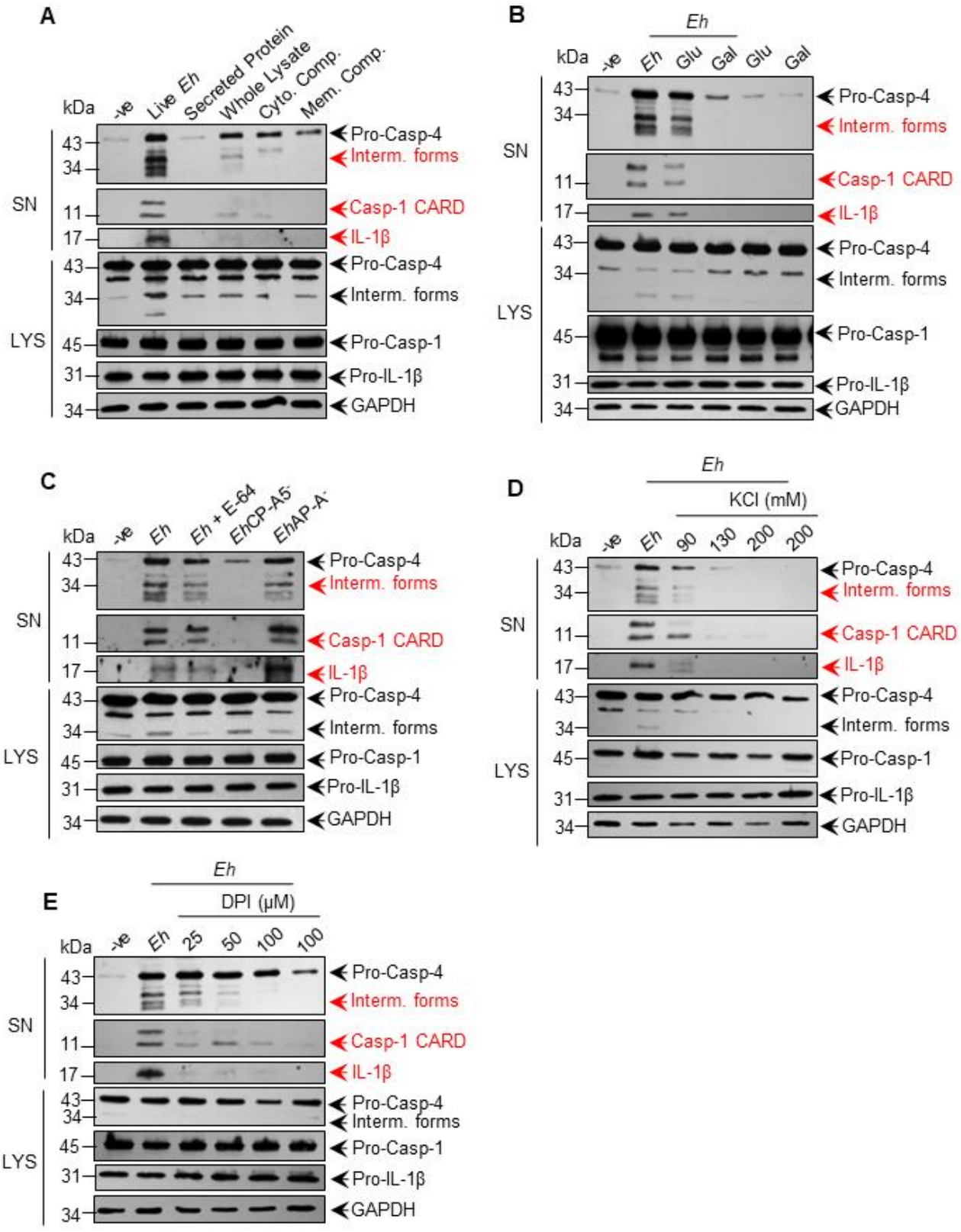
A
kDa
-ve
Live Eh
Secreted Protein
Whole Lysate
Cyto. Comp.
Mem. Comp.
SN
LYS
43
34
11
17
45
31
Pro-Casp-4
Interm. forms
Casp-1 CARD
IL-1β
Pro-Casp-1
Pro-IL-1β
GAPDH
B
Eh
kDa
-ve
Eh
Glu
Gal
Glu
Gal
C
Eh + E-64
EhCP-A5
EhAP-A
D
Eh
KCl (mM)
90
130
200
200
E
Eh
DPI (μM)
25
50
100
100

Figure 3.2 *E. histolytica*-induced caspase-4 activation parallels caspase-1 requiring live parasite and contact via Gal-lectin and EhCP-A5 and involves cellular perturbations.

THP-1 macrophages were incubated with (A) different preparations of *Eh* including live *Eh*, whole lysates, or with membrane or cytoplasmic fractions of equal amounts of *Eh* for 60 min. (B) THP-1 macrophages were pretreated for 5 min with 55 mM D-galactose (Gal), or glucose (Glu) as an osmotic control prior to incubation with *Eh* for 60 min at a 1:20 ratio (optimal dosage from Fig 1A). (C) THP-1 macrophages were incubated with *Eh*, E-64 treated *Eh*, *Eh*CP-A5^{-} and *Eh*AP-A^{-} (1:20) for 60 min. THP-1 macrophages were pre-treated with exogenous (D) potassium chloride (KCl) or (E) diphenyleneiodonium chloride (DPI) for 1h prior to stimulation with *Eh* for 60 min. Cell supernatant was TCA precipitated and cells were washed and lysed. Equal amounts of lysates were loaded onto SDS-PAGE gel and immunoblotted with the indicated antibodies. Immunoblot analysis was performed for caspase-4, caspase-1, IL-1β in both the supernatants (SN) and lysates (LYS), and blots were reprobed for GAPDH. Western blots are representative of three independent experiments. Jeanie Quach performed the experiment from cell harvesting, SDS-PAGE, imaging, and data analysis.

3.3 *E. histolytica*-induced caspase-4 activation is independent of NLRP3 and ASC

Caspase-1 is well studied with regard to its mechanisms of activation requiring NLRP3 and ASC recruitment into a complex for its activation. To determine if the NLRP3 inflammasome complex was required for caspase-4 activation, NLRP3 CRISPR/Cas9 KO THP-1 macrophages and WT controls were treated with *Eh* for 10-60 min and caspase-4 activation was quantified by densitometric analysis. The intermediate forms of caspase-4 was used for densitometric analysis and unlike the lysates which have GAPDH as a housekeeping control, there was no control available for the supernatants. The densitometry of the treatments was compared to cells only as the control. Caspase-4 activation in NLRP3 KO cells was unaffected (**Figure 3.3A** and **3.3B**). Not surprising, MSU required both NLRP3 and ASC for its activation and hence, there was less caspase-1 and IL-1β secretion. IL-1β protein levels were absent in the NLRP3 CRISPR/Cas9 KO compared to WT THP-1 macrophages, supporting the notion that the NLRP3 inflammasome is the central inflammasome activated by *Eh*. Caspase-4 levels were similar in THP-1 defASC macrophages when treated with *Eh* for 10-60 min (**Figure 3.3C** and **3.3D**). THP-1 defASC macrophages displayed less caspase-1 CARD and IL-1β secretion, supporting the requirement of the ASC adaptor to be recruited to a molecular complex, along with NLRP3 for activating caspase-1. In the immunoblot for ASC, there was still the presence of ASC detected in the THP-1 defASC macrophages, indicating that the gene is silenced and it is not a complete KO.

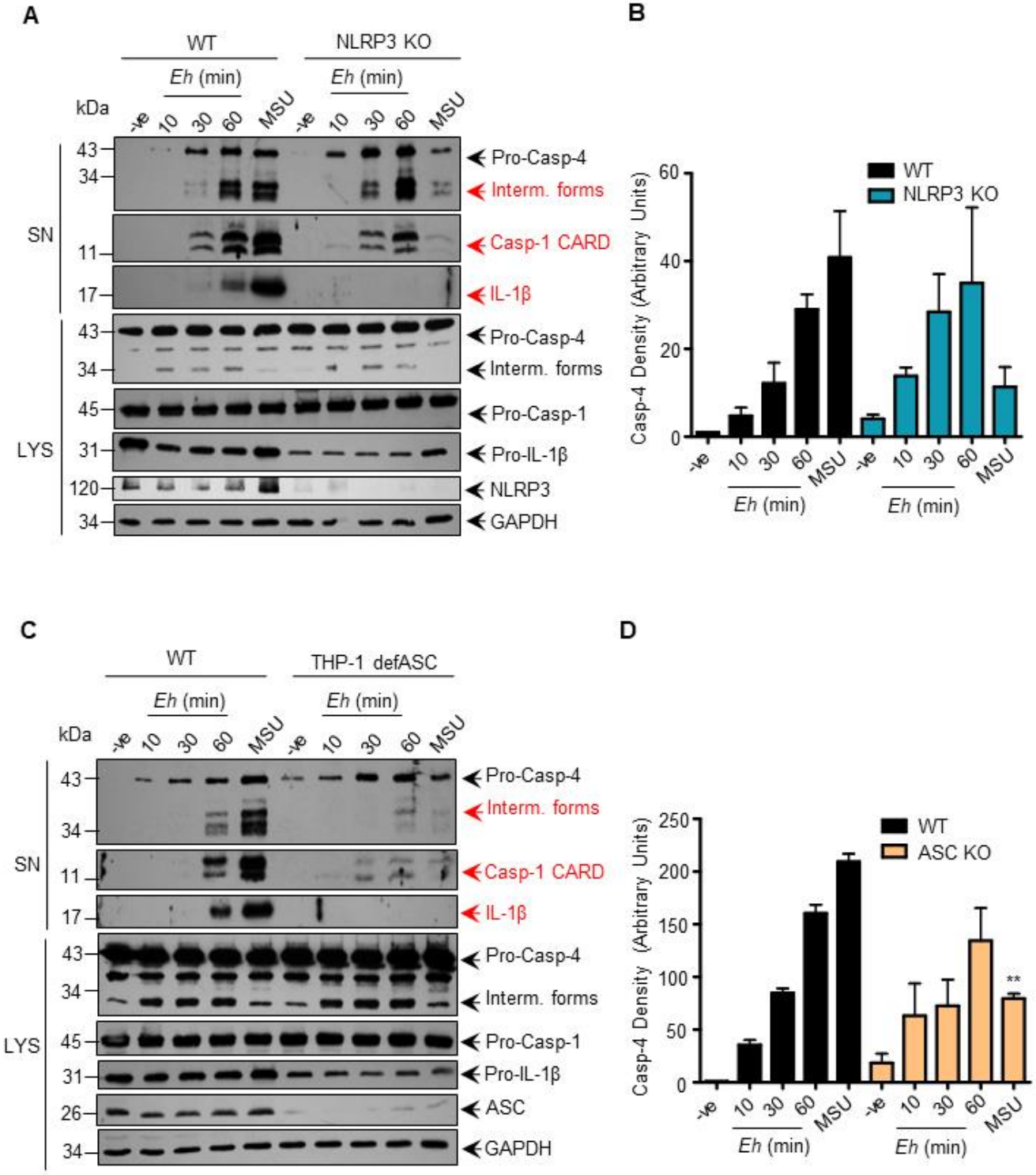
A
WT
NLRP3 KO
Eh (min)
Eh (min)
kDa
-ve
10
30
60
MSU
-ve
10
30
60
MSU
SN
LYS
43
34
11
17
43
34
45
31
120
34
Pro-Casp-4
Interm. forms
Casp-1 CARD
IL-1β
Pro-Casp-4
Interm. forms
Pro-Casp-1
Pro-IL-1β
NLRP3
GAPDH
B
Casp-4 Density (Arbitrary Units)
60
40
20
0
WT
NLRP3 KO
-ve
10
30
60
MSU
-ve
10
30
60
MSU
Eh (min)
Eh (min)
C
WT
THP-1 defASC
Eh (min)
Eh (min)
kDa
-ve
10
30
60
MSU
-ve
10
30
60
MSU
SN
LYS
43
34
11
17
43
34
45
31
26
34
Pro-Casp-4
Interm. forms
Casp-1 CARD
IL-1β
Pro-Casp-4
Interm. forms
Pro-Casp-1
Pro-IL-1β
ASC
GAPDH
D
Casp-4 Density (Arbitrary Units)
250
200
150
100
50
0
WT
ASC KO
**
-ve
10
30
60
MSU
-ve
10
30
60
MSU
Eh (min)
Eh (min)

Figure 3.3 *E. histolytica*-induced caspase-4 activation is independent of inflammasome components.

(A, B) WT, NLRP3 CRISPR/Cas9 KO THP-1 macrophages, and (C, D) THP-1 defASC macrophages were incubated with *Eh* (1:20) at increasing time points, cell supernatant was TCA precipitated and cells were washed and lysed. Equal amounts of lysates were loaded onto SDS-PAGE gel and immunoblotted with the indicated antibodies. Immunoblot analysis was performed for caspase-4, caspase-1, and IL-1β in the supernatants (SN) and along with NLRP3 and ASC in lysates (LYS), and blots were reprobed for GAPDH. Quantifications of caspase-4 proteins were performed by densitometric analysis from three independent experiments, and the negative (cells only) acted as an internal control. Data are representative of three experiments and statistical significance was calculated with Student's *t*-test in the KO as compared to WT (**$p<0.01$). Bars represent ± SEM. Jeanie Quach performed the experiment from cell harvesting, SDS-PAGE, imaging, and data analysis. Christina Sandall generated the NLRP3 CRISPR/Cas9 KO THP-1 cells.

3.4 *E. histolytica*-induced caspase-1 activation is dependent on caspase-4 and caspase-4 activation is independent of caspase-1

To interrogate whether caspase-1 required caspase-4 for its activation, CASP4 CRISPR/Cas9 KO THP-1 macrophages were stimulated with *Eh* for 10-60 min and monitored for caspase-4 and -1 activation and IL-1β release. Intriguingly, caspase-1 activation and IL-1β release were significantly lower (73% and 97% respectively, $p<0.05$) in CASP4 CRISPR/Cas9 KO compared to WT THP-1 macrophages as shown by western blot and densitometric analysis (**Figure 3.4A-C**; red highlighted box) suggesting a requirement of caspase-4 in caspase-1 activation. This requirement of caspase-4 by caspase-1 was also observed with the positive control MSU (**Figure 3.4A**). A regulatory role of caspase-4 in caspase-1 activation was previously shown in keratinocytes transfected with LPS and UVB irradiated [121,165,166] but no studies to date have shown this response towards a parasitic infection. Furthermore, the orthologue of caspase-4 found in mouse known as caspase-11, also points to the requirement of caspase-11 in caspase-1-mediated IL-1β secretion in response to gram-negative bacteria [167]. To determine whether caspase-4 activation required caspase-1, CASP1 CRISPR/Cas9 KO THP-1 macrophages were stimulated with *Eh* for 10-60 min. While there was less IL-1β secretion, there were no significant differences in caspase-4 activation suggesting that caspase-1 is not upstream of caspase-4 (**Figure 3.4D** and **3.4E**). MSU stimulation also showed less caspase-1 activation and IL-1β secretion, but no difference in caspase-4 activation. Taken together, these results support the notion that caspase-4 is upstream of caspase-1 to activate IL-1β secretions in response to *Eh*. This is

in contrast to studies that found reduced secretion of caspase-4 in caspase-1 KO in UVB-irradiated keratinocytes, indicating the effects are agonist-dependent [121]. To confirm a role for caspase-4 enzymatic activity in caspase-1 activation, in preliminary studies we used Z-LEVD-FMK to inhibit caspase-4 activity in WT macrophages stimulated with *Eh* and it did inhibit caspase-1 activation. To test the specificity of this inhibitor, we used it on CASP4 CRISPR/Cas9 KO cells stimulated with *Eh* and it also inhibited caspase-1 activation, indicating that it is non-specific and that the caspase substrates overlap [168].

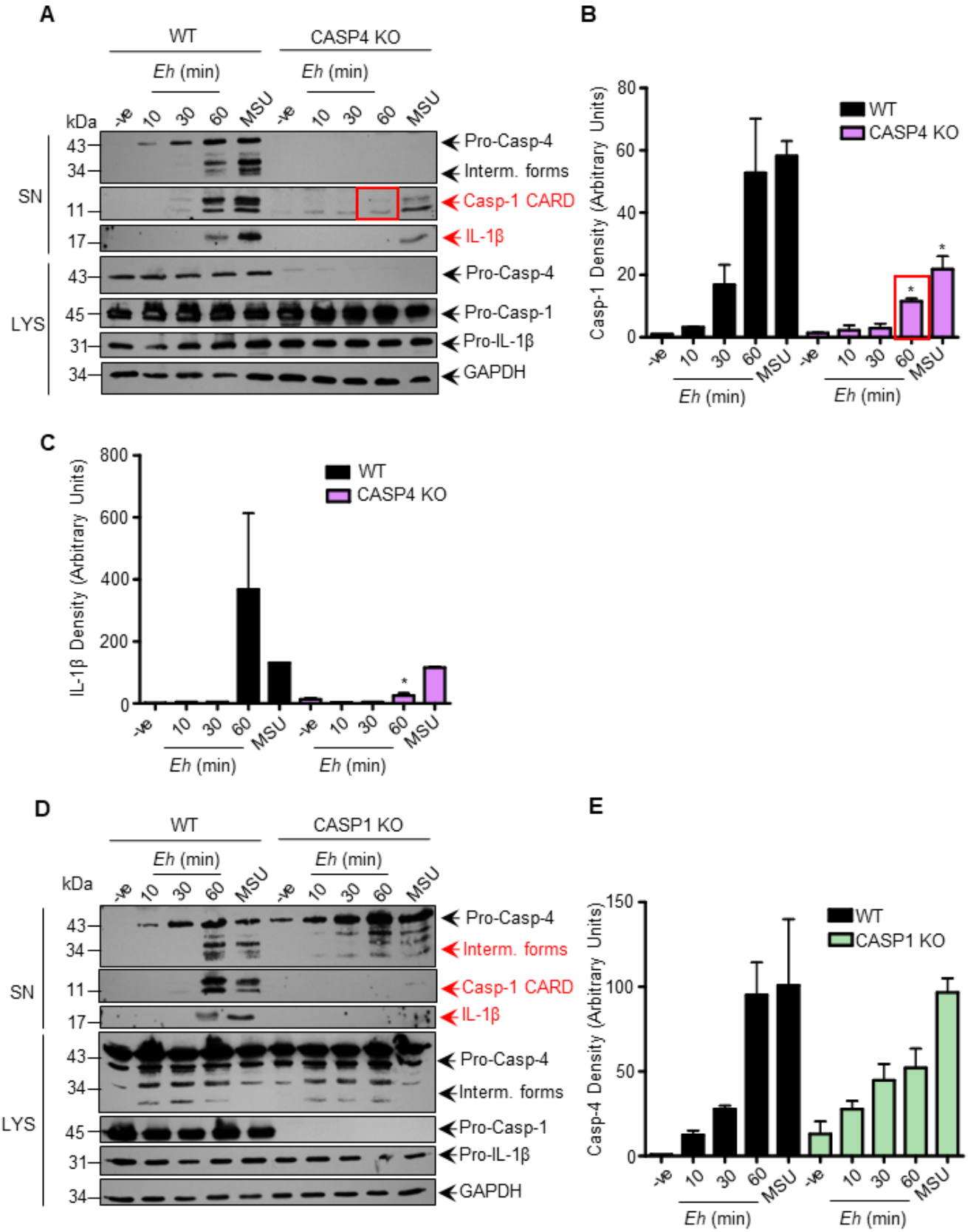
A
WT
CASP4 KO
Eh (min)
Eh (min)
kDa
-ve
10
30
60
MSU
-ve
10
30
60
MSU
SN
LYS
43
34
11
17
43
45
31
34
Pro-Casp-4
Interm. forms
Casp-1 CARD
IL-1β
Pro-Casp-4
Pro-Casp-1
Pro-IL-1β
GAPDH
B
Casp-1 Density (Arbitrary Units)
WT
CASP4 KO
Eh (min)
Eh (min)
C
IL-1β Density (Arbitrary Units)
WT
CASP4 KO
Eh (min)
Eh (min)
D
WT
CASP1 KO
Eh (min)
Eh (min)
kDa
SN
LYS
Pro-Casp-4
Interm. forms
Casp-1 CARD
IL-1β
Pro-Casp-4
Interm. forms
Pro-Casp-1
Pro-IL-1β
GAPDH
E
Casp-4 Density (Arbitrary Units)
WT
CASP1 KO
Eh (min)
Eh (min)

Figure 3.4 *E. histolytica*-induced caspase-1 activation is dependent on caspase-4 and caspase-4 activation is independent of caspase-1.

(A-C) WT, CASP4 CRISPR/Cas9 KO and (D, E) CASP1 CRISPR/Cas9 KO THP-1 macrophages were incubated with *Eh* (1:20) at increasing time points and cell supernatant was TCA precipitated and cells were washed and lysed. Equal amounts of lysates were loaded onto SDS-PAGE gel and immunoblotted with the indicated antibodies. Immunoblot analysis was performed for caspase-4, caspase-1, IL-1β in both the supernatants (SN) and lysates (LYS), and blots were reprobed for GAPDH. Quantifications of caspase-1 and IL-1β (5A) and caspase-4 (5D) were performed by densitometric analysis from three independent experiments, and the negative (cells only) acted as an internal control. Data are representative of three experiments and statistical significance was calculated with Student's *t*-test (*$p<0.05$). Bars represent ± SEM.

3.5 *E. histolytica*-induced IL-1β is dependent on caspase-1 and caspase-4

To determine the distinct role of caspase-4 in regulating IL-1β and other pro-inflammatory molecules, a human cytokine array focused 13-plex was used to screen for differences in cytokines/chemokines in CASP4 CRISPR/Cas9 KO compared to WT macrophages stimulated with *Eh*. The most interesting finding was that IL-1β levels were 90% lower in CASP4 CRISPR/Cas9 KO macrophages, which was consistent with the results seen by western blots of CASP1 and CASP4 CRISPR/Cas9 KO THP-1 macrophages (**Figure 3.4A** and **3.4D, Figure 3.5A**). To determine if the IL-1β released was bioactive, we used the SEAP assay that showed significantly ($p<0.001$) less bioactive IL-1β released by CASP4 CRISPR/Cas9 KO as compared to WT THP-1 macrophages (**Figure 3.5B**; highlighted histogram), suggesting there is cross talk between caspase-4 and -1 in regulating IL-1β release. The positive control, MSU displayed significantly less bioactive IL-1β levels in CASP1 CRISPR/Cas9 KO ($p<0.001$), but unexpectedly higher bioactive IL-1β in CASP4 CRISPR/Cas9 KO as compared to WT THP-1 macrophages ($p<0.001$). LDH levels in CASP1 and CASP4 CRISPR/Cas9 KO as compared to WT THP-1 macrophages were not significantly different when stimulated with *Eh* from 1-3 h, indicating that there was no cytotoxicity or caspase-4 and -1 related pyroptotic differences (**Figure 3.5C**). IL-1β was actively secreted and not due to cell death.

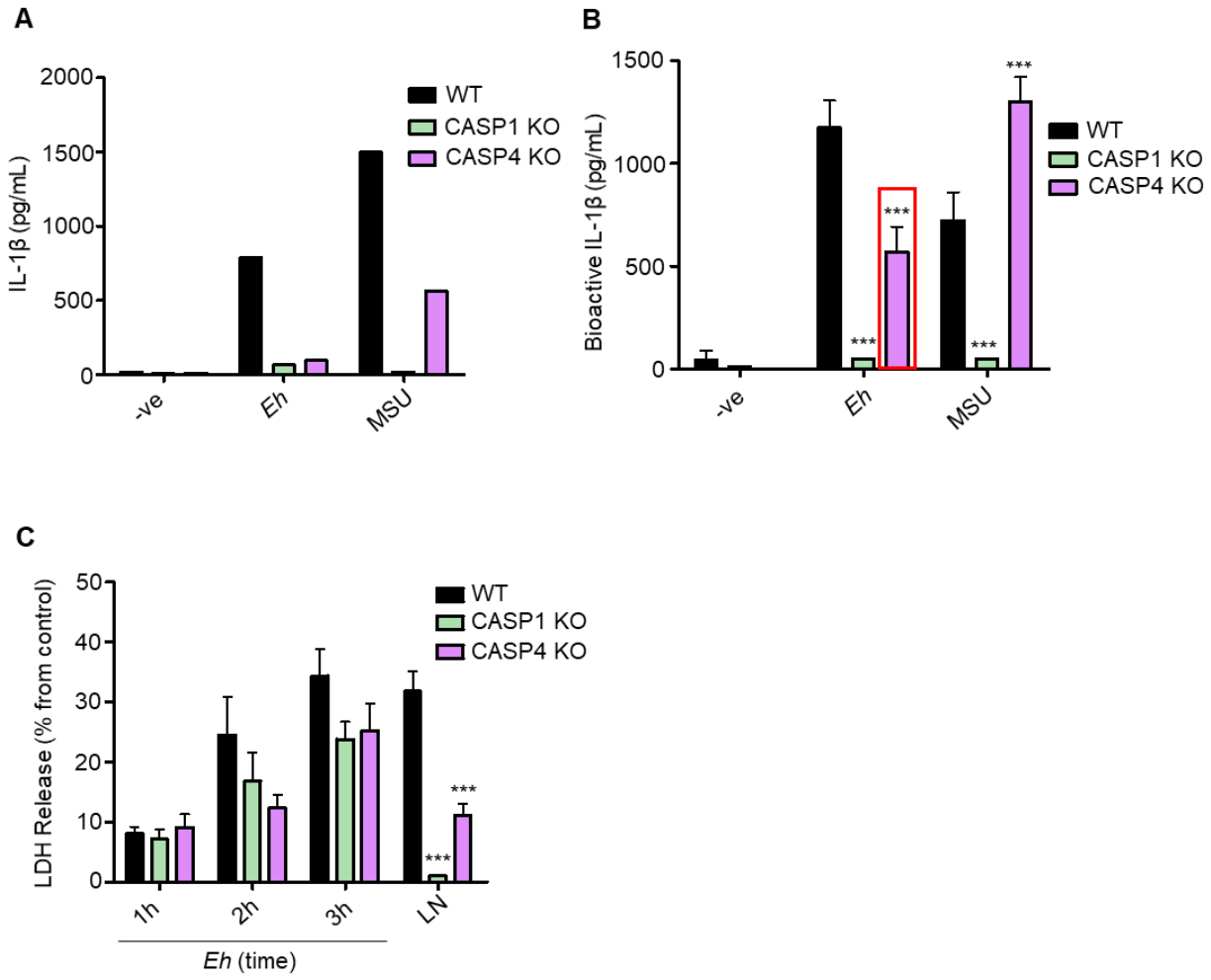

Figure 3.5 *E. histolytica*-induced IL-1β secretion is dependent on caspase-4 and -1 activation.

(A) WT, CASP4 CRISPR/Cas9 KO and CASP1 CRISPR/Cas9 KO THP-1 macrophages were incubated with *Eh* for 60 min and cell supernatant was quantified by human focused 13-plex cytokine/chemokine arrays. (B) Cell supernatant was added to HEK-Blue™ reporter cells to detect bioactive IL-1β using the SEAP assay. Cell death was measured by LDH release into the culture supernatant and is shown as a percentage of LDH release from cells without stimulation (control) (C). Data are representative of three experiments and statistical significance was calculated with one-way ANOVA and a Bonferroni post-hoc test (***p<0.001). Bars represent ± SEM. Jeanie Quach performed the experiment from cell harvesting, SDS-PAGE, imaging, and data analysis.

3.6 Overexpression of caspase-4 rescued *E. histolytica*-induced IL-1β secretion in CASP4 CRISPR/Cas9 KO macrophages

To confirm that caspase-4 has a role in enhancing IL-1β secretion, CASP4 CRISPR/Cas9 KO THP-1 macrophages were nucleofected with pro-caspase-4 expression plasmid and stimulated with *Eh* for 60 min. As indicated on the western blot, there was efficient restoration of pro-caspase-4 band (~41 kDa) slightly lower than the endogenous form of pro-caspase-4 in WT macrophages (**Figure 3.6A**). There was also higher caspase-1 and IL-1β protein expression in the CASP4 CRISPR/Cas9 KO macrophages treated with *Eh* compared to non-stimulated control cells. Strikingly, there was increased caspase-1 activation (highlighted box) and IL-1β protein expression in CASP4 CRISPR/Cas9 KO transfected with the caspase-4 plasmid when stimulated with *Eh* as compared to non-stimulated transfected CASP4 CRISPR/Cas9 KO THP-1 macrophages. More importantly, bioactive IL-1β secretion was rescued when pro-caspase-4 was overexpressed in CASP4 CRISPR/Cas9 KO THP-1 macrophages and stimulated with *Eh* as compared to control ($p<0.01$, **Figure 3.6B**; highlighted histogram). These results suggest that overexpressed pro-caspase-4 when stimulated with *Eh* stimulation enhanced caspase-1 processing at the CARD domain to enhance caspase-1-dependent maturation of IL-1β.

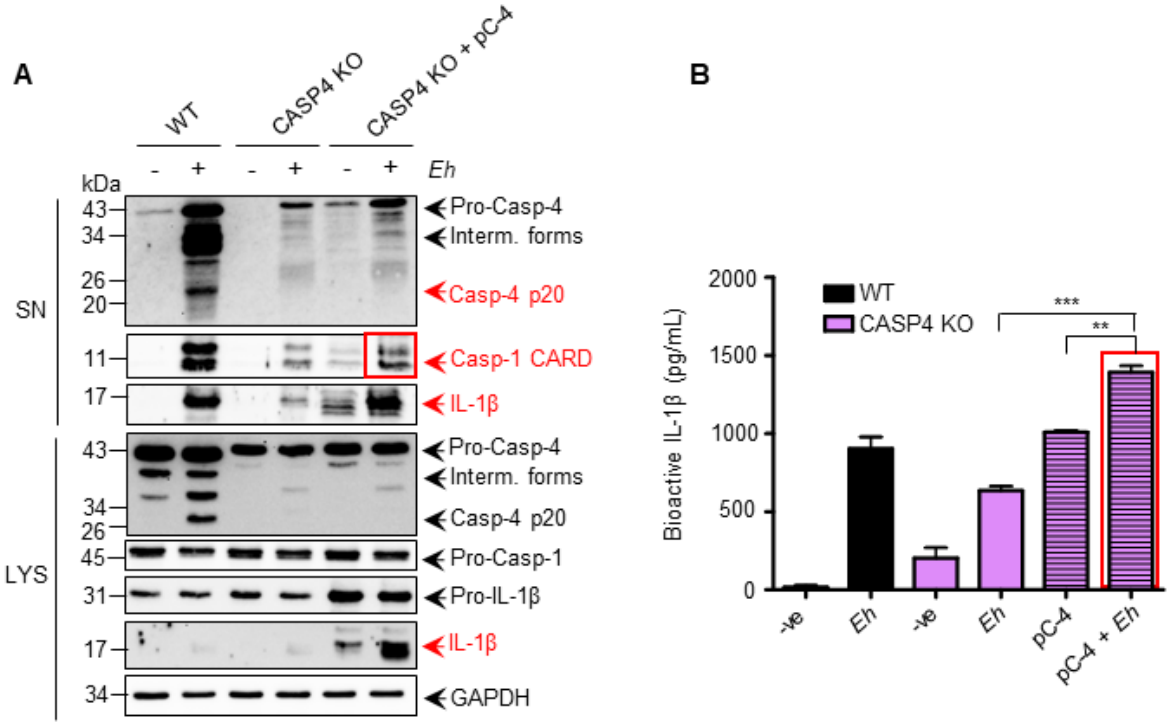

Figure 3.6 Overexpression of caspase-4 rescues *E. histolytica*-induced IL-1β secretion in CASP4 deficient macrophages.

(A) CASP4 CRISPR/Cas9 KO THP-1 macrophages were nucleofected with caspase-4 expression plasmid (pC-4) and left to rest for 24h before stimulating with *Eh* (1:20) for 60 min. (B) Cell supernatant from stimulated macrophages was also added to HEK-Blue™ reporter cells to detect bioactive IL-1β using the SEAP assay. Cell supernatant was TCA precipitated and cells were washed and lysed. Equal amounts of lysates were loaded onto SDS-PAGE gel and immunoblot analysis was performed for caspase-4, caspase-1, and IL-1β in both the supernatants (SN) and lysates (LYS), and blots were reprobed for GAPDH. Data are representative of three experiments and statistical significance was calculated with one-way ANOVA and a Bonferroni post-hoc test (**p<0.01, ***p<0.001). Bars represent ± SEM. France Moreau performed the nucleofections. Jeanie Quach performed the experiment from cell harvesting, SDS-PAGE, imaging, and data analysis.

3.7 *E. histolytica*-induced IL-1β secretion is dependent on caspase-4 interaction with caspase-1

To determine if the caspases specifically interacted with each other, COS-7 cells were transfected with pro-caspase-1, pro-caspase-4, and pro-IL-1β plasmids. We used COS-7 cells as they are easy to transfect with more than 90% transfection efficiency using GFP and they do not express ASC or NLRP3 facilitating the interactions between the caspases independent of the inflammasome complex (**Figure 3.7A**). Although weak pro-caspase-1 and pro-caspase-4 were detected by western blot under basal conditions, they were not activated unless stimulated with *Eh*. Transfection with GFP served as the control. When pro-caspase-1, pro-caspase-4, and pro-IL-1β plasmids were transfected and stimulated with *Eh*, pro-caspase-1 was cleaved into active caspase-1 p20 fragment and pro-caspase-4 was cleaved into the large subunit detectable in cell lysates (26 kDa, highlighted box; **Figure 3.7A**). This subsequently led to the cleavage of IL-1β from 31 kDa to 17 kDa. LPS and ATP stimulation (abbreviated LA) did not yield detectable caspase-4 or caspase-1 activation in the supernatant, but was present in the lysates (**Figure 3.7B**). This indicates a similar intracellular inflammatory pathway was initiated and LA served as another agonist for caspase-4-caspase-1 interaction in mediating IL-1β release. Although differences in protein expression were not detectable for the caspases under *Eh* stimulation, the SEAP assay yielded significant IL-1β differences. Importantly, the transfection of all three plasmids led to an additive effect, with more bioactive IL-1β secretion ($p<0.001$) than transfection of caspase-1 and IL-1β plasmids or the transfection

of caspase-4 and IL-1β with *Eh* stimulation (**Figure 3.7C**; highlighted histogram). As a positive control, LPS was used to prime cells and then stimulated with ATP (LA) in cells transfected with all three plasmids (**Figure 3.7B**). The combination of all three plasmids yielded greater caspase-1 activation and IL-1β secretion. This provides further evidence that the presence of caspase-4 enhances caspase-1 activation and therefore higher amounts of IL-1β secretion. In our study the use of COS-7 cells was advantageous as they basally express inactive caspase-4 and -1 (both are pro-forms) while COS-1 cells basally expressed active caspase-4 as indicated by the intermediate forms (**Figure 3.7D**). COS-7 cells allowed us to investigate *Eh*-induced activation of caspases.

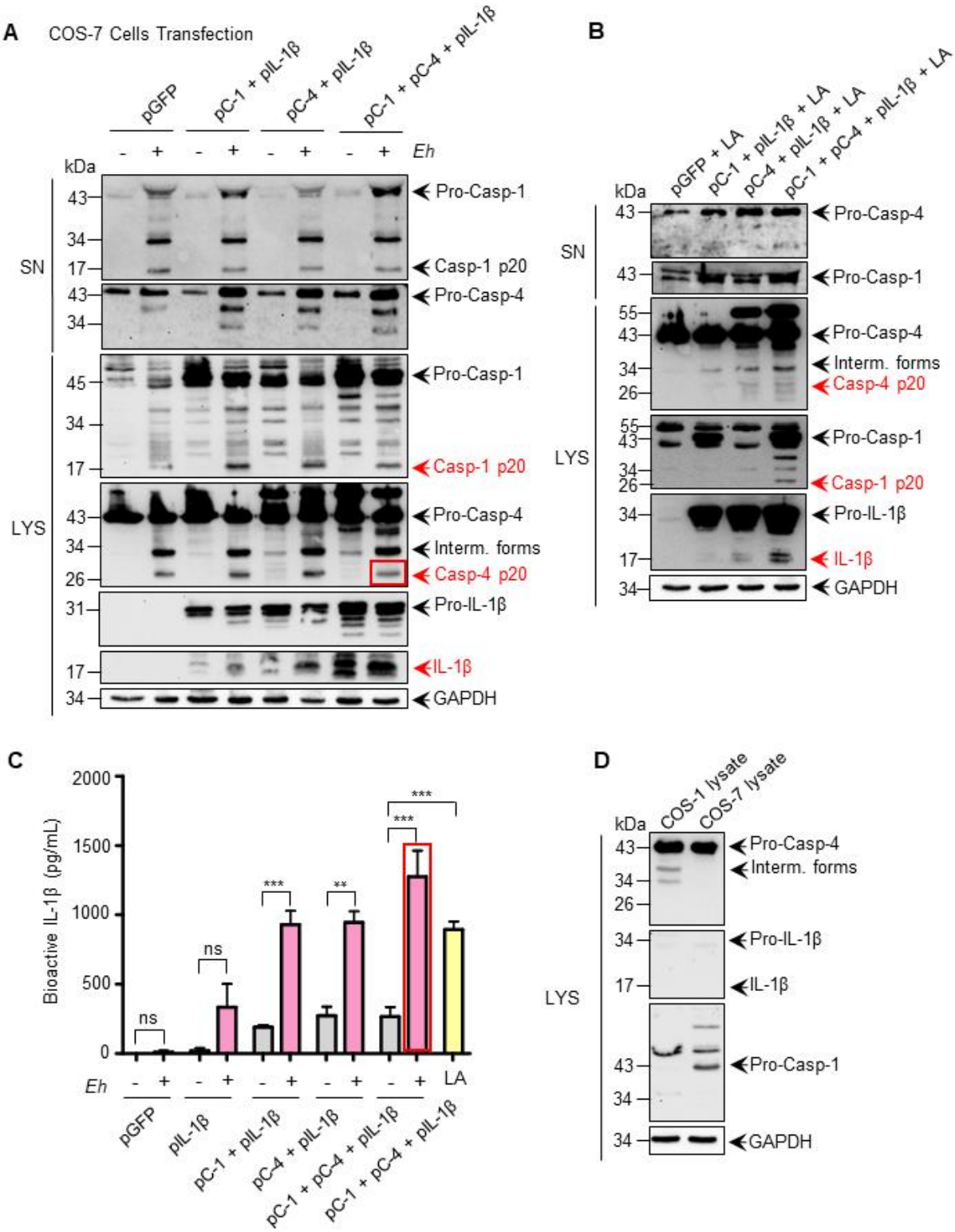
A
COS-7 Cells Transfection
pGFP
pC-1 + pIL-1β
pC-4 + pIL-1β
pC-1 + pC-4 + pIL-1β
Eh
kDa
SN
LYS
Pro-Casp-1
Casp-1 p20
Pro-Casp-4
Interm. forms
Casp-4 p20
Pro-IL-1β
IL-1β
GAPDH
B
pGFP + LA
pC-1 + pIL-1β + LA
pC-4 + pIL-1β + LA
pC-1 + pC-4 + pIL-1β + LA
C
Bioactive IL-1β (pg/mL)
ns
***
**
LA
D
COS-1 lysate
COS-7 lysate

Figure 3.7 *E. histolytica*-induced IL-1β secretion is dependent on caspase-4 interaction with caspase-1.

(A) COS-7 cells were transfected with pro-caspase-1 (abbreviated pC-1, 100 ng), pro-caspase-4 (abbreviated pC-4, 10 ng), pro-IL-1β (1 μg) plasmids, or GFP (1 μg) as a control and stimulated with *Eh* (1:2) for 30 min or (B) LPS (50 ng/mL for 2h to prime) and ATP (3 mM for 60 min) abbreviated LA, served as the control for IL-1β release. (C) Cell supernatant from stimulated macrophages was added to HEK-Blue™ reporter cells to detect bioactive IL-1β using the SEAP assay. (D) Protein expression of caspase-4, caspase-1, IL-1β was compared in COS-1 and COS-7 lysates to indicate basal expression and rationale for usage of COS-7 cells. Cell supernatant was TCA precipitated and cells were washed and lysed. Equal amounts of lysates were loaded onto SDS-PAGE gel and immunoblot analysis was performed for caspase-4 and -1 in the supernatants (SN) and along with IL-1β in the lysates (LYS), and blots were reprobed for GAPDH. Data are representative of three experiments and statistical significance was calculated with one-way ANOVA and a Bonferroni post-hoc test (**$p<0.01$, ***$p<0.001$, ns = not significant). Bars represent ± SEM. France Moreau performed the nucleofections. Jeanie Quach performed the experiment from cell harvesting, SDS-PAGE, imaging, and data analysis.

3.8 Pro-caspase-4 interacts with pro-caspase-1 in *Eh*-stimulated THP-1 macrophages

To confirm that caspase-4 was directly interacting with caspase-1, THP-1 macrophages were stimulated with *Eh* for 20 min followed by 0.8% formaldehyde treatment for 7 min at room temperature to covalently cross-link and stabilize the protein-protein interactions [169]. Antibodies against caspase-4 and -1 were then used to pull-down (PD) the complex and immunoblotted for caspase-4 and -1 (**Figure 3.8A**). This method is valuable because it allows for the detection of transient interacting proteins. However, as detection of cross-linked proteins is highly dependent on the antibody, we screened several caspase-4 antibodies from different companies and observed a high molecular weight complex around 92 kDa (cross-linked complex) only with the caspase-4 M029-3 antibody and not with the others (**Figure 3.11A**). The mouse IgG antibody detected the heavy (50 kDa) and light (25 kDa) chains. The cross-linked complex containing caspase-4 was detected at 92 kDa when the sample was incubated at 65°C and rapidly dissociated when the sample was boiled to 99°C demonstrating specificity for the protein-protein complex (**Figure 3.8B**). Pro-caspase-4 was also detected using the caspase-4 M029-3 antibody (**Figure 3.8B**). Immunoprecipitation with caspase-1 sc-56036 antibody following stimulation with *Eh* and formaldehyde treated, detected pro-caspase-1 (**Figure 3.8C**) and when immunoblotting for caspase-4 detected a band at 43 kDa (**Figure 3.8D** and **3.8E**; highlighted box) indicating that pro-caspase-1 engages pro-caspase-4.

To validate these observations, COS-7 cells were transfected with pro-caspase-1, pro-caspase-4, and pro-IL-1β plasmids and stimulated with *Eh* and pulled-down using both caspase-4 and -1 antibodies. As predicted, the high molecular weight cross-linked complex was detected at 92 kDa and when cells were subjected to caspase-1 pull-down, pro-caspase-4 was detected (**Figure 3.8F;** highlighted box). Conversely, when cells were subjected to caspase-4 pull-down, pro-caspase-1 was detected (**Figure 3.8G;** highlighted box). These results provide compelling evidence that caspase-1 and caspase-4 directly interacted with each other.

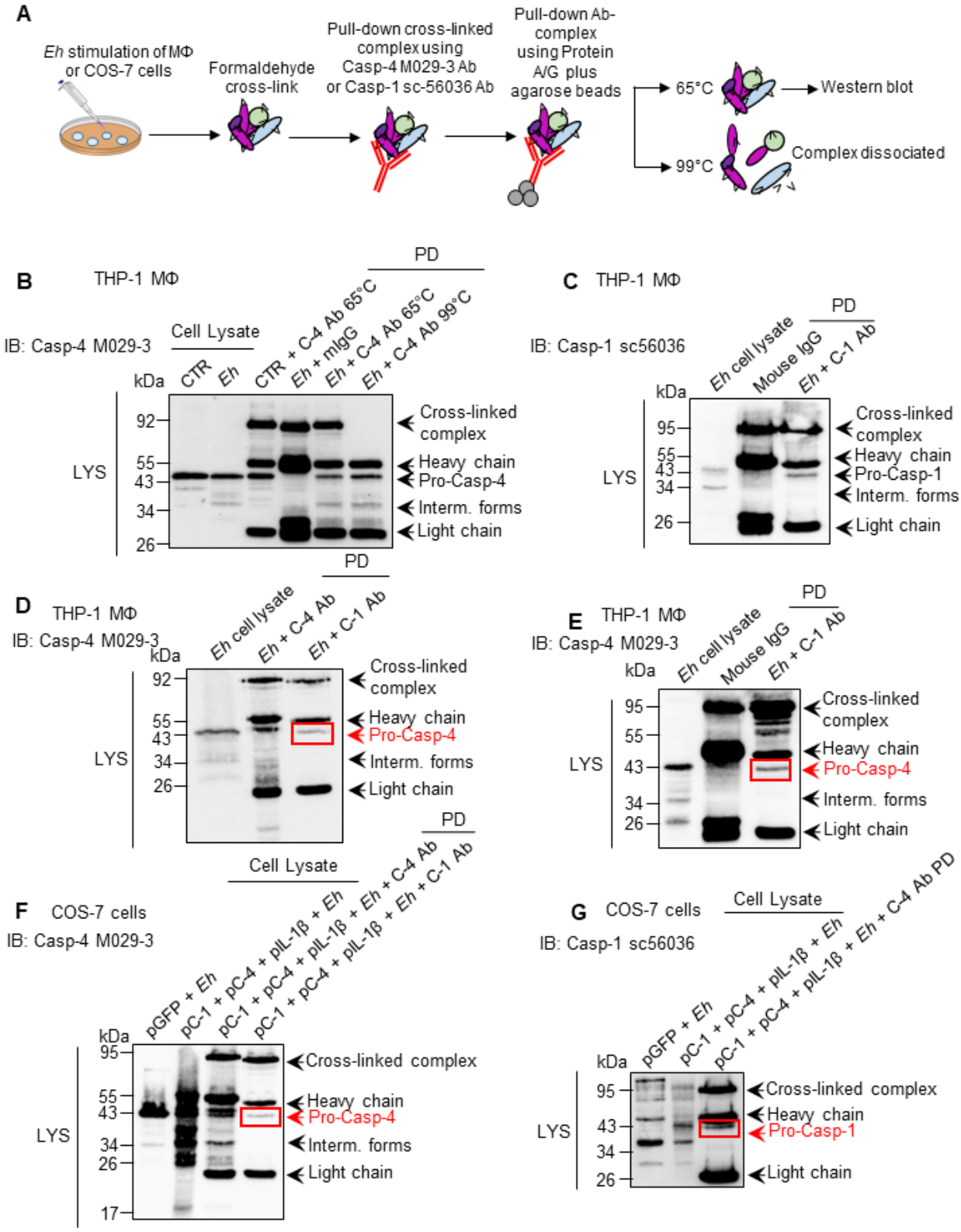
A
Eh stimulation of MΦ or COS-7 cells
Formaldehyde cross-link
Pull-down cross-linked complex using Casp-4 M029-3 Ab or Casp-1 sc-56036 Ab
Pull-down Ab-complex using Protein A/G plus agarose beads
65°C
Western blot
99°C
Complex dissociated
B
THP-1 MΦ
IB: Casp-4 M029-3
Cell Lysate
PD
CTR
Eh
CTR + C-4 Ab 65°C
Eh + mIgG
Eh + C-4 Ab 65°C
Eh + C-4 Ab 99°C
kDa
LYS
92
55
43
34
26
Cross-linked complex
Heavy chain
Pro-Casp-4
Interm. forms
Light chain
C
THP-1 MΦ
IB: Casp-1 sc56036
PD
Eh cell lysate
Mouse IgG
Eh + C-1 Ab
kDa
LYS
95
55
43
34
26
Cross-linked complex
Heavy chain
Pro-Casp-1
Interm. forms
Light chain
D
THP-1 MΦ
IB: Casp-4 M029-3
PD
Eh cell lysate
Eh + C-4 Ab
Eh + C-1 Ab
kDa
LYS
92
55
43
34
26
Cross-linked complex
Heavy chain
Pro-Casp-4
Interm. forms
Light chain
E
THP-1 MΦ
IB: Casp-4 M029-3
PD
Eh cell lysate
Mouse IgG
Eh + C-1 Ab
kDa
LYS
95
55
43
34
26
Cross-linked complex
Heavy chain
Pro-Casp-4
Interm. forms
Light chain
F
COS-7 cells
IB: Casp-4 M029-3
Cell Lysate
PD
pGFP + Eh
pC-1 + pC-4 + pIL-1β + Eh
pC-1 + pC-4 + pIL-1β + Eh + C-4 Ab
pC-1 + pC-4 + pIL-1β + Eh + C-1 Ab
kDa
LYS
95
55
43
34
26
17
Cross-linked complex
Heavy chain
Pro-Casp-4
Interm. forms
Light chain
G
COS-7 cells
IB: Casp-1 sc56036
Cell Lysate
pGFP + Eh
pC-1 + pC-4 + pIL-1β + Eh
pC-1 + pC-4 + pIL-1β + Eh + C-4 Ab PD
kDa
LYS
95
43
34
26
Cross-linked complex
Heavy chain
Pro-Casp-1
Light chain

Figure 3.8 Pro-caspase-4 interacts with pro-caspase-1 in *E. histolytica*-stimulated THP-1 macrophages.

(A) A schematic workflow of cell preparations to quantify caspase-1 and caspase-4 interaction by pull-down and western blot. Cells were stimulated with *Eh*, treated with formaldehyde, lysed and cross-linked complexes (black triangles with oval shapes) were pulled-down (PD) with antibodies (Y-shaped) and protein A/G plus agarose beads (grey circles). (B-E) THP-1 macrophages or COS-7 cells were stimulated with *Eh* for 20 min and 0.8% formaldehyde treated for 7 min at room temperature. Cells were subjected to pull-down (PD) with caspase-4 M029-3 or caspase-1 sc-56036 antibody at 1.5 µg and immunoblotted for caspase-4 or caspase-1. (F, G) COS-7 cells were transfected with caspase-1 (60 ng), caspase-4 (500 ng), or IL-1β (1.5 µg) plasmids, or GFP (1 µg) as a control prior to stimulating with *Eh* (2:1). Cells were subjected to pull-down with caspase-4 M029-3 or caspase-1 sc-56036 antibody at 1.5 µg and immunoblotted for caspase-4 or caspase-1. Corresponding mouse (mIgG) controls were used. Lysates were loaded onto SDS-PAGE gel and immunoblotted with the indicated antibodies. Western blots are representative of three independent experiments. France Moreau performed the nucleofections and assisted with formaldehyde treatment of cells. Jeanie Quach performed the experiment from cell harvesting, SDS-PAGE, imaging, and data analysis.

3.9 Caspase-4 siRNA knockdown in THP-1 macrophages decreases IL-1β secretion induced by *E. histolytica*.

The CRISPR/Cas9 gene editing tool was not available early during the course of my PhD, hence the logical approach to study the function of caspase-4 was to silence the gene through siRNA. To determine whether there was a role for caspase-4 in regulating caspase-1, caspase-1 as well as IL-1β was detected in both the supernatants and lysates in knock down cells. Caspase-4 siRNA was about 50% silenced as indicated by protein levels in the lysates and there was no processing of caspase-4 in the supernatants in response to *Eh* (**Figure 3.9A**). Interestingly, caspase-1 CARD protein was not different in the caspase-4 siRNA treated cells as compared to scrambled siRNA. This suggests that the presence of caspase-4 proteolytic activity allowed for cleavage of the caspase-1 CARD domain. Despite that, there was reduced IL-1β levels in caspase-4 silenced cells as compared to controls in response to *Eh*, and this was supported by the IL-1β ELISA (**Figure 3.9B**). In retrospect, this is valuable data because it indicates that siRNA silencing is effective, however, optimization is needed to ensure the balance between low cell death and maximal gene silencing.

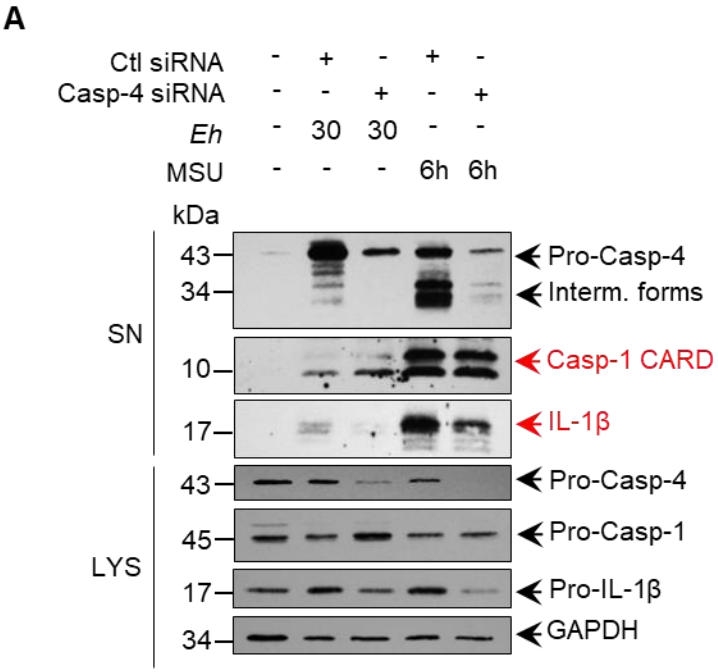
A
Ctl siRNA - + - + -
Casp-4 siRNA - - + - +
Eh - 30 30 - -
MSU - - - 6h 6h
kDa
SN
43
34
Pro-Casp-4
Interm. forms
10
Casp-1 CARD
17
IL-1β
LYS
43
Pro-Casp-4
45
Pro-Casp-1
17
Pro-IL-1β
34
GAPDH

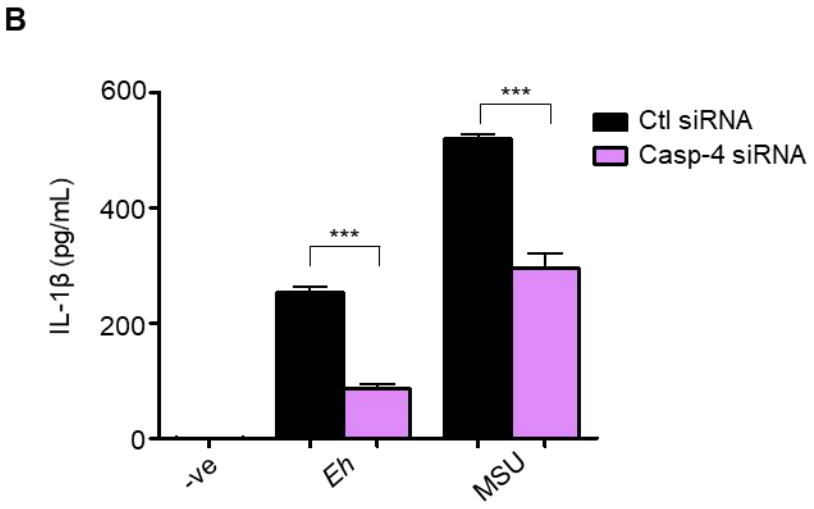
B
600
400
200
0
IL-1β (pg/mL)
***
***
Ctl siRNA
Casp-4 siRNA
-ve
Eh
MSU

Figure 3.9 Caspase-4 siRNA knockdown in THP-1 macrophages decreases IL-1β secretion induced by *E. histolytica*.

(A) PMA-differentiated THP-1 macrophages were transfected with caspase-4 (Casp-4) siRNA or control (Ctl) siRNA (50 nM) using 10 μL INTERFERin reagent per reaction and left for 48h. *Eh* (1:20) was added for 60 min and MSU stimulation for 300 μg/mL for 6h was the positive control. Cell supernatant was TCA precipitated and cells were washed and lysed. Equal amounts of lysates were loaded onto SDS-PAGE gel and immunoblot analysis was performed for caspase-4, caspase-1, IL-1β in both the supernatants (SN) and lysates (LYS), and blots were reprobed for GAPDH. (B) Cell supernatant was used to determine IL-1β levels using an IL-1β ELISA. Data are representative of three independent experiments and statistical significance was calculated with an unpaired Student's *t*-test (***$p<0.001$). Bars represent ± SEM. Jeanie Quach performed the experiment from cell harvesting, SDS-PAGE, imaging, and data analysis.

3.10 Overexpression of caspase-4 in THP-1 macrophages enhances bioactive IL-1β secretion and overexpression of caspase-1 in CASP1 CRISPR/Cas9 KO is lethal.

To determine the interaction between caspase-4 and -1 in regulating the overall IL-1β output, THP-1 macrophages were nucleofected with caspase-4 expression plasmid to determine how it affects IL-1β secretions. Intriguingly, overexpressed caspase-4 in THP-1 macrophages (**Figure 3.10A**) that were stimulated with *Eh* or ATP led to increased IL-1β secretions as compared to the GFP control. In addition to restoring caspase-4 in CASP4 CRISPR/Cas9 KO macrophages, we also attempted to restore caspase-1 in CASP1 CRISPR/Cas9 KO macrophages. While it was successful with the CASP4 CRISPR/Cas9 KO macrophages, the CASP1 CRISPR/Cas9 KO macrophages suffered from major cell death (**Figure 3.10B** and **3.10C**). It was speculated that caspase-1 induced pyroptosis as the cells observed under the microscope had membranes that look dissolved and spewing out its contents. As a control, WT THP-1 macrophages were able to tolerate the caspase-1 plasmid much better.

A

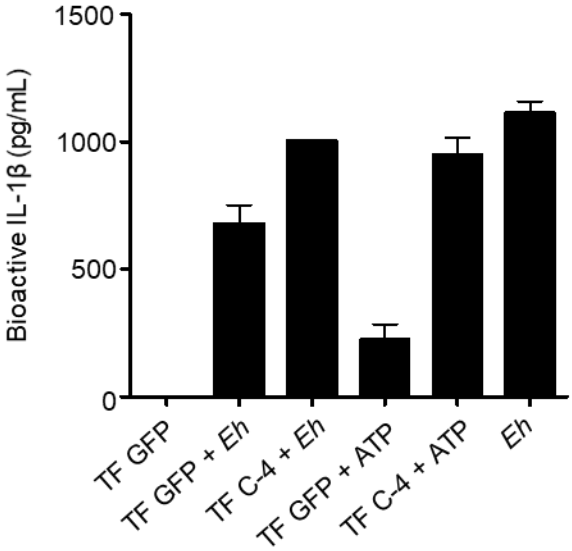
Bioactive IL-1β (pg/mL)
1500
1000
500
0
TF GFP
TF GFP + Eh
TF C-4 + Eh
TF GFP + ATP
TF C-4 + ATP
Eh

B

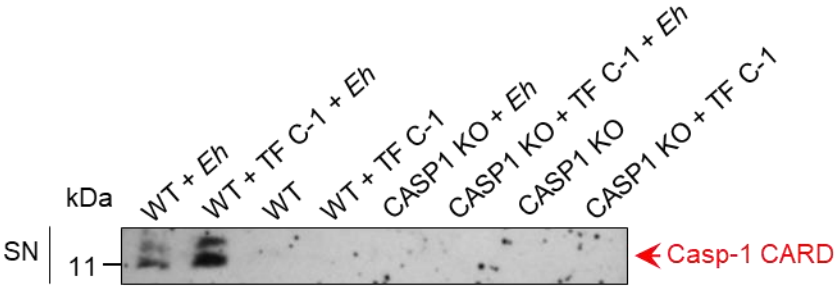
kDa
WT + Eh
WT + TF C-1 + Eh
WT
WT + TF C-1
CASP1 KO + Eh
CASP1 KO + TF C-1 + Eh
CASP1 KO
CASP1 KO + TF C-1
SN
11
Casp-1 CARD

C

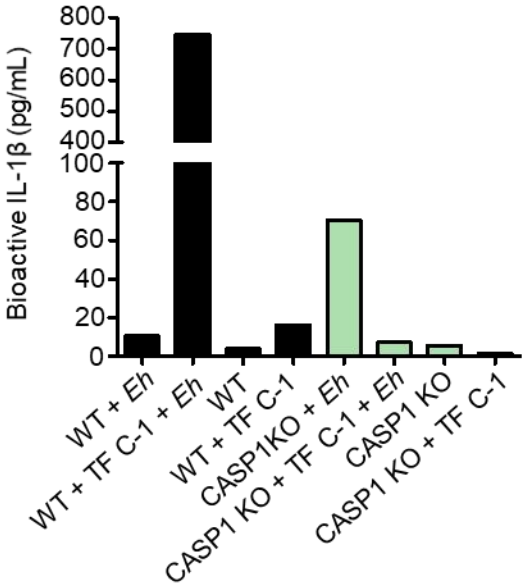
Bioactive IL-1β (pg/mL)
800
700
600
500
400
100
80
60
40
20
0
WT + Eh
WT + TF C-1 + Eh
WT
WT + TF C-1
CASP1KO + Eh
CASP1 KO + TF C-1 + Eh
CASP1 KO
CASP1 KO + TF C-1

Figure 3.10 Overexpression of caspase-4 in THP-1 macrophages enhances bioactive IL-1β secretion and overexpression of caspase-1 in CASP1 CRISPR/Cas9 KO is lethal.

(A) THP-1 macrophages were nucleofected with caspase-4 (1 μg) and left overnight prior to stimulating with *Eh* or ATP for 60 min. (B) Attempts to restore caspase-1 in CASP-1 CRISPR/Cas9 KO macrophages by nucleofecting with pro-caspase-1 plasmid (60 ng) resulted in high cell death. The surviving cells showed no caspase-1 secretion as indicated by the absence of caspase-1 CARD bands. Furthermore, there was minimal bioactive IL-1β in the CASP1 CRISPR/Cas9 KO THP-1 macrophages transfected with caspase-1 plasmid (see C). (C) Supernatants of THP-1 macrophages stimulated with *Eh* were added to HEK-Blue™ reporter cells to detect bioactive IL-1β using the SEAP assay. Data are representative of two independent experiments. France Moreau performed the nucleofections. Jeanie Quach performed the experiment from cell harvesting, SDS-PAGE, imaging, and data analysis.

3.11 Screening of caspase-4 and -1 antibodies on the formaldehyde cross-linked complex.

To determine caspase-4 and -1 interaction in a complex, formaldehye was used to treat cells post stimulation with *Eh*. This technique requires a lot of time dedicated to optimize the incubation time of *Eh* to macrophages where the caspase-4 and -1 interactions are occurring at its peak. The final timepoint that was chosen was 20 min and caspase-4 and -1 interactions were detected. Though it was only the pro-forms, a longer incubation time of *Eh* (40 or 60 min) may possibly yield the intermediate forms of caspase-4 that is interacting with pro-caspase-1, as we believe is the case if caspase-1 is a substrate for caspase-4. Several different antibodies for both caspase-4 and -1 were tested to determine their potential for detecting epitopes that may have been modified post formaldehyde treatment. Out of the antibodies tested for caspase-4, only caspase-4 M029-3 was able to pick up the cross-linked complex (92 kDa) (**Figure 3.11A**). A control without stimulation was used to compare *Eh* stimulated cells and both samples were pulled down with caspase-4 M029-3 antibody. In the *Eh* stimulated cells, the intermediate forms were also detected, providing evidence that the active forms can also be recognized post formaldehyde treatment. A Coomassie Blue staining was performed to determine if the high molecular weight band (around 92 kDa) in the *Eh* stimulation with the mouse IgG control is the same band as the *Eh* treatment with the caspase-4 M029-3 antibody and it looks to be a different band (**Figure 3.11B**). The caspase-1 antibodies that were tested had two potential candidates, caspase-1 sc-56036 or caspase-1 sc-622. The caspase-1 sc-56036 was chosen because it had less background and cleaner bands (**Figure 3.11C**).

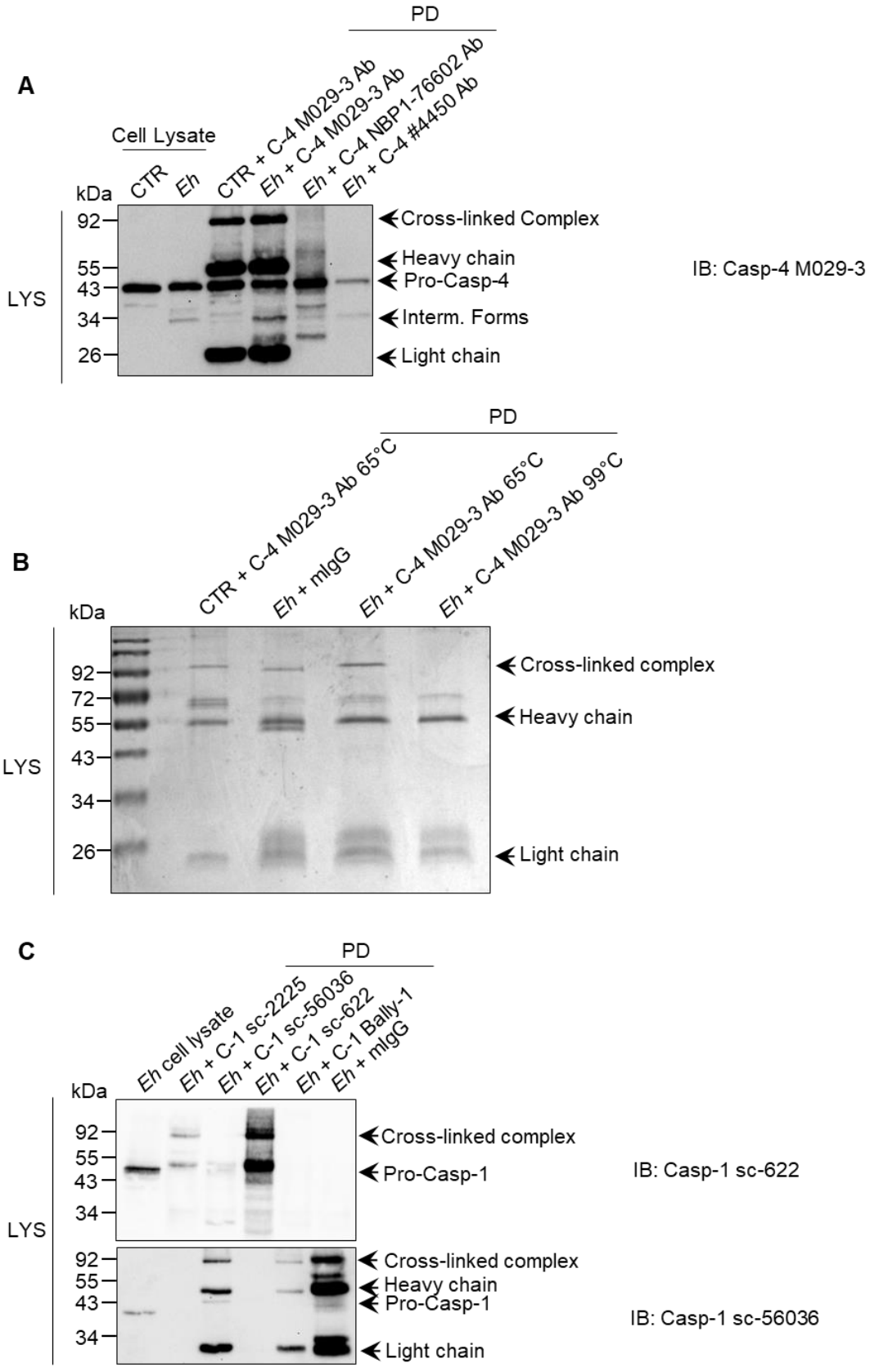
A
PD
Cell Lysate
CTR
Eh
CTR + C-4 M029-3 Ab
Eh + C-4 M029-3 Ab
Eh + C-4 NBP1-76602 Ab
Eh + C-4 #4450 Ab
kDa
92
55
43
34
26
LYS
Cross-linked Complex
Heavy chain
Pro-Casp-4
Interm. Forms
Light chain
IB: Casp-4 M029-3
B
PD
CTR + C-4 M029-3 Ab 65°C
Eh + mIgG
Eh + C-4 M029-3 Ab 65°C
Eh + C-4 M029-3 Ab 99°C
kDa
92
72
55
43
34
26
LYS
Cross-linked complex
Heavy chain
Light chain
C
PD
Eh cell lysate
Eh + C-1 sc-2225
Eh + C-1 sc-56036
Eh + C-1 sc-622
Eh + C-1 Bally-1
Eh + mIgG
kDa
92
55
43
34
LYS
Cross-linked complex
Pro-Casp-1
IB: Casp-1 sc-622
92
55
43
34
Cross-linked complex
Heavy chain
Pro-Casp-1
Light chain
IB: Casp-1 sc-56036

Figure 3.11 Screening of caspase-4 and -1 antibodies on the formaldehyde cross-linked complex.

(A) THP-1 macrophages were stimulated with *Eh* for 20 min and formaldehyde treated for 7 min prior to incubation with caspase-4 antibodies to pull-down (PD) the cross-linked complex. Several caspase-4 antibodies from different companies (MBL International Corporation, Novus Biologicals, and Cell Signaling) were used to determine the appropriate antibody for detecting a cross-linked complex at 92 kDa by western blot as well as on (B) SDS-PAGE stained with Coomassie Blue. Caspase-4 M029-3 pulled-down (PD) the caspase-4 cross-linked complex from formaldehyde treated cells. (**C**) Several caspase-1 antibodies from different companies (Santa Cruz and Adipogen) were used to determine the appropriate antibody for detecting cross-linked complex at 92 kDa. Caspase-1 sc-56036 pulled-down the caspase-1 cross-linked complex from formaldehyde treated cells. Data are representative of two independent experiments. France Moreau assisted with formaldehyde treatment of cells. Jeanie Quach performed the experiment from cell harvesting, SDS-PAGE, imaging, and data analysis.

3.12 IL-8 and MCP-1 level changes in CASP1 and CASP4 deficient macrophages stimulated with *E. histolytica*

To determine the distinct cytokines/chemokines regulated by caspase-4, we used the Human Focused 13-Plex Cytokine/Chemokine Array which included the following: GM-CSF, IFN-γ, IL-1β, IL-2, IL-4, IL-6, IL-8, IL-10, IL-12, MCP-1, TNF-α, IL-13, IL-5. The majority of cytokines/chemokines were undetectable, however, we found interesting results with IL-1β that was reduced in the CASP1 and CASP4 CRISPR/Cas9 KO macrophages. Please note that this is shown in the manuscript. IL-8 levels were slightly up regulated in the CASP4 CRISPR/Cas9 KO macrophages as compared to WT macrophages when stimulated with *Eh* and MSU (**Figure 3.12A**), but we do not know if this is significant because only one experiment was performed. IL-8 levels are important as a neutrophil chemoattractant [4,64], therefore repeating the experiment with increased time of treatment with *Eh* and/or utilizing the IL-8 ELISA would be interesting to explore further. Additionally, there were increased levels of MCP-1 in the CASP1 CRISPR/Cas9 KO macrophages, but no difference in the CASP4 CRISPR/Cas9 KO macrophages with *Eh* stimulation (**Figure 3.12B**). MCP-1 is a monocyte chemoattractant protein that regulates monocyte and macrophage migration to inflamed sites [170]. Although no conclusions can be made about these studies, it shows that there are other cytokines/chemokines that may be regulated by caspase-4. Although not explored, both IL-18 and IL-1α have been shown to be regulated by the inflammasome or caspase-4 [126,159], respectively and so are also worth exploring.

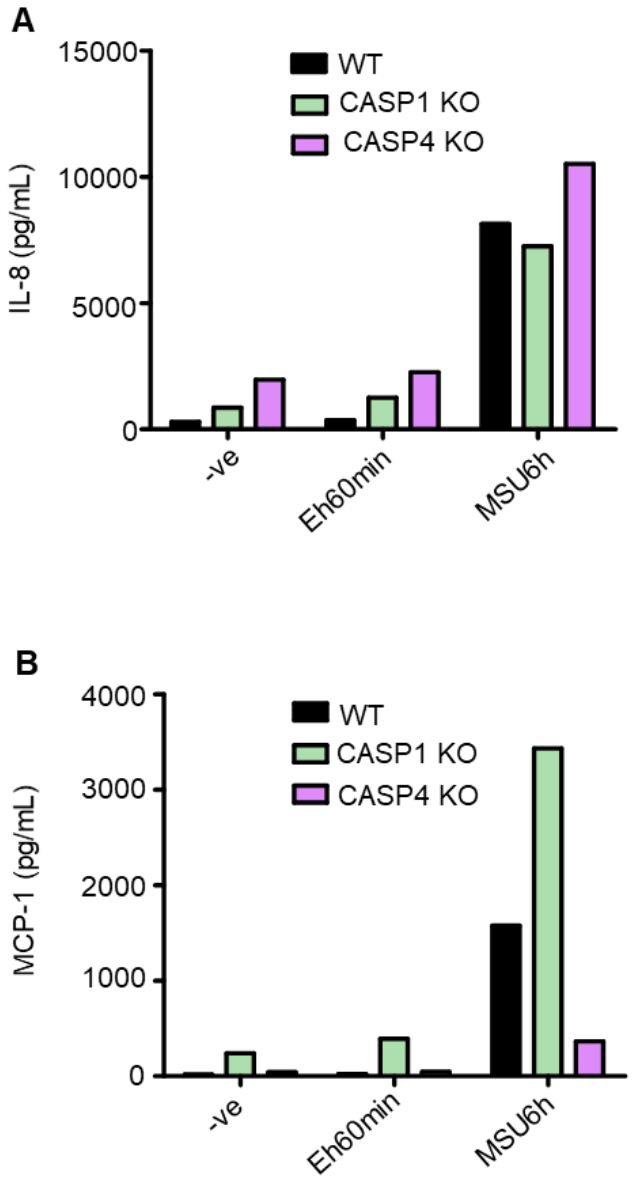

Figure 3.12 IL-8 and MCP-1 levels in CASP1 and CASP4 CRISPR/Cas9 KO macrophages stimulated with *E. histolytica*.

(A, B) WT, CASP4 CRISPR/Cas9 KO and CASP1 CRISPR/Cas9 KO THP-1 macrophages were incubated with *Eh* for 60 min and cell supernatant was quantified by human focused 13-plex cytokine/chemokine arrays. IL-8 levels (pg/mL) are in (A) and MCP-1 levels (pg/mL) are in (B). One experiment was performed. Jeanie Quach performed the experiment from cell harvesting, SDS-PAGE, imaging, and data analysis.

3.13 Interacting partners of caspase-4 in *Eh*-stimulated macrophages

In order to better understand the function of caspase-4 in inflammation, studying the proteins that caspase-4 interacts with would lend some clues. To determine the interacting partners for caspase-4, THP-1 macrophages were stimulated with *Eh* and then exposed to formaldehyde for cross-linking. Following the cross-link, the beads were boiled and then ran on an SDS-PAGE gel, with the band excised and then sent for liquid chromatography–mass spectrometry (LC-MS/MS). The number of matched peptides for caspase-4 was rather low, with only 7. It was expected that caspase-1 would be pulled down with caspase-4 in the complex, but we did not observe that. Interestingly, there were other proteins namely adenylyl cyclase-associated protein 1 isoform X2 which is involved in regulating the actin cytoskeleton [171], immunoglobulin lambda-like polypeptide 5 isoform 1 is part of the light chain involved in antigen binding, and moesin is involved in regulating actin cytoskeleton [172] (**Table 3.1**). Plastin-2 is also involved in actin binding [172], clathrin heavy chain is involved in the formation of vesicles [173], and peroxiredoxin-1 is an antioxidant that fight oxidative stress [174].

Table 3.1 List of proteins that interact with caspase-4 using LC-MS/MS in THP-1 macrophages stimulated with *E. histolytica* and formaldehyde cross-linked

Accession Number	Description	Number of Matched Peptides
NP_001216	caspase-4 isoform alpha precursor	7
NP_001337411	adenylyl cyclase-associated protein 1 isoform X2	7
NP_001171597	immunoglobulin lambda-like polypeptide 5 isoform 1	6
NP_002435	moesin	3
NP_002289	plastin-2	3
NP_004850	clathrin heavy chain 1 isoform 1	2
NP_001407	eukaryotic initiation factor 4A-I isoform 1	2
NP_001189360	peroxiredoxin-1	2

France Moreau assisted with formaldehyde treatment of cells. Jeanie Quach performed the experiment from cell harvesting, SDS-PAGE, imaging, and data analysis.

3.14 Interacting partners of caspase-4 in *Eh*-stimulated COS-7 cells

To determine the interacting partners for caspase-4, COS-7 cells were utilized because of their high transfection efficiency. COS-7 cells were transfected with pro-caspase-4, pro-caspase-1, and pro-IL-1β, stimulated with *Eh* and then exposed to formaldehyde for cross-linking. Following the cross-link, the beads were subjected to several washes to remove traces of contaminants suitable for mass spectrometry. This experiment yielded better caspase-4 (with 32 matched peptides) because the beads were used instead of excising the band from a gel (**Table 3.2**). One protein with a top hit is glutathione S-transferase P, important for regulating Cdk5 kinase activity and implicated in Alzheimer's Disease [175]. Since IL-1β was transfected into the cells, it was not surprising to see this as an interacting protein. The immunoglobulin lambda-like polypeptide 5 isoform 1 is involved in receptor binding and vimentin isoform x1 are filaments involved in stabilizing collagen mRNAs [176]. Most remarkably, caspase-1 was not found as one of the targets and it could be that the interaction is weak or it is transient. As shown, the detection of caspase-1 by mass spectrometry was difficult due to a variety of factors including timepoint of *Eh* stimulation, formaldehyde cross-link procedure, and the usage of mass spectrometry. As cross-link is not a common procedure conducted at the SAMS centre, it would be valuable to send samples to the UVic Genome BC Protein Centre (Victoria, British Columbia) as they have good experience with cross-linked proteins. Detecting the presence of caspase-1 in caspase-4 pull down studies and vice versa would lend supporting evidence to the important interactions between caspase-4 and -1 in regulating IL-1β secretions.

Table 3.2 List of proteins that interact with caspase-4 using LC-MS/MS in transfected COS-7 cells stimulated with *E. histolytica* and formaldehyde cross-linked

Accession Number	Description	Number of Matched Peptides
NP_001216	caspase-4 isoform alpha precursor	32
NP_000843	glutathione S-transferase P	76
NP_000567	interleukin-1 beta proprotein	7
NP_001171597	immunoglobulin lambda-like polypeptide 5 isoform 1	7
XP_006717563	vimentin isoform X1	6
NP_001093588	DNA repair protein XRCC3	5
NP_001137232	eukaryotic translation initiation factor 5A-1 isoform A	5
XP_011509088	1-phosphatidylinositol 3-phosphate 5-kinase isoform X8	3
NP_004850	clathrin heavy chain 1 isoform 1	2
NP_002435	Moesin	2
NP_001189360	peroxiredoxin-1	2
NP_006187	poly(rC)-binding protein 1	2

France Moreau assisted with formaldehyde treatment of cells. Jeanie Quach performed the experiment from cell harvesting, SDS-PAGE, imaging, and data analysis.

Caspase-11 Murine Studies

3.15 *E. histolytica*-induced caspase-11 activation is independent of inflammasome components

As murine caspase-11 is believed to be the ortholog to human caspase-4, we used mouse bone marrow-derived macrophages (BMDM) deficient in Asc and Nlrp3 to explore whether the requirements are similar. Control, *Asc*$^{-/-}$ and *Nlrp3*$^{-/-}$ BMDM were stimulated with *Eh* for 5, 30, or 60 min. LPS and cholera toxin B (CTB) activates the non-canonical inflammasome, so they were used as positive controls. Caspase-11 activation occurred as early as 5 mins in both the lysates and supernatants, whereas for caspase-1 activation, it started to occur at 60 mins. Robust caspase-11 activation was detected in the supernatants at 60 min; however, there was no difference in caspase-11 protein levels (p43 and p38) between *Asc*$^{-/-}$ and *Asc*$^{+/+}$ BMDM (**Figure 3.13A**). Predictably, cleavage of the caspase-1 p20 and IL-1β (17 kDa) was absent in *Asc*$^{-/-}$ showing a dependency of caspase-1 activation on inflammasome complex formation. Additionally, there was also no difference in caspase-11 protein levels between *Nlrp3*$^{-/-}$ compared to *Nlrp3*$^{+/+}$ BMDM (**Figure 3.13B**). The cleavage of caspase-1 p20 was absent in *Nlrp3*$^{-/-}$ and IL-1β was reduced compared to *Nlrp3*$^{+/+}$ BMDM. This indicates that both human caspase-4 and murine caspase-11 are activated similarly, being independent of NLRP3 and ASC.

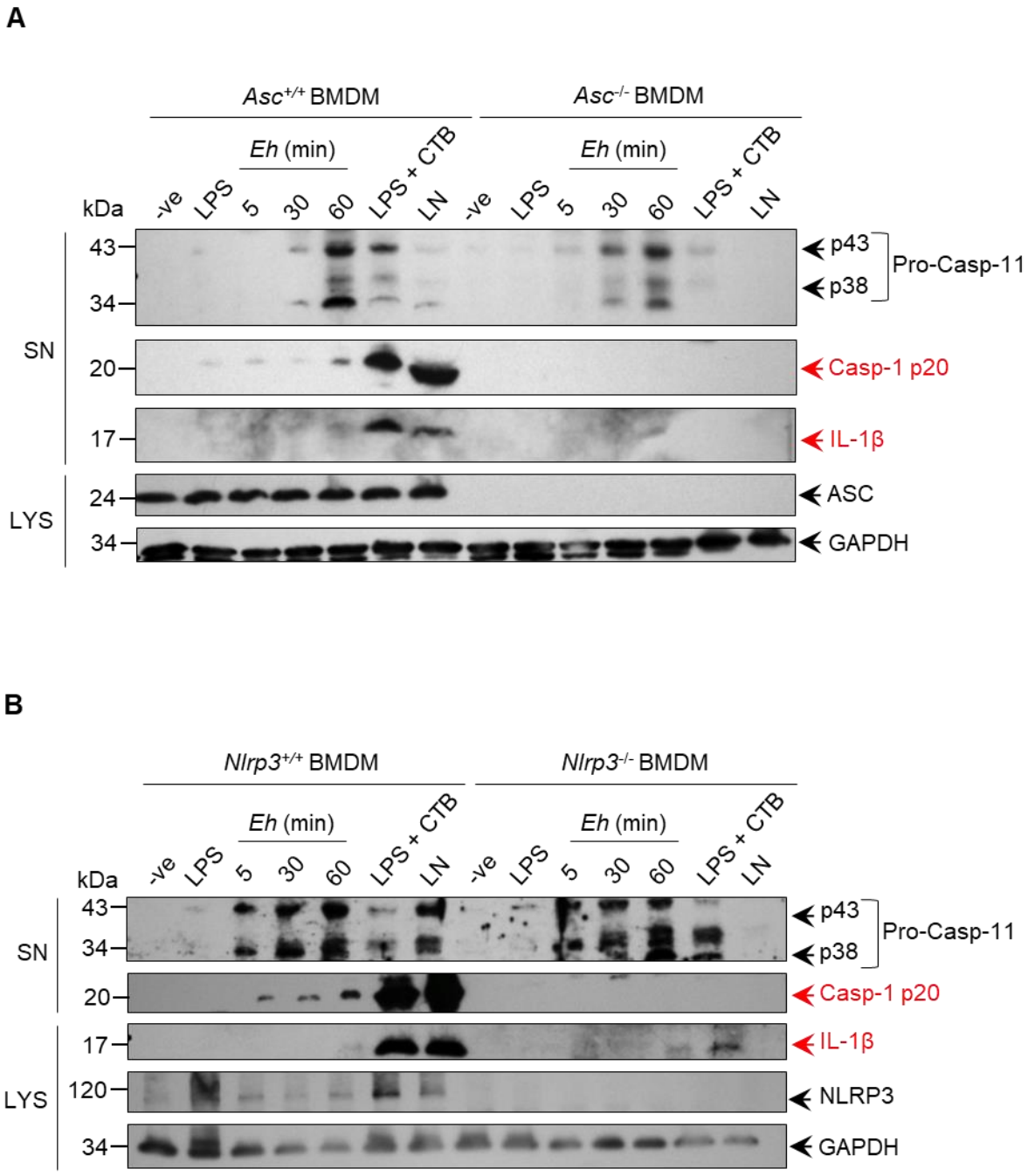
A
Asc+/+ BMDM
Asc-/- BMDM
Eh (min)
Eh (min)
kDa
-ve
LPS
5
30
60
LPS + CTB
LN
-ve
LPS
5
30
60
LPS + CTB
LN
SN
LYS
43
34
20
17
24
34
p43
p38
Pro-Casp-11
Casp-1 p20
IL-1β
ASC
GAPDH
B
Nlrp3+/+ BMDM
Nlrp3-/- BMDM
Eh (min)
Eh (min)
kDa
-ve
LPS
5
30
60
LPS + CTB
LN
-ve
LPS
5
30
60
LPS + CTB
LN
SN
LYS
43
34
20
17
120
34
p43
p38
Pro-Casp-11
Casp-1 p20
IL-1β
NLRP3
GAPDH

Figure 3.13 *E. histolytica*-induced caspase-11 activation is independent of inflammasome components.

(A) BMDM derived from *Asc*$^{+/+}$ and *Asc*$^{-/-}$ and (B) *Nlrp3*$^{-/-}$ and *Nlrp3*$^{-/-}$ were LPS primed (100 ng/mL) for 3.5h before incubation with *Eh* (1:20) at increasing time points. LPS (2 μg/mL) and cholera toxin B (CTB, 20 ng/mL) was added for 16h and LPS (50 ng/mL) and nigericin (10 μM) was added for 30 min (LN). Cell supernatant was TCA precipitated and cells were washed and lysed. Equal amounts of lysates were loaded onto SDS-PAGE gel and immunoblot analysis was performed for caspase-11, caspase-1, IL-1β in the supernatants (SN), and ASC, NLRP3 in the lysates (LYS) and blots were reprobed for GAPDH. Western blots are representative of three independent experiments. Jeanie Quach performed the experiment from cell harvesting, SDS-PAGE, imaging, and data analysis.

3.16 *E. histolytica*-induced caspase-1 activation is independent of caspase-11

Studies were also done on BMDMs derived from *Casp11*$^{-/-}$ mice stimulated with *Eh* for 5, 30, and 60 min and there were no differences in caspase-1 p20 and IL-1β protein expression as compared to *Casp11*$^{+/+}$ controls (**Figure 3.14A**). The positive control LPS and cholera toxin B (CTB) showed slightly less activation in *Casp11*$^{-/-}$ as compared to *Casp11*$^{+/+}$ macrophages. These findings indicate that although caspase-11 has similar parasite requirements in the activation of caspase-4, it may serve different functions. Predictably, using *Casp1*$^{-/-}$*Casp11*$^{-/-}$ there was less IL-1β as compared to *Casp1*$^{+/+}$*Casp11*$^{+/+}$ macrophages when stimulated with *Eh* (**Figure 3.14B**). Interestingly, caspase-1 activation was not dependent on caspase-11, suggesting that caspase-4 and caspase-11 may play different roles.

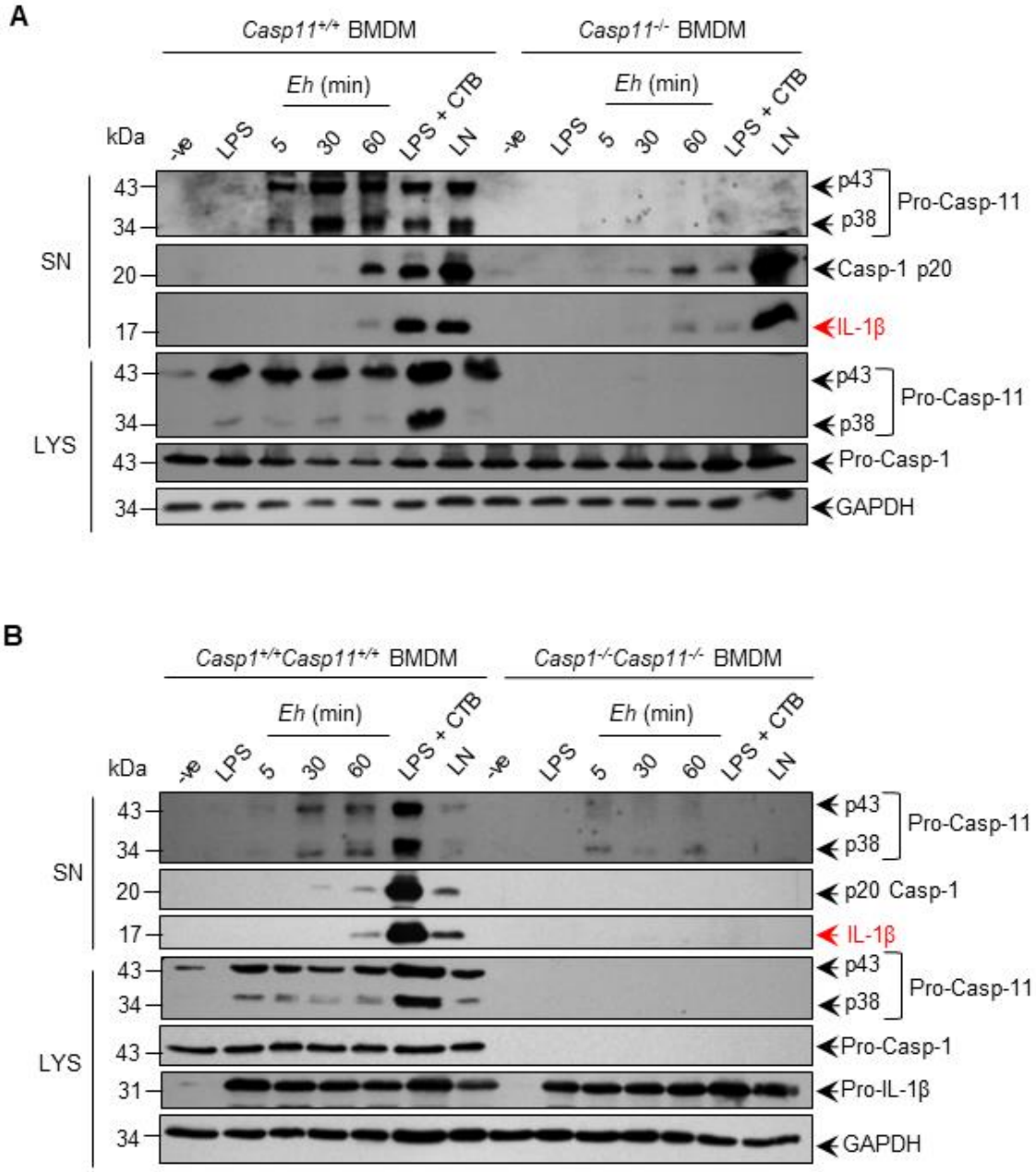
A
Casp11+/+ BMDM
Casp11-/- BMDM
Eh (min)
Eh (min)
kDa
-ve
LPS
5
30
60
LPS + CTB
LN
-ve
LPS
5
30
60
LPS + CTB
LN
SN
LYS
43
34
20
17
43
34
43
34
p43
p38
Pro-Casp-11
Casp-1 p20
IL-1β
p43
p38
Pro-Casp-11
Pro-Casp-1
GAPDH
B
Casp1+/+Casp11+/+ BMDM
Casp1-/-Casp11-/- BMDM
Eh (min)
Eh (min)
kDa
-ve
LPS
5
30
60
LPS + CTB
LN
-ve
LPS
5
30
60
LPS + CTB
LN
SN
LYS
43
34
20
17
43
34
43
31
34
p43
p38
Pro-Casp-11
p20 Casp-1
IL-1β
p43
p38
Pro-Casp-11
Pro-Casp-1
Pro-IL-1β
GAPDH

Figure 3.14 *E. histolytica*-induced caspase-1 activation is independent of caspase-11.

(A) *Casp11*$^{+/+}$ and *Casp11*$^{-/-}$ and (B) *Casp1*$^{+/+}$*Casp11*$^{+/+}$ and *Casp1*$^{-/-}$*Casp11*$^{-/-}$ BMDMs were LPS primed (100 ng/mL) for 3.5h before incubation with *Eh* at increasing time points (1:20). LPS (2 μg/mL) and cholera toxin B (CTB, 20 ng/mL) was added for 16h and LPS (50 ng/mL) and nigericin (10 μM) was added for 30 min (LN). Cell supernatant was TCA precipitated and cells were washed and lysed. Equal amounts of lysates were loaded onto SDS-PAGE gel and immunoblot analysis was performed for caspase-11, caspase-1, IL-1β in the supernatants (SN) and caspase-11, caspase-1 in the lysates (LYS), and blots were reprobed for GAPDH. Western blots are representative of three independent experiments. Jeanie Quach performed the experiment from cell harvesting, SDS-PAGE, imaging, and data analysis.

3.17 Summary of Results

It was shown in this study that *Eh* can induce robust activation of caspase-4 and -1 and they occur simultaneously at 30 min and accumulates up until 60 mins. The activation of caspase-4 and -1 also require the presence of the live parasite and *Eh* Gal-lectin binding to macrophage surfaces. More interestingly, it is the *Eh*CP-A5 that is involved in turning on these inflammatory caspases. In addition to caspases, IL-1β secretions have been shown to be high at 60 min post caspase activation, indicating that caspases have a regulatory role in IL-1β output. This was supported by studies involving the use of CASP4 and CASP1 CRISPR/Cas9 KO macrophages. While it is expected that caspase-1 have a critical role in cleaving IL-1β from its pro-form, CASP4 CRISPR/Cas9 KO macrophages also displayed reduced IL-1β. This reduced IL-1β levels was also seen with caspase-4 siRNA silenced cells as well. The Human Focused 13-Plex Cytokine/Chemokine Array provided a good idea of key cytokines/chemokines that could be modulated by caspase-4, including IL-8 and MCP-1, but would require further studies to confirm this. Further experiments including the nucleofection of the caspase-4 rescued IL-1β levels in CASP4 CRISPR/Cas9 KO macrophages with *Eh* stimulation as compared to controls (without caspase-4 nucleofection). In addition to using THP-1 macrophages, using another cell line, COS-7 cells that do not express ASC or NLRP3, the overexpression of caspase-4, -1, and IL-1β showed that they directly interact to enhance IL-1β secretions. This showed that caspase-4 and -1 directly interacted via enhancing the cleavage of the CARD domain to increase caspase-1 activity and subsequent IL-1β secretions. Using formaldehyde treatment to stabilize weak and transient interactions,

pro-caspase-4 was pulled down with pro-caspase-1 in a high molecular weight complex (92 kDa). In reverse, pro-caspase-1 was also pulled down with caspase-1 in a complex. Although caspase-4-caspase-1 interaction was not detected via mass spectrometry, the immunoblots provide strong evidence that they do interact.

Chapter Four: **Discussion and Conclusions**

4.1 Discussion of Results

4.1.1 *Human Caspase-4*

This is the first comparative study that addresses the distinct roles of inflammatory caspases in *Eh*-macrophage interaction in the regulation of IL-1β. The most intriguing fact about this parasite is that it can live in harmony with the host without causing any symptoms, but in a small number of infected individuals, it invades the mucosal barrier to cause disease. During *Eh* invasion, the immune response that is initiated by the host is a contributing factor that tips the balance between *Eh* clearance (resolution) and disease. Understanding why a raging tissue-damaging pro-inflammatory response occurs when *Eh* invades seem to be central in the early development of amebic lesions. At present, we have limited information on how this process is initiated. Although studies have investigated the role of caspases in *Eh* infection, none have addressed inflammatory caspase-4. For instance, caspase-3 has been shown to be involved in Jurkat T cell apoptosis induced by *Eh* [48]. Additionally, using a general caspase inhibitor in *Eh*-challenged mice results in smaller liver abscesses [177]. Petri *et al.* also showed that blocking K^+ channel activity and using specific inhibitors of caspase-1, -3, and a pan-caspase inhibitor protected HT-29 intestinal epithelial cells and THP-1 macrophages from amebic killing [178]. Prior studies in our laboratory have implicated caspase-1 and -6 in *Eh*-induced pro-inflammatory responses and in particular, IL-1β secretion [33,155,156]. My study has filled another gap in our knowledge of the pro-inflammatory response,

where activated caspase-4 has been shown to enhance the cleavage of caspase-1 to increase its bioactivity and to augment IL-1β secretions in response to live parasites.

We investigated three different aspects of caspase-4 within macrophages upon interaction with *Eh*: 1) is caspase-4 activated in a manner similar to caspase-1 using the same parasite factors, 2) does caspase-4 act upstream to regulate caspase-1 activation and IL-1β secretion or vice versa, and 3) is the function of caspase-4 distinct from caspase-1. A dose and time-dependent response with *Eh* stimulation showed that 1:20 *Eh* to macrophage ratio and 60 min was optimal for conducting experiments with *Eh*. To elucidate the parasite factors involved in caspase-4 activation, exogenous Gal-lectin was added to block *Eh* binding to macrophage surface. Moreover, *Eh*CP-A5^{-} was used to determine its involvement in caspase-4 activation. Using western blot, we found that the requirements for activating caspase-4 were the same as caspase-1 in that live *Eh* via Gal-lectin contact and *Eh*CP-A5 was necessary for initiating inflammatory caspase-4 and -1 activation in macrophage leading to high IL-1β output. The requirement of *Eh*CP-A5 is supported by Mortimer *et al.* showing that *Eh*CP-A5 RGD motif engages $\alpha_5\beta_1$ integrin to induce ATP release through pannexin-1 channels. This subsequently signals through the $P2X_7$ receptor to activate the NLRP3 inflammasome [155]. Preliminary experiments using RGD blocking peptide to block *Eh*CP-A5 engagement of $\alpha_5\beta_1$ integrin did not work We have attempted to use the RGD blocking peptide to determine its involvement in activating caspase-4, but we were unable to get inhibition of caspase-1 activation as shown by Mortimer *et al*. Further work would be required to optimize the dose of RGD blocking peptide.

The common signals that induce NLRP3 inflammasome activation include perturbations to ion concentrations such as the drop in cytosolic K^+ or the production of ROS. Potassium efflux has been shown to be the minimal requirement by many agonists to activate the NLRP3 inflammasome [179]. To investigate whether caspase-4 activation involves K^+ or ROS, we used exogenous KCl and DPI to alter K^+ and to block ROS generation, respectively. Our experiments demonstrated that a decrease in cytosolic K^+ or the production of ROS were also involved in caspase-4 processing. The same cellular changes were also observed for *Eh*-induced caspase-1 activation in the Mortimer *et al.*'s study [155].

The NLRP3 inflammasome has been well described as requiring the recruitment of ASC, NLRP3, and pro-caspase-1 into a high multimeric complex for the activation of caspase-1. Following this event, the pro-inflammatory cytokines IL-1β and IL-18 are cleaved into their bioactive form and secreted. To determine whether caspase-4 uses the same platform, we used NLRP3 CRISPR/Cas9 KO macrophages and THP-1 macrophages deficient in ASC. Our studies demonstrated *Eh*-induced caspase-4 activation and secretion was independent of NLRP3 and ASC, indicating that caspase-4 requires alternate proteins or it can be auto-catalytically cleaved upon dimerization. It has been shown that LPS can bind to the CARD domain of caspase-4, allowing it to undergo homo-oligomerization and activation [125]. It is unclear from these studies how caspase-4 is activated. CASP1 CRISPR/Cas9 KO macrophages stimulated with *Eh* have similar caspase-4 activation compared to WT macrophages, suggesting caspase-1 is not involved

in caspase-4 activation. Further studies are warranted to assess how caspase-4 activation occurs. Mass spectrometry would allow us screen for interacting partners and although we did perform this, there was no particular protein that was relevant in host-parasite interactions. Optimization of the protocol for sample preparation for mass spectrometry would be required before proceeding to examine specific proteins of interest.

In order to examine the role of caspase-4 in *Eh*-induced IL-1β production, we used the CASP4 CRISPR/Cas9 KO macrophages. CASP4 CRISPR/Cas9 KO macrophages stimulated with *Eh* had significantly reduced caspase-1 CARD domain and IL-1β secretions shown by western blotting, compared to WT macrophages. The release of bioactive IL-1β was also quantified using the SEAP assay and it was shown to be 50% less in the CASP4 CRISPR/Cas9 KO macrophages compared to WT macrophages. This led us to speculate that 1) caspase-4 can cleave IL-1β or 2) caspase-4 is interacting with caspase-1 to regulate IL-1β. Many studies have suggested that caspase-4 cannot cleave IL-1β [107,158,180] but caspase-4 can directly bind to caspase-1 and cleave it [120]. Based on these observations we speculated that caspase-1 could be a substrate for caspase-4. To test this hypothesis, we overexpressed caspase-4 in THP-1 macrophages and COS-7 cells.

Using caspase-4 deficient THP-1 macrophages, we overexpressed caspase-4 and stimulated with *Eh* and we found that this rescued both caspase-1 activation and IL-1β secretions. Furthermore, COS-7 cells with overexpressed caspase-4, caspase-1, and IL-1β also enhanced IL-1β release in response to *Eh*. These findings implicate an important role

for caspase-4 in regulating caspase-1 and this occurred by enhancing the cleavage of the CARD domain. Sollberger *et al.* demonstrated that when the caspase-4 cysteine residue was mutated, the protein lost its proteolytic function, therefore it is likely that caspase-1 activation by caspase-4 is mediated by the cysteine residue [121]. In order to test if the cysteine site is required for activation, future experiments would involve mutating this site and determining its effect on caspase-1 CARD domain cleavage and IL-1β secretion. In contrast to what Sollberger *et al.* reported with MSU in terms of IL-1β being reduced in caspase-4 knockdown [121], we saw no difference in IL-1β between the WT and CASP4 CRISPR/Cas9 KO macrophages when stimulated with MSU. Our studies suggest that caspase-4 enhancing effect is unique to *Eh,* and it is the live parasite that alerts the immune system to activate several effector molecules to trigger an appropriate response. Altogether, caspase-4 acts in a similar manner to NLRP3, where it is able to sense cellular perturbations to further activate caspase-1 to regulate IL-1β secretion. Thus, IL-1β secretions are dictated by two checkpoints. Caspase-4 is needed to boost caspase-1 activation only in the presence of live *Eh*. Caspase-1 activation alone, on the other hand, was sufficient to mount an immune response to MSU.

Caspases were originally categorized as involved in: 1) cell death or 2) regulating inflammatory processes, but there is emerging evidence to indicate that caspases have more than one function. For instance, caspase-8, unlike its conventional role in apoptosis, was shown to mediate IL-1β processing in response to *Candida albicans* and *Aspergillus fumigatus* in dendritic cells [145]. There are some other functions of caspase-4 that have been described in the field. Intracellular LPS and gram-negative bacterial pathogens have

been shown to activate caspase-4 [125,159]. Caspase-4 was found to be critical in mediating IL-1α and cell death in response to gram-negative pathogens, *Yersinia pseudotuberculosis, Salmonella enterica* serovar Typhimurium, and *Legionella pneumophila* [159]. To exclude a role for caspase-4 in mediating cell death, an LDH assay was performed with CASP4 CRISPR/Cas9 KO and CASP1 CRISPR/Cas9 KO macrophages. Cell death was not observed to be dependent on caspase-4 in response to *Eh* and neither did cell death differ among the caspase knockout macrophages.

As the raging pro-inflammatory response elicited upon *Eh* invasion is also characterized by the release of several other cytokines/chemokines, I quantified those that may be regulated by caspase-4 using a Human Focused-13 Plex Cytokine/Chemokine Array. Only two chemokines have been detected using this array and the other cytokines/chemokines were undetectable. In order to detect TNF-α levels and other chemokines, treatment with *Eh* would need to be extended to 3h. There was increased IL-8 production in both the CASP1 and CASP4 CRISPR/Cas9 KO macrophages compared to WT macrophages in response to *Eh*. Additionally, CASP1 CRISPR/Cas9 KO macrophages displayed increased MCP-1 compared to WT macrophages in response to *Eh*. Clearly further studies will be needed to confirm these results.

Studying protein-protein interactions when *Eh* forms an intercellular bridge with macrophages also provided clues for a better understanding of signaling processes in macrophages and mechanisms in *Eh* pathogenesis. After establishing that the presence of caspase-4, caspase-1, and IL-1β all interact to cleave pro-IL-1β into its active form, we

wanted to know if this occurred via direction interactions between caspase-4 and -1. To study caspase-4-caspase-1 interactions, formaldehyde was used as a cross-linker to stabilize weak and transient protein-protein interactions. Different conditions were performed to determine the optimal protocol for cross-linking caspase-4 and -1. These included varying formaldehyde concentrations (0 to 2%), reaction temperature (optimal at room temperature), and incubation times (maximum 10 min). The best formaldehyde concentration to yield the highest amount cross-linked complex was 0.8% and up. In addition to optimizing the protocol, several antibodies had to be tested to determine the suitable antibody to detect the protein after formaldehyde modification. The caspase-4 M-029-3 antibody that was used for all the earlier experiments was suitable for formaldehyde treated cells, however, a different caspase-1 antibody, sc-56036 that detects the pro-form and p10 was used for the detection of caspase-1 for formaldehyde treated cells. Caspase-4 and -1 cross-linked complexes was stabilized using formaldehyde treatment, allowing the interacting proteins to be clearly detected in pull-down studies using caspase-1 and -4 antibodies. Samples of caspase-4 cross-linked proteins were also sent for mass spectrometry, however caspase-1 was not detected. The reason for this could be the conditions optimized for immunoblot may not necessarily work for mass spectrometry. Another reason could be due to high levels of albumin contamination associated with the beads, as seen in the COS-7 cells experiment, that could have masked the detection of caspase-1. There were many other proteins that were detected, but the top 3 hits from the COS-7 cells did not seem to be potential routes to pursue from a host-parasite interactions perspective. It is more relevant to look at caspase-4 interacting

proteins in THP-1 macrophages, but in addition to that, COS-7 cells had high transfection efficiency for us to study if caspase-4 and -1 interacted independent of NLRP3 and ASC.

These studies underline the importance of inflammatory caspases in disease pathogenesis and its importance in alleviating *Eh* infection. Our study is the first to show that an extracellular parasite can induce caspase-4 activation. This suggests that there are several signals that are sensed by caspases. A schematic diagram depicting how *Eh* stimulates both caspase-4 and -1 independently to regulate high IL-1β output in macrophages is shown (**Figure 4.1**).

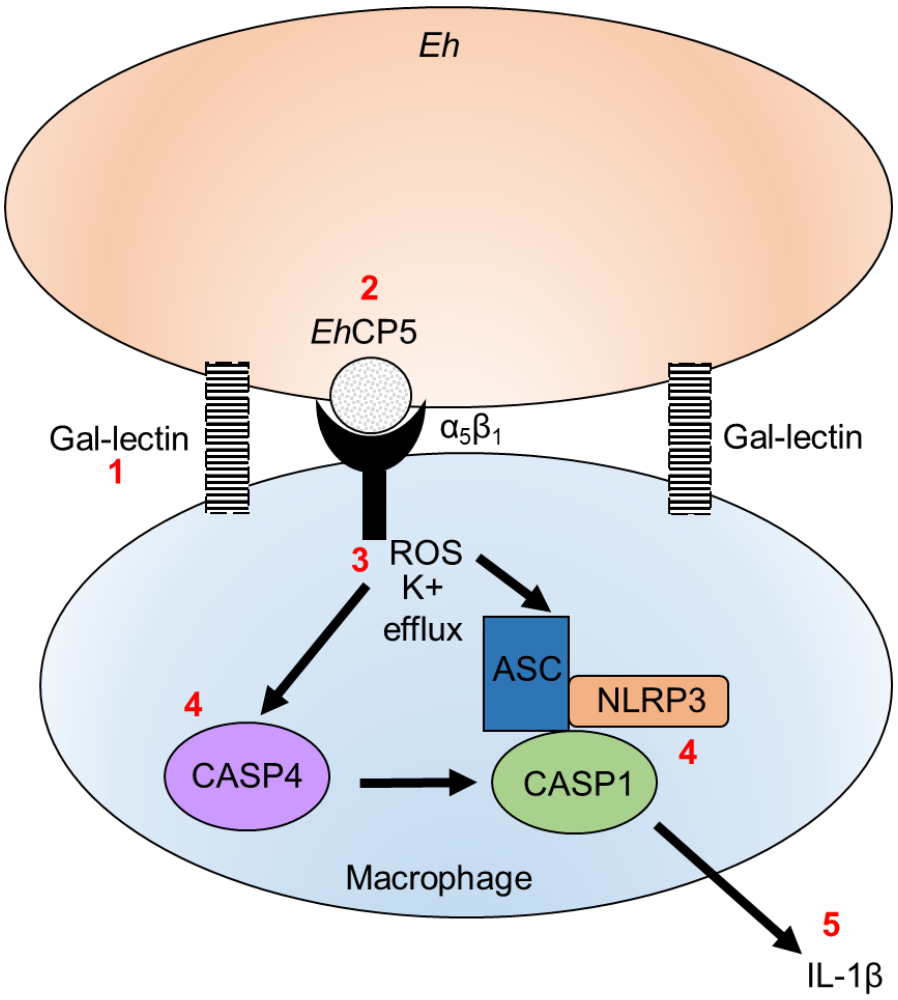

Figure 4.1 Schematic representation of *E. histolytica*-macrophage interaction and induction of caspase-4 and -1 activation.

The first step of caspase activation is *Eh* adherence to macrophage contact via the Gal-lectin adhesin that binds to Gal/GalNAc residues on the macrophage surfaces (1). *Eh*CP5 is a cysteine protease that is highly expressed on the surface of *Eh* and was shown to activate both caspase-4 and -1 (2). *Eh*CP5 binds to $\alpha_5\beta_1$ integrin on macrophage surface to activate the NLRP3 inflammasome. K^+ efflux and the generation of reactive oxygen species then converge to activate the NLRP3 inflammasome and caspase-4 (3). Caspase-4 is simultaneously activated with caspase-1 (4) and caspase-4 enhances caspase-1 activity by cleaving the caspase-1 CARD domains independent of the inflammasome complex to regulate IL-1β activation (5).

4.1.2 *Murine Caspase-11*

Some of the studies that were performed with human macrophages to examine caspase-4 were repeated in mouse BMDMs to examine caspase-11 including dose and time-dependent experiments. To determine the optimal dose and time of *Eh* treatment for the activation of both caspase-11 and -1, *Eh* was added for 5, 30, and 60 min to macrophages and at 1:40, 1:20, and 1:10 ratios. In contrast to caspase-4, caspase-11 activation was seen as early as 5 min in both the lysates and supernatants and did not parallel that of caspase-1 activation. Caspase-1 activation and secretion did not appear until 60 min. It was difficult to detect caspase-1 p20 activation and IL-1β secretions in the supernatants consistently with *Eh* stimulation, therefore optimization is required to determine the best *Eh* to macrophage ratio or to increase the number of wells pooled per treatment. Caspase-11 was detectable upon *Eh* stimulation, but the bands were saturated and this could have masked subtle differences between the different time points. Therefore, loading less supernatant may better help differentiate the time points. Interestingly, some papers have reported the p26 subunit using the same antibody [118], caspase-11 17D9, however, we were unable to detect this band for *Eh* or LPS and CTB stimulation due to degradation or because there was too little protein to be detected. We have also determined that caspase-11 activation was dependent on both Gal-lectin binding and *Eh*CP-A5, which is similar to caspase-4.

The IL-1β ELISA is a standard assay used in the field to examine inflammasome activation as it is a readout of caspase-1 activation. Some of the earlier studies that we

performed with BMDMs involved using the IL-1β ELISA and attempts were made to elucidate the effects of *Casp1*$^{-/-}$*Casp11*$^{-/-}$ and *Casp-11*$^{-/-}$ on IL-1β secretions in response to *Eh*. *Casp1*$^{-/-}$*Casp11*$^{-/-}$ BMDMs displayed comparable levels of IL-1β with the *Casp1*$^{+/+}$*Casp11*$^{+/+}$ BMDMs in response to *Eh* stimulation. In contrast, western blots indicated that there was no IL-1β present in the *Casp1*$^{-/-}$*Casp11*$^{-/-}$ BMDMs. The results of the IL-1β ELISA did not support the western blots and this could due to the detection of pro-IL-1β in cell supernatants using the IL-1β ELISA. Thus, it was concluded that with the success of the use of HEK-IL-1β reporter cells, the availability of a cell line for animal studies would be valuable to interrogate the bioactive levels of IL-1β in BMDMs.

The NLRP3 sensor and ASC adaptor are important for activating caspase-1, and we were interested in knowing whether it was also important for activating caspase-11. To determine whether *Eh*-induced caspase-11 activation depended on NLRP3 and ASC, we used *Nlrp3*$^{-/-}$ BMDMs and *Asc*$^{-/-}$ BMDMs. Caspase-11 activation, similar to caspase-4, occurred independently of NLRP3 and ASC. Interestingly, the murine ortholog of human caspase-4, caspase-11 was shown to also enhance caspase-1 processing and IL-1β production in response to *Escherichia coli* and cholera toxin B [118]. To determine whether caspase-11 is involved in caspase-1 activation, we used *Casp11*$^{-/-}$ BMDMs stimulated with *Eh* for different time points. In response to *Eh*, caspase-11 did not seem to play a role in mediating caspase-1 p20 activation. Altogether, these studies suggest that caspase-4 and -11 may play different roles in inflammation, each interacting with different proteins or regulating different cytokine/chemokines. Further studies are needed to address this.

In addition to utilizing BMDMs, examining IL-1β secretions in *Casp-11*$^{-/-}$ ameba colonic loop models would lend further clues as to whether there is any regulatory role for caspase-11 in IL-1β secretions. If there is evidence for caspase-11 in regulating IL-1β secretions, the next question would be to ask if it is through caspase-1 interaction or if caspase-11 can cleave IL-1β. Using a relevant animal model like mice can unravel the role of the caspases in the context of disease, in this case amebiasis. Furthermore, elucidating the relationship between human caspase-4 and murine caspase-11 is important in helping to understand whether mice models are useful for understanding the human inflammatory conditions.

The novelty of these studies is that there is cross talk between caspase-4 and -1. The activation of these inflammatory caspases is shown to be induced by an extracellular parasite through outside-in signaling. Elucidating the inflammatory caspase-caspase interacting proteins have been important not only for understanding *Eh* pathogenesis, but also on how inflammation is regulated in infectious and inflammatory diseases. NLRP3 inflammasome and specifically caspase-1 has been implicated in a variety of conditions including sepsis and inflammatory bowel disease [104,181]. As current knowledge of caspase-4 biology in inflammatory diseases is limited, our study highlights a critical role of this protein in amplifying IL-1β secretion. Since caspase-4 plays an essential role in mediating caspase-1 bioactivity, it poses to be a novel therapeutic target for treating uncontrolled inflammation.

4.1.3 *Applications of Research Findings*

It is important that *in vitro* studies can be translated to human diseases and we are particularly interested in amebiasis. Patients with amebic colitis display various clinical manifestations including diarrhea, bloody stool, and abdominal pain [182]. Endoscopic findings reveal inflamed colons and multiple ulcers attributed to *Eh* invasion and host immune responses. These clinical results reflect the many different interactions happening at the cellular level between host and the parasite and among host cells themselves that drive disease pathogenesis. With this in perspective, it shows how the early host immune response is vital for resolving *Eh* infections. My studies addressed several novel targets from the parasite and/or host that can help with treating the disease or aid in vaccine development.

In our study we showed that *Eh* Gal-lectin-mediated contact is the critical first step in eliciting the activation of inflammasome and caspase-4. Thus, limiting *Eh* contact with host cells during colonization in the colon could be a strategy to inhibit disease. In this regard, the Gal-lectin is the best candidate for generating neutralizing/blocking antibodies as a vaccine candidate to limit colonization and prevent against disease. On the host side, this study brought to light that caspase-4 is another sensor for detecting and responding to live parasites during tissue invasion and could be a novel target to develop intervention strategies to control inflammation. Currently there is no specific caspase-4 inhibitor available. In fact, no caspase inhibitory drugs are available on the market [183,184]. As the output that is regulated by caspase-4 is IL-1β, targeting IL-1β could be a promising

therapeutic approach. Canakinumab, a human anti-IL-1β monoclonal antibody has been approved for use as treatment of Familial Cold Auto inflammatory Syndrome and Muckle-Wells Syndrome [185], and therefore can be used to control inflammation in amebiasis. Importantly, the inhibitors would need to be tested in an *in vivo* model of invasive amebiasis and in the field for clinical efficacy.

4.1.4 *Technical Limitations in Studying Caspase-4*

We tried different approaches to examine caspase-4 and to study its function in inflammation. The most relevant technique to use for studying caspase-4 is western blotting to determine protein levels because caspase-4 is a protease and is modified post-translationally by cleavage. However, we have experienced inconsistencies in western blots from each experiment. To overcome this, we have tried to maintain similar conditions and repeated more experiments. For most publications in this field, only representative blots are shown, however, for subtle differences, it is necessary to apply densitometric analyses to establish any significant results. In our studies, it has been particularly tricky to quantify caspase-4, since the active intermediate forms appear as a triplet band rather than one band. Moreover, the bands do not necessarily all appear consistently and it is difficult to separate the bands for analysis. Despite this, we have applied densitometric analyses for many experiments to allow for greater confidence in the data.

A second approach to examine caspase-4 is to measure its proteolytic activity since one of its function is to cleave substrates ending with the residues LEVD. The rationale for utilizing this assay was to study caspase-4 activity to correlate caspase-4 protein activation by western blot, as cleavage of the intermediate forms does not always equate to caspase activation. In order to measure caspase enzymatic activity, the 7-amino-4-trifluoromethyl coumarin (AFC)-LEVD (as a probe for caspase-4) or AFC-YVAD (as a probe for caspase-1) [100] have been used. However, when we attempted to use the caspase-4 enzymatic assay, both the positive and negative controls were not working. Different controls would need to be used for optimizing the assay first before proceeding with *Eh* stimulation. Other controls that could be used include ATP treatment or transfecting LPS into macrophages.

A third approach that we used to study caspase-4 is through the use of pharmacological inhibitors. We realized though that the use of pharmacological inhibitors is not the ideal method to tease out differences between caspases because the substrates overlap. This was observed when we utilized the caspase-4 inhibitor, Z-LEVD-FMK (Enzo Life Sciences, ALX-260-142-R100). In the caspase-4 CRISPR/Cas9 KO macrophages, we used the caspase-4 inhibitor and found that it also inhibited caspase-1 activation. Although substrates are useful in studying purified caspases, it becomes more complicated for cell lysates because cells express a variety of caspases. Substrates are not specific for one caspase and this was also reported by several other groups [129,132].

When CRISPR/Cas9 gene editing was not available, we relied on utilizing siRNA knockdown of caspase-4 to elucidate its function. A limitation to siRNA knockdown is the difficulty in achieving a high percentage of transfection and silencing required to see its downstream effects. As evident from our studies, caspase-4 siRNA knockdown did not change caspase-1 CARD levels, but we saw reduced IL-1β levels, indicating that even the presence of a small quantity of caspase-4 can alter caspase-1 CARD levels. In this case, we saw that the presence of caspase-4 was able to cleave the caspase-1 CARD domain in the caspase-4 siRNA knockdown and the levels seen were comparable to scrambled siRNA with *Eh* stimulation. When we obtained the CASP4 CRISPR/Cas9 KO cells, we were able to clearly elucidate that caspase-1 CARD was reduced in the CASP4 CRISPR/Cas9 KO macrophages when stimulated with *Eh*. The results obtained from using CASP4 CRISPR/Cas9 KO macrophages clarified the caspase-4 siRNA experiments and brought to light that caspase-1 CARD was actually reduced in the caspase-4 deficient macrophages compared to WT. It provided another line of evidence that IL-1β levels are reduced in the absence of caspase-4.

For earlier studies, we used an IL-1β ELISA as the main assay for measuring IL-1β secretions in macrophages stimulated with *Eh*. However, it was difficult to achieve consistency between experiments. An explanation for this is that the IL-1β ELISA uses two antibodies that may recognize both pro-IL-1β and IL-1β, and therefore should not be used as a measurement of bioactive IL-1β. As a test for usability of the ELISA, caspase-1 CRISPR/Cas9 KO macrophages were stimulated with *Eh* and the supernatants were used to determine IL-1β levels. Surprisingly, there were similar levels of IL-1β in the CASP1

CRISPR/Cas9 KO compared to WT macrophages. It is expected that IL-1β levels are reduced in CASP1 CRISPR/Cas9 KO macrophages because it was observed to be absent by western blotting. In place of the IL-1β ELISA, the HEK-IL-1β reporter cells were used for all subsequent studies, as it is more specific in measuring only bioactive IL-1β levels through the production of SEAP. The SEAP assay yielded much more consistency between experiments and when we used the CASP1 CRISPR/Cas9 KO macrophages, there was 90% significantly less IL-1β secretions, which supports our previous finding that *Eh*-induced IL-1β secretion is dependent on caspase-1 [156].

Although we have elucidated an important role for caspase-4 in enhancing IL-1β activation, we do not know whether the effects are significant in an *in vivo* context. For instance, we do not know whether the enhanced IL-1β response would help clear *Eh* infection or even how it alters the pro-inflammatory response because there are multiple other immune cells, cytokines, and chemokines that could be at play as well. Existing models for *Eh* infection include gerbils for amebic liver abscesses and the colonic loop model is suitable as an early acute inflammatory response model. Although our studies have highlighted that caspase-11 may not be a direct ortholog of caspase-4, it would still be valuable to explore whether *Casp11*$^{-/-}$ mice have any alterations to IL-1β compared to *Casp11*$^{+/+}$ mice injected with *Eh* in colonic loops.

4.2 Future Directions

4.2.1 *Determining the Domains for Caspase-4 and -1 Interaction*

In our pull-down studies, we have shown that caspase-4 and -1 interact, but there are still many unanswered questions as to where they interact. Although it was reported that the p20 of caspase-4 binds to the p20 of caspase-1 [121], it is unclear which domains interact under *Eh* stimulation. Using CASP4 CRISPR/Cas9 KO macrophages, full-length caspase-1 could be pulled-down and subsequently be exposed to recombinant caspase-4 to quantify the cleavage sites by sequencing. Alternatively, constructs of the possible cleaved domains on caspase-1 (including different CARD cleavages and p20 and p10 subunits) could be designed based on caspase-4 preferential cleavage site, LEVD [109] and transfected into COS-7 cells. Following that, immunoprecipitation of the different caspase-1 constructs would be performed and then immunoblotting for caspase-4 would allow us to determine the specific domain that is important for interacting with caspase-4. To further investigate caspase-4-caspase-1 interaction, constructs of caspase-4 can be generated in the same way to determine the specific caspase-4 domain that directly interacts with caspase-1.

Inflammatory caspase activation happens quite rapidly and is exported into the extracellular space. To determine the sequence of events that occur during the cleavage of caspase-1 by caspase-4, different cleavage sites on caspase-1 could be mutated and then IL-1β levels could be quantified. This would lend clues to the rate-limiting step in this proteolytic cascade, as it is unclear whether cleavages of each subunit occur at the same

time or whether one occurs before the next. To explore whether caspase-4 activity is necessary for caspase-1 activation, the catalytic cysteine site (285) could also be mutated to an alanine residue. The mutated caspase-4 plasmid could be transfected along with caspase-1 and IL-1β in COS-7 cells, stimulated with *Eh* and the proteins would be detected via immunoblot and IL-1β via the SEAP assay. This would provide evidence that the cysteine site is the critical residue for mediating enzymatic activity to enhance caspase-1 bioactivity. In our studies we have only used caspase-1 sc-622 antibody to detect the CARD domain, but it would be interesting to determine if the p20 and p10 subunits protein levels align with that of the CARD as it is the formation of the heterotetramer that exhibits proteolytic activity.

4.2.2 *Studying Inflammasomes in Other Cells*

THP-1 cells are a human acute monocytic leukemia cell line isolated from a 1-year old male and they have been used extensively to study monocyte and macrophage functions [186]. The most effective differentiation reagent for THP-1 cells to differentiate into macrophages is PMA. THP-1 macrophages are known to be the best model for studying inflammasomes because they highly express NLRP3, ASC, and pro-caspase-1. Alternatives to THP-1 macrophages include human peripheral blood mononuclear cells (PMBCs), however, it is associated with drawbacks such as high variability from donors, slower growth rate, and limited availability of PMBCs as they cannot be stored in liquid nitrogen [187]. In addition to THP-1 macrophages, there is increasing evidence for the importance of inflammasomes in epithelial cells. In particular, Knodler *et al.* examined

the role of non-canonical caspase-4 inflammasome in epithelial cells in extruding *Salmonella* [126]. Although *Eh* is an extracellular parasite, it has the ability to induce outside-in signaling as seen with this study and since epithelial cells are the first to make contact with *Eh*, it is also critical to study epithelial defenses in disease pathogenesis. Although IL-18 was not explored in this study, it may be more apparent in caspase-4 activation in epithelial cells.

4.2.3 *The Role of Caspase-4 in Other Pathogen Models or Inflammatory Diseases*

An interesting question to answer is whether other pathogens could activate caspase-4 to trigger the same pathway of caspase-1 activation or if this role is unique to *Eh* or even extracellular pathogens in general. There are a plethora of parasites that activate the inflammasome including *Plasmodium* [188], *Trypanosoma* [189], and *Toxoplasma* [190], so it is worth investigating whether the function of caspase-4 in regulating caspase-1 is conserved across different pathogens. Malaria has one of the highest rates of morbidity and mortality worldwide due to a parasite, accounting for 730,500 deaths in 2015, so application to other parasites may be beneficial [191]. Interestingly, increased caspase-4 and -5 expression are observed in inflamed and dysplastic tissue of patients with colitis-associated colorectal cancer [192]. Investigating whether IL-1β levels differ in inflamed tissues versus controls would also lend some insight into whether secretions of this cytokine is driven by caspase-4 and -1 as well. Understanding whether this caspase-4-caspase-1-IL-1β pathway is operating in other diseases can definitely shed light on therapeutic options for controlling inflammation.

4.2.4 *Studying Other Inflammatory Caspases*

Caspase-5 is another inflammatory caspase that shares high homology to human caspase-4, caspase-1, and murine caspase-11, so it would be an important avenue of research because the understanding of caspase-5 is even more limited compared to caspase-4. Caspase-5 is expressed in macrophages. Caspase-5 was shown to bind to LPS via its CARD domain, similar to caspase-4 and caspase-11 [125]. It was also reported to be important in regulating cell death and IL-1β in response to *Salmonella typhimurium* in THP-1 monocytes [166]. Interestingly, double deletion of both caspase-5 and -4 resulted in greater IL-1β reduction [166]. Moreover, a recent study showed that caspase-5 functions independently of ASC to activate IL-1β [193]. ASC deficient keratinocytes that were UVB-irradiated had induced caspase-5 expression and IL-1β release [193]. These studies indicate that there may be functional redundancies between caspase-4 and -5. It would be interesting to assess whether caspase-5 and -4 cross talk by immunoblotting for caspase-5 in CASP4 CRISPR/Cas9 to determine any potential interactions and if they act synergistically to regulate IL-1β secretions.

4.3 Conclusions

Inflammasomes were first discovered in 2002 and the discoveries made to date have advanced out understanding of how host immune defenses are activated upon pathogenic and sterile insults. Identifying alternate pathways of caspase-1 regulation is central to understanding how the pro-inflammatory response contributes to ameba pathogenesis.

My studies examined both the parasite requirements for activating caspase-4 and the role of caspase-4 in regulating IL-1β secretions. This is a huge progression not only for the field of inflammasomes, but also for amebiasis. Although amebiasis still remains a problem worldwide today, advances in molecular biology have allowed for a better understanding of *Eh* pathogenesis and have shed light on the complexities of host-parasite interactions. Although there are currently no clinical trials for an *Eh* vaccine, early studies on potential vaccine candidates have been explored. The conclusions of our studies exploring the molecular mechanisms of *Eh* pathogenesis have provided novel insights into therapeutic targets for limiting disease and inflammation.

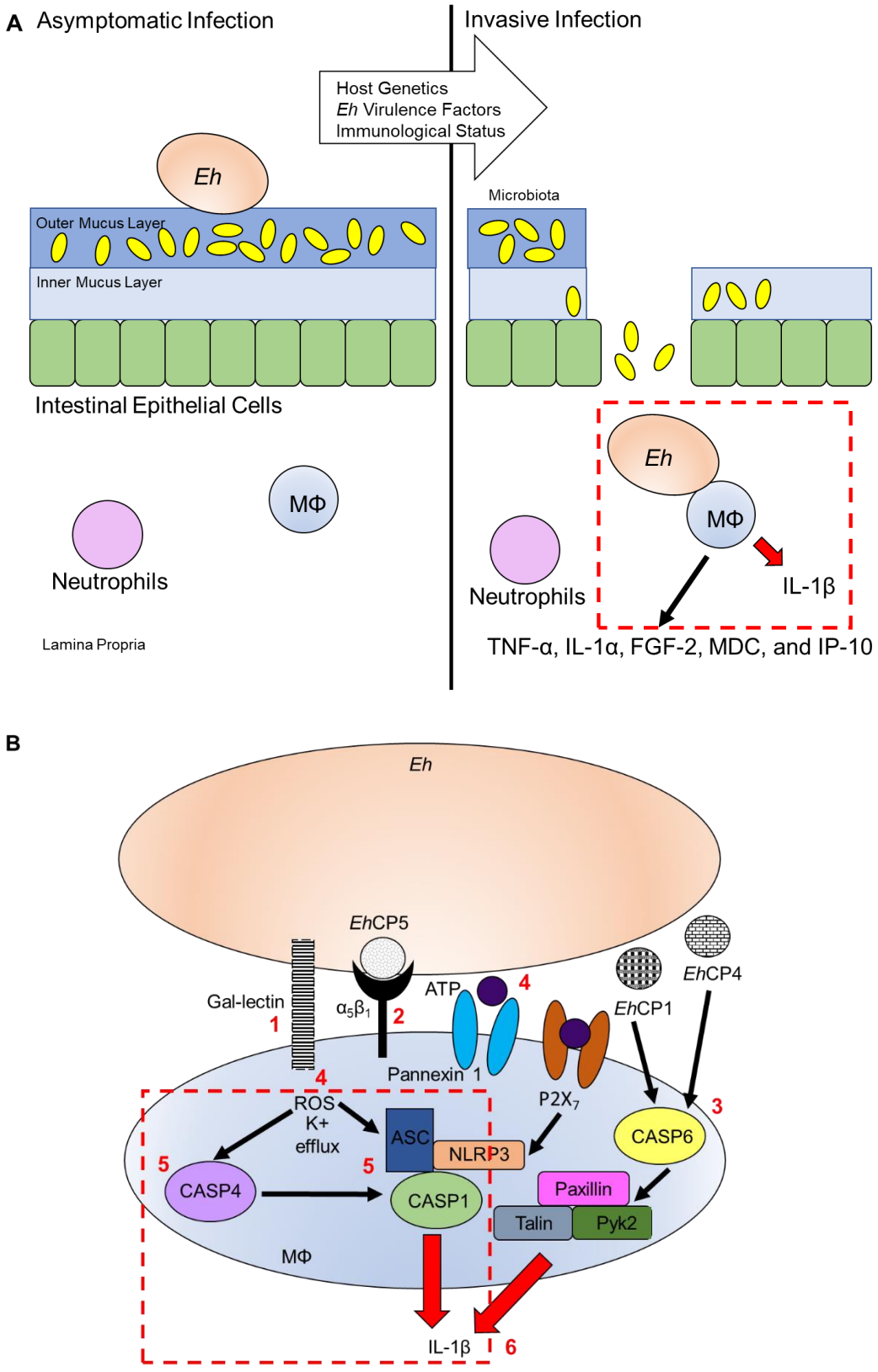
A
Asymptomatic Infection
Invasive Infection
Host Genetics
Eh Virulence Factors
Immunological Status
Eh
Outer Mucus Layer
Inner Mucus Layer
Intestinal Epithelial Cells
Microbiota
MΦ
Neutrophils
Lamina Propria
Eh
MΦ
Neutrophils
IL-1β
TNF-α, IL-1α, FGF-2, MDC, and IP-10
B
Eh
EhCP5
EhCP4
EhCP1
Gal-lectin
1
α5β1
2
ATP
4
Pannexin 1
4
P2X7
ROS
K+
efflux
ASC
NLRP3
CASP6
3
5
5
CASP4
CASP1
Paxillin
Talin
Pyk2
MΦ
IL-1β
6

Figure 4.2 Conceptual diagrams of how my research findings fit in the pathogenesis of amebiasis.

(A) In asymptomatic infection, *Eh* colonizes the colon by binding of the Gal-lectin adhesion to galactose and *N*-acetyl galactosamine residues of MUC2 mucin. Here the parasite feeds on bacteria and dead slough cells and patients show no symptoms of disease. During *Eh* invasion, *Eh* degrades the mucus bilayers through cysteine proteases and glycosidases allowing the parasite to make contact with mucosal epithelial cells. Susceptibility to invasion is due to various factors including host genetics, *Eh* virulence factors and immunological status of the host. When *Eh* breaches the surface epithelial cells it encounters several immune cells in the lamina propria including neutrophils and macrophages. The key interaction during this early invasion are *Eh*-macrophage interactions and the production of many cytokines/chemokines including IL-1α, FGF-2, MDC, IP-10, and TNF-α. Of importance is high-output IL-1β secretion (dash box in red). (B) *Eh* first makes contact with a macrophage via binding through the Gal-lectin adhesin (1), followed by the *Eh*CP-A5 ligation of α5β1 integrin (2) and then the activation of various signaling pathways. The earliest pathway that is activated is caspase-6 mediated degradation of cytoskeletal proteins including paxillin, talin, and Pyk2 occurring within 5 min. Several cellular events subsequently occur during the next 30 min including the release of ATP through the pannexin-1 channel that signals back through the $P2X_7$ receptor, K^+ efflux, and the generation of ROS (4), followed by the activation of caspase-4 and the NLRP3 inflammasome consisting of the recruitment of NLRP3, ASC, and pro-caspase-1 (5). The resulting IL-1β secretion (6) is the final output of the various different signaling pathways. My studies have made the intriguing finding that only live parasite can activate caspase-4, which in turn amplifies caspase-1 activation for high output IL-1β production (dash box in red).

4.4 References

1. Naghavi M, Wang H, Lozano R, Davis A, Liang X, Zhou M, et al. Global, regional, and national age-sex specific all-cause and cause-specific mortality for 240 causes of death, 1990-2013: A systematic analysis for the Global Burden of Disease Study 2013. Lancet. 2015;385: 117–171.
2. Tanyuksel M, Petri WA. Laboratory diagnosis of amebiasis. Clin Microbiol Rev. 2003;16: 1–18.
3. Espinosa-Cantellano M, Martínez-Palomo A. Pathogenesis of intestinal amebiasis: from molecules to disease. Clin Microbiol Rev. 2000;13: 318–331.
4. Prathap K, Gilman R. The histopathology of acute intestinal amebiasis. A rectal biopsy study. Am J Pathol. 1970;60: 229–246.
5. WHO. Amebiasis. Wkly Epidemiol Rec. 1997;7: 97–100.
6. Ximénez C, Morán P, Rojas L, Valadez A, Gómez A. Reassessment of the epidemiology of amebiasis: state of the art. Infect Genet Evol. 2009;9: 1023–1032.
7. Mondal D, Haque R, Sack RB, Kirkpatrick BD, Petri WA. Short report: attribution of malnutrition to cause-specific diarrheal illness: evidence from a prospective study of preschool children in Mirpur, Dhaka, Bangladesh. Am J Trop Med. 2009;80: 824–826.
8. Duggal P, Guo X, Haque R, Peterson KM, Ricklefs S, Mondal D, et al. A mutation in the leptin receptor is associated with *Entamoeba histolytica* infection in children. J Clin Invest. 2011;121: 1191–1198.
9. Korpe PS, Stott BR, Nazib F, Kabir M, Haque R, Herbein JF, et al. Short report:

Evaluation of a rapid point-of-care fecal antigen detection test for *Entamoeba histolytica*. Am J Trop Med Hyg. 2012;86: 980–981.

10. Mortimer L, Chadee K. The immunopathogenesis of *Entamoeba histolytica*. Exp Parasitol. 2010;126: 366–380.
11. Chadee K, Johnson ML, Orozco E, Petri WA, Ravdin JI. Binding and internalization of rat colonic mucins by the galactose/N-acetyl-D-galactosamine adherence lectin of *Entamoeba histolytica*. J Infect Dis. 1988;158: 398–406.
12. Petri WA, Chapman MD, Snodgrass T, Mann BJ, Broman J, Ravdin JI. Subunit structure of the galactose and N-acetyl-D-galactosamine-inhibitable adherence lectin of *Entamoeba histolytica*. J Biol Chem. 1989;264: 3007–3012.
13. Pillai DR, Wan PSK, Yau YCW, Ravdin JI, Kain KC. The cysteine-rich region of the *Entamoeba histolytica* adherence lectin (170-kilodalton subunit) is sufficient for high-affinity Gal/GalNac-specific binding in vitro. Infect Immun. 1999;67: 3836–3841.
14. Chadee K, Petri WA, Innes DJ, Ravdin JI. Rat and human colonic mucins bind to and inhibit adherence lectin of *Entamoeba histolytica*. J Clin Invest. 1987;80: 1245–1254.
15. Bracha R, Mirelman D. Adherence and ingestion of *Escherichia coli* serotype 055 by trophozoites of *Entamoeba histolytica*. Infect Immun. 1983;40: 882–887.
16. Ravdin JI, Guerrant RL. Role of adherence in cytopathogenic mechanisms of *Entamoeba histolytica*. Study with mammalian tissue culture cells and human erythrocytes. J Clin Invest. 1981;68: 1305–1313.
17. Abd-Alla MD, Jackson TFGH, Rogers T, Reddy S, Ravdin JI. Mucosal immunity

to asymptomatic *Entamoeba histolytica* and *Entamoeba dispar* infection is associated with a peak intestinal anti-lectin immunoglobulin A antibody response. Infect Immun. 2006;74: 3897–3903.

18. Ravdin JI, Abd-alla MD, Welles SL, Reddy S, Jackson TFHG. Intestinal antilectin immunoglobulin A antibody response and immunity to *Entamoeba dispar* infection following cure of amebic liver abscess. Infect Immun. 2003;71: 6899–6905.

19. Haque R, Ali IM, Sack RB, Farr BM, Ramakrishnan G, Petri WA. Amebiasis and mucosal IgA antibody against the *Entamoeba histolytica* adherence lectin in Bangladeshi children. J Infect Dis. 2001;183: 1787–1793.

20. Haque R, Duggal P, Ali IM, Hossain MB, Mondal D, Sack RB, et al. Innate and acquired resistance to amebiasis in Bangladeshi children. J Infect Dis. 2002;186: 547–552.

21. Petri WA, Ravdin JI. Protection of gerbils from amebic liver abscess by immunization with the galactose-specific adherence lectin of *Entamoeba histolytica*. Infect Immun. 1991;59: 97–101.

22. Soong C-J, Kain KC, Abd-Alla M, Jackson TFHG, Ravdin JI. A recombinant cysteine-rich section of the *Entamoeba histolytica* galactose-inhibitable lectin is efficacious as a subunit vaccine in the gerbil model of amebic liver abscess. J Infect Dis. 1995;171: 645–651.

23. Abd-alla MD, Jackson TFGH, Soong GC, Mazanec M, Ravdin JI. Identification of the *Entamoeba histolytica* galactose-inhibitable lectin epitopes recognized by human immunoglobulin A antibodies following cure of amebic liver abscess.

Infect Immun. 2004;72: 3974–3980.

24. Ivory CPA, Chadee K. Activation of dendritic cells by the Gal-lectin of *Entamoeba histolytica* drives Th1 responses in vitro and in vivo. Eur J Immunol. 2007;37: 385–394.

25. Séguin R, Mann BJ, Keller K, Chadee K. Identification of the galactose-adherence lectin epitopes of *Entamoeba histolytica* that stimulate tumor necrosis factor-alpha production by macrophages. Proc Natl Acad Sci USA. 1995;92: 12175–12179.

26. Campbell D, Mann BJ, Chadee K. A subunit vaccine candidate region of the *Entamoeba histolytica* galactose-adherence lectin promotes interleukin-12 gene transcription and protein production in human macrophages. Eur J Immunol. 2000;30: 423–430.

27. Kammanadiminti SJ, Mann BJ, Dutil L, Chadee K. Regulation of Toll-like receptor-2 expression by the Gal-lectin of *Entamoeba histolytica*. FASEB. 2003;18: 155–185.

28. Reed SL, Keene WE, McKerrow JH. Thiol proteinase expression and pathogenicity of *Entamoeba histolytica*. J Clin Microbiol. 1989;27: 2772–2777.

29. Bruchhaus I, Loftus BJ, Hall N, Tannich E. The intestinal protozoan parasite *Entamoeba histolytica* contains 20 cysteine protease genes, of which only a small subset is expressed during in vitro cultivation. Eukaryot Cell. 2003;2: 501–509.

30. Lidell ME, Moncada DM, Chadee K, Hansson GC. *Entamoeba histolytica* cysteine proteases cleave the MUC2 mucin in its C-terminal domain and dissolve the protective colonic mucus gel. Proc Natl Acad Sci U S A. 2006;103: 9298–9303.

31. Hou Y, Mortimer L, Chadee K. *Entamoeba histolytica* cysteine proteinase 5 binds

integrin on colonic cells and stimulates NFκB-mediated pro-inflammatory responses. J Biol Chem. 2010;285: 35497–35504.

32. Cornick S, Moreau F, Chadee K. *Entamoeba histolytica* cysteine proteinase 5 evokes mucin exocytosis from colonic goblet cells via αvβ3 integrin. PLoS Pathog. 2016;12: 1–24.

33. St-Pierre J, Moreau F, Cornick S, Quach J, Begum S, Aracely Fernandez L, et al. The macrophage cytoskeleton acts as a contact sensor upon interaction with *Entamoeba histolytica* to trigger IL-1β secretion. PLoS Pathog. 2017;13: e1006592.

34. Garcia-Nieto RM, Rico-Mata R, Arias-Negrete S, Avila EE. Degradation of human secretory IgA1 and IgA2 by *Entamoeba histolytica* surface-associated proteolytic activity. Parasitol Int. 2008;57: 417–423.

35. Kelsall BL, Ravdin JI. Degradation of Human IgA by *Entamoeba histolytica*. J Infect Dis. 1993;168: 1319–1322.

36. Zhang Z, Yan L, Wang L, Seydel KB, Li E, Ankri S, et al. *Entamoeba histolytica* cysteine proteinases with interleukin-1 beta converting enzyme (ICE) activity cause intestinal inflammation and tissue damage in amoebiasis. Mol Microbiol. 2000;37: 542–548.

37. Leippe M, Andra J, Nickel R, Tannich E, Muller-eberhard HJ. Amoebapores, a family of membranolytic peptides from cytoplasmic granules of *Entamoeba histolytica*: isolation, primary structure, and pore bacterial cytoplasmic membranes. Mol Microbiol. 1994;14: 895–904.

38. Bracha R, Nuchamowitz Y, Leippe M, Mirelman D. Antisense inhibition of

amoebapore expression in *Entamoeba histolytica* causes a decrease in amoebic virulence. Mol Microbiol. 1999;34: 463–472.

39. Zhang X, Zhang Z, Alexander D, Bracha R, Mirelman D, Stanley SL. Expression of amoebapores is required for full expression of *Entamoeba histolytica* virulence in amebic liver abscess but is not necessary for the induction of inflammation or tissue damage in amebic colitis. Infect Immun. 2004;72: 678–683.

40. Stenson WF, Zhang Z, Riehl T, Stanley J. Amebic infection in the human colon induces cyclooxygenase-2. Infect Immun. 2001;69: 3382–3388.

41. Dey I, Keller K, Belley A, Chadee K. Identification and characterization of a cyclooxygenase-like enzyme from *Entamoeba histolytica*. Proc Natl Acad Sci U S A. 2003;100: 13561–13566.

42. Lejeune M, Moreau F, Chadee K. Prostaglandin E2 produced by *Entamoeba histolytica* signals via EP4 receptor and alters claudin-4 to increase ion permeability of tight junctions. Am J Pathol. 2011;179: 807–818.

43. Dey I, Chadee K. Prostaglandin E2 produced by *Entamoeba histolytica* binds to EP4 receptors and stimulates interleukin-8 production in human colonic cells. Infect Immun. 2008;76: 5158–5163.

44. Orozco E, Guarneros G, Martínez-Palomo A, Tomas S. *Entamoeba histolytica* phagocytosis as a virulence factor. J Exp Med. 2010;158: 1511–1521.

45. Rodriguez MA, Orozco E. Isolation and characterization of phagocytosis- and virulence-deficient mutants of *Entamoeba histolytica*. J Infect Dis. 1986;154: 27–32.

46. Sateriale A, Vaithilingam A, Donnelly L, Miller P, Huston CD. Feed-forward

regulation of phagocytosis by *Entamoeba histolytica*. Infect Immun. 2012;80: 4456–4462.

47. Huston CD, Boettner DR, Miller-Sims V, Petri WA. Apoptotic killing and phagocytosis of host cells by the parasite *Entamoeba histolytica*. Infect Immun. 2003;71: 964–972.

48. Huston CD, Houpt ER, Mann BJ, Hahn CS, Petri WA. Caspase 3-dependent killing of host cells by the parasite *Entamoeba histolytica*. Cell Microbiol. 2000;2: 617–625.

49. Ragland BD, Ashley LS, Vaux DL, Petri WA. *Entamoeba histolytica*: Target cells killed by trophozoites undergo DNA fragmentation which is not blocked by Bcl-2. Exp Parasitol. 1994;79: 460–467.

50. González-Ruiz A, Haque R, Aguirre A, Castañón G, Hall A, Guhl F, et al. Value of microscopy in the diagnosis of dysentery associated with invasive *Entamoeba histolytica*. J Clin Pathol. 1994;47: 236–239.

51. Boettner DR, Huston CD, Sullivan JA, Petri WA. *Entamoeba histolytica* and *Entamoeba dispar* utilize externalized phosphatidylserine for recognition and phagocytosis of erythrocytes. Infect Immun. 2005;73: 3422–3430.

52. Ralston KS, Solga MD, MacKey-Lawrence NM, Somlata, Bhattacharya A, Petri WA. Trogocytosis by *Entamoeba histolytica* contributes to cell killing and tissue invasion. Nature. 2014;508: 526–530.

53. Johansson ME V, Ambort D, Pelaseyed T, Schütte A, Gustafsson JK, Ermund A, et al. Composition and functional role of the mucus layers in the intestine. Cell Mol Life Sci. 2011;68: 3635–3641.

54. Johansson ME V., Larsson JMH, Hansson GC. The two mucus layers of colon are organized by the MUC2 mucin, whereas the outer layer is a legislator of host-microbial interactions. Proc Natl Acad Sci. 2011;108: 4659–4665.

55. Gum JR, Hicks JW, Toribara NW, Siddiki B, Kim YS. Molecular cloning of human intestinal mucin (MUC2) cDNA. Identification of the amino terminus and overall sequence similarity to prepro-von Willebrand factor. J Biol Chem. 1994;269: 2440–2446.

56. Moncada D, Keller K, Chadee K. Entamoeba histolytica-secreted products degrade colonic mucin oligosaccharides. Infect Immun. 2005;73: 3790–3793.

57. Moncada D, Keller K, Chadee K. *Entamoeba histolytica* cysteine proteinases disrupt the polymeric structure of colonic mucin and alter its protective function. Infect Immun. 2003;71: 838–844.

58. Moncada DM, Keller K, Ankri S, Mirelman D, Chadee K. Antisense inhibition of *Entamoeba histolytica* cysteine proteases inhibits colonic mucus degradation. Gastroenterology. 2006;130: 721–730.

59. Kissoon-Singh V, Moreau F, Trusevych E, Chadee K. *Entamoeba histolytica* exacerbates epithelial tight junction permeability and proinflammatory responses in Muc2(-/-) mice. Am J Pathol. 2013;182: 852–865.

60. Neurath MF, Becker C, Barbulescu K. Role of NF-κB in immune and inflammatory responses in the gut. Gut. 1998;43: 856–860.

61. Kammanadiminti SJ, Dey I, Chadee K. Induction of monocyte chemotactic protein 1 in colonic epithelial cells by *Entamoeba histolytica* is mediated via the phosphatidylinositol 3-kinase/p65 pathway. Infect Immun. 2007;75: 1765–1770.

62. Betanzos A, Javier-Reyna R, García-Rivera G, Bañuelos C, González-Mariscal L, Schnoor M, et al. The EhCPADH112 complex of *Entamoeba histolytica* interacts with tight junction proteins occludin and claudin-1 to produce epithelial damage. PLoS One. 2013;8: e65100.

63. Goplen M, Lejeune M, Cornick S, Moreau F, Chadee K. *Entamoeba histolytica* contains an occludin-like protein that can alter colonic epithelial barrier function. PLoS One. 2013;8: 1–6.

64. Yu Y, Chadee K. *Entamoeba histolytica* stimulates interleukin 8 from human colonic epithelial cells without parasite-enterocyte contact. Gastroenterology. 1997;112: 1536–1547.

65. Guerrant RL, Brush J, Ravdin JI, Sullivan JA, Mandell GL. Interaction between *Entamoeba histolytica* and human polymorphonuclear neutrophils. J Infect Dis. 1981;143: 83–93.

66. Sateriale A, Huston CD. A sequential model of host cell killing and phagocytosis by *Entamoeba histolytica*. J Parasitol Res. 2011; 1–10.

67. Salata RA, Ravdin JI. The interaction of human neutrophils and *Entamoeba histolytica* increases cytopathogenicity for liver cell monolayers. J Infect Dis. 1986;154: 19–26.

68. Chadee K, Denis M. Human neutrophils activated by interferon-γ and tumour necrosis factor-α kill *Entamoeba histolytica* trophozoites in vitro. J Leukoc Biol. 1989;46: 270–274.

69. Smith PD, Smythies LE, Shen R, Greenwell-Wild T, Gliozzi M, Wahl SM. Intestinal macrophages and response to microbial encroachment. Mucosal

Immunol. 2011;4: 31–42.

70. Dinarello CA. Interleukin-18. Methods. 1999;19: 121–32.

71. Van der Meer JW, Vogels M TE, Netea MG, Kullberg BJ. Proinflammatory cytokines and treatment of disease. Ann New York Acad Sci. 2006;856: 243–251.

72. Gabay C, Lamacchia C, Palmer G. IL-1 pathways in inflammation and human diseases. Nat Rev Rheumatol. 2010;6: 232–241.

73. Lin J, Seguin R, Keller K, Chadee K. Tumor necrosis factor alpha augments nitric oxide-dependent macrophage cytotoxicity against *Entamoeba histolytica* by enhanced expression of the nitric oxide synthase gene. Infect Immun. 1994;62: 1534–1541.

74. Lin JY, Chadee K. Macrophage cytotoxicity against *Entamoeba histolytica* trophozoites is mediated by nitric oxide from L-arginine. J Immunol. 1992;148: 3999–4005.

75. Siman-Tov R, Ankri S. Nitric oxide inhibits cysteine proteinases and alcohol dehydrogenase 2 of *Entamoeba histolytica*. Parasitol Res. 2003;89: 146–149.

76. Ghadirian E, Denis M. *Entamoeba histolytica* extract and interferon-gamma activation of macrophage-mediated amoebicidal function. Immunobiology. 1992;185: 1–10.

77. Denis M, Chadee K. Cytokine activation of murine macrophages for in vitro killing of *Entamoeba histolytica* trophozoites. Infect Immun. 1989;57: 1750–1756.

78. Ivory CPA, Prystajecky M, Jobin C, Chadee K. Toll-like receptor 9-dependent macrophage activation by *Entamoeba histolytica* DNA. Infect Immun. 2008;76: 289–297.

79. Moonah SN, Abhyankar MM, Haque R, Petri WA. The macrophage migration inhibitory factor homolog of *Entamoeba histolytica* binds to and immunomodulates host macrophages. Infect Immun. 2014;82: 3523–3530.

80. Bruchhaus I, Tannich E. Induction of the iron-containing superoxide dismutase in *Entamoeba histolytica* by a superoxide anion-generating system or by iron chelation. Mol Biochem Parasitol. 1994;67: 281–288.

81. Bruchhaus I, Richter S, Tannich E. Recombinant expression and biochemical characterization of an NADPH:flavin oxidoreductase from *Entamoeba histolytica*. Biochem J. 1998;1221: 1217–1221.

82. Bruchhaus I, Richter S, Tannich E. Removal of hydrogen peroxide by the 29 kDa protein of *Entamoeba histolytica*. Biochem J. 1997;326: 785–789.

83. Wang W, Keller K, Chadee K. *Entamoeba histolytica* modulates the nitric oxide synthase gene and nitric oxide production by macrophages for cytotoxicity against amoebae and tumour cells. Immunology. 1994;83: 601–610.

84. Elnekave K, Siman-tov R, Ankri S. Consumption of L-arginine mediated by *Entamoeba histolytica* L-arginase (EhArg) inhibits amoebicidal activity and nitric oxide production by activated macrophages. Parasite Immunol. 2004;25: 597–608.

85. Wang W, Chadee K. *Entamoeba histolytica* suppresses gamma interferon-induced macrophage class II major histocompatibility complex Ia molecule and I-A beta mRNA expression by a prostaglandin E2-dependent mechanism. Infect Immun. 1995;63: 1089–1094.

86. Reed SL, Ember JA, Herdman DS, DiScipio RG, Hugti TE, Gigli I. The extracellular neutral cysteine proteinase of *Entamoeba histolytica* degrades

anaphylatoxins C3a and C5a. J Immunol. 1995;155: 266–274.

87. Köhl J. Anaphylatoxins and infectious and non-infectious inflammatory diseases. Mol Immunol. 2001;38: 175–187.

88. Ventura-Juárez J, Campos-Rodríguez R, Jarillo-Luna RA, Muñoz-Fernández L, Escario-G-Trevijano JA, Pérez-Serrano J, et al. Trophozoites of *Entamoeba histolytica* express a CD59-like molecule in human colon. Parasitol Res. 2009;104: 821–826.

89. Braga LL, Ninomiya H, McCoy JJ, Eacker S, Wiedmer T, Pham C, et al. Inhibition of the complement membrane attack complex by the galactose-specific adhesin of *Entamoeba histolytica*. J Clin Invest. 1992;20: 1131–1137.

90. Espinosa-Cantellano M, Martínez-Palomo A. *Entamoeba histolytica*: mechanism of surface receptor capping. Exp Parasitol. 1994;79: 424–435.

91. Baxt LA, Baker RP, Singh U, Urban S. An *Entamoeba histolytica* rhomboid protease with atypical specificity cleaves a surface lectin involved in phagocytosis and immune evasion. Genes Dev. 2008;22: 1636–1646.

92. Chadee K, Meerovitch E. The Mongolian gerbil (Meriones unguiculatus) as an experimental host for *Entamoeba histolytica*. Am J Trop Med Hyg. 1984;33: 47–54.

93. Shibayama M, Navarro-García F, López-Revilla R, Martínez-Palomo A, Tsutsumi V. In vivo and in vitro experimental intestinal amebiasis in Mongolian gerbils *(Meriones unguiculatus)*. Parasitol Res. 1997;83: 170–176.

94. Tsutsumi V, Shibayama M. Experimental amebiasis: a selected review of some in vivo models. Arch Med Res. 2006;37: 210–220.

95. Seydel KB, Li E, Swanson PE, Stanley SL. Human intestinal epithelial cells produce proinflammatory cytokines in response to infection in a SCID mouse-human intestinal xenograft model of amebiasis. Infect Immun. 1997;65: 1631–1639.

96. Bansal D, Ave P, Kerneis S, Frileux P, Boché O, Baglin AC, et al. An ex-vivo human intestinal model to study *Entamoeba histolytica* pathogenesis. PLoS Negl Trop Dis. 2009;3: 1–11.

97. Chadee K, Keller K, Forstner J, Innes DJ, Ravdin JI. Mucin and nonmucin secretagogue activity of *Entamoeba histolytica* and cholera toxin in rat colon. Gastroenterology. 1991;100: 986–997.

98. Kumar H, Kawai T, Akira S. Pathogen recognition by the innate immune system. Int Rev Immunol. 2011;30: 16–34.

99. Franchi L, Warner N, Viani K, Nuñez G. Function of Nod-like receptors in microbial recognition and host defense. Immunol Rev. 2009;227: 106–128.

100. Black RA, Kronheim SR, Merriam JE, March CJ, Hopp TP. A pre-aspartate-specific protease from human leukocytes that cleaves prointerleukin-1beta. J Biol Chem. 1989;264: 5323–5326.

101. Chowdhury I, Tharakan B, Bhat GK. Caspases - an update. Comp Biochem Physiol Part B. 2008;151: 10–27.

102. Lamkanfi M, Declercq W, Kalai M, Saelens X, Vandenabeele P. Alice in caspase land. A phylogenetic analysis of caspases from worm to man. Cell Death Differ. 2002;9: 358–361.

103. Miller DK, Myerson J, Becker JW. The interleukin-1β converting enzyme family

of cysteine proteases. J Cell Biochem. 1997;64: 2–10.

104. Scott A, Saleh M. The inflammatory caspases: guardians against infections and sepsis. Cell Death Differ. 2007;14: 23–31.

105. Martinon F, Tschopp J. Inflammatory caspases: linking an intracellular innate immune system to autoinflammatory diseases. Cell. 2004;117: 561–574.

106. Martinon F, Burns K, Tschopp J. The inflammasome: a molecular platform triggering activation of inflammatory caspases and processing of proIL-β. Mol Cell. 2002;10: 417–426.

107. Kamens J, Paskind M, Hugunin M, Talanian R V, Allen H, Banach D, et al. Identification and characterization of ICH-2, a novel member of the interleukin-1β-converting enzyme family of cysteine proteases. J Biol Chem. 1995;270: 15250–15256.

108. Maelfait J, Vercammen E, Janssens S, Schotte P, Haegman M, Magez S, et al. Stimulation of Toll-like receptor 3 and 4 induces interleukin-1β maturation by caspase-8. J Exp Med. 2008;205: 1967–1973.

109. Talanian R V., Quinlan C, Trautz S, Hackett MC, Mankovich JA, Banach D, et al. Substrate specificities of caspase family proteases. J Biol Chem. 1997;272: 9677–9682.

110. Miao EA, Leaf IA, Treuting PM, Mao DP, Dors M, Sarkar A, et al. Caspase-1-induced pyroptosis is an innate immune effector mechanism against intracellular bacteria. Nat Immunol. 2010;11: 1136–1142.

111. Kang S-J, Wang S, Hara H, Peterson EP, Namura S, Amin-Hanjani S, et al. Dual role of caspase-11 in mediating activation of caspase-1 and caspase-3 under

pathological conditions. J Cell Biol. 2000;149: 613–622.

112. Schauvliege R, Vanrobaeys J, Schotte P, Beyaert R. Caspase-11 gene expression in response to lipopolysaccharide and interferon-gamma requires nuclear factor-kappa B and signal transducer and activator of transcription (STAT) 1. J Biol Chem. 2002;277: 41624–41630.

113. Wang S, Miura M, Jung Y, Zhu HZ, Gagliardini V, Shi L, et al. Identification and characterization of Ich-3, a member of the interleukin-1 converting enzyme (ICE)/Ced-3 family and an upstream regulator of ICE. J Biol Chem. 1996;271: 20580–20587.

114. Li J, Brieher WM, Scimone ML, Kang SJ, Zhu H, Yin H, et al. Caspase-11 regulates cell migration by promoting Aip1-cofilin-mediated actin depolymerization. Nat Cell Biol. 2007;9: 276–286.

115. Akhter A, Caution K, Abu Khweek A, Tazi M, Abdulrahman BA, Abdelaziz DHA, et al. Caspase-11 promotes the fusion of phagosomes harboring pathogenic bacteria with lysosomes by modulating actin polymerization. Immunity. 2012;37: 35–47.

116. Wang S, Miura M, Jung YK, Zhu H, Li E, Yuan J. Murine caspase-11, an ICE-interacting protease, is essential for the activation of ICE. Cell. 1998;92: 501–509.

117. Wang SY, Miura M, Jung YK, Zhu H, Gagliardini V, Shi LF, et al. Identification and characterization Of Ich-3, a member of the interleukin-1β converting enzyme (ICE) ced-3 family and an upstream regulator Of ICE. J Biol Chem. 1996;271: 20580–20587.

118. Kayagaki N, Warming S, Lamkanfi M, Walle L Vande, Louie S, Dong J, et al.

Non-canonical inflammasome activation targets caspase-11. Nature. 2011;479: 117–121.

119. Demon D, Kuchmiy A, Fossoul A, Zhu Q, Kanneganti T-D, Lamkanfi M. Caspase-11 is expressed in the colonic mucosa and protects against dextran sodium sulfate-induced colitis. Mucosal Immunol. 2014;7: 1504–15116.

120. Kajiwara Y, Schiff T, Voloudakis G, Gama Sosa MA, Elder G, Bozdagi O, et al. A critical role for human caspase-4 in endotoxin sensitivity. J Immunol. 2014;193: 335–343.

121. Sollberger G, Strittmatter GE, Kistowska M, French LE, Beer H-D. Caspase-4 is required for activation of inflammasomes. J Immunol. 2012;188: 1992–2000.

122. Cheung KT, Sze DM yuen, Chan KH, Leung PH mei. Involvement of caspase-4 in IL-1 beta production and pyroptosis in human macrophages during dengue virus infection. Immunobiology. 2017;223: 356–364.

123. Karki P, Dahal GR, Park I-S. Both dimerization and interdomain processing are essential for caspase-4 activation. Biochem Biophys Res Commun. 2007;356: 1056–1061.

124. Lakshmanan U, Porter AG. Caspase-4 interacts with TNF receptor-associated factor 6 and mediates lipopolysaccharide-induced NF-κB-dependent production of IL-8 and CC chemokine ligand 4 (macrophage-inflammatory protein-1). J Immunol. 2007;179: 8480–8490.

125. Shi J, Zhao Y, Wang Y, Gao W, Ding J, Li P, et al. Inflammatory caspases are innate immune receptors for intracellular LPS. Nature. 2014;514: 187–192.

126. Knodler LA, Crowley SM, Sham HP, Yang H, Ma C, Ernst RK, et al. Non-

canonical inflammasome activation of caspase-4/caspase-11 mediates epithelial defenses against enteric bacterial pathogens. Cell Host Microbe. 2015;16: 249–256.

127. Kobayashi T, Ogawa M, Sanada T, Mimuro H, Kim M, Ashida H, et al. The Shigella OspC3 effector inhibits caspase-4, antagonizes inflammatory cell death, and promotes epithelial infection. Cell Host Microbe. 2013;13: 570–583.

128. Bian Z-M, Elner SG, Elner VM. Dual involvement of caspase-4 in inflammatory and ER stress-induced apoptotic responses in human retinal pigment epithelial cells. Invest Ophthalmol Vis Sci. 2009;50: 6006–6014.

129. Li C, Wei J, Li Y, He X, Zhou Q, Yan J, et al. Transmembrane protein 214 (TMEM214) mediates endoplasmic reticulum stress-induced caspase 4 enzyme activation and apoptosis. J Biol Chem. 2013;288: 17908–17917.

130. Martinon F, Mayor A, Tschopp J. The inflammasomes: guardians of the body. Annu Rev Immunol. 2009;27: 229–265.

131. Sushmita J, Brickey WJ, Ting JP-Y. Inflammasomes in myeloid cells: warriors within. Microbiol Spectr. 2017;21: 129–139.

132. Ting JPY, Lovering RC, Alnemri ES, Bertin J, Boss JM, Davis BK, et al. The NLR gene family: a standard nomenclature. Immunity. 2008;28: 285–287.

133. Galliher-Beckley AJ, Lan L-Q, Aono S, Wang L, Shi J. Caspase-1 activation and mature interleukin-1β release are uncoupled events in monocytes. World J Biol Chem. 2013;4: 30–34.

134. Ogura Y, Sutterwala FS, Flavell RA. The inflammasome: first line of the immune response to cell stress. Cell. 2006;126: 659–662.

135. Andrei C, Dazzi C, Lotti L, Torrisi MR, Chimini G, Rubartelli A. The secretory route of the leaderless protein interleukin 1β involves exocytosis of endolysosome-related vesicles. Mol Biol Cell. 1999;10: 1463–1475.

136. Keller M, Rüegg A, Werner S, Beer H-D. Active caspase-1 is a regulator of unconventional protein secretion. Cell. 2008;132: 818–831.

137. Qu Y, Franchi L, Nunez G, Dubyak GR. Nonclassical IL-1 secretion stimulated by P2X7 receptors is dependent on inflammasome activation and correlated with exosome release in murine macrophages. J Immunol. 2007;179: 1913–1925.

138. Nickel W, Rabouille C. Mechanisms of regulated unconventional protein secretion. Nat Rev Mol Cell Biol. 2009;10: 148–155.

139. Dinarello CA. Immunological and inflammatory functions of the interleukin-1 family. Annu Rev Immunol. 2009;27: 519–550.

140. Hornung V, Bauernfeind F, Halle A, Samstad EO, Kono H, Rock KL, et al. Silica crystals and aluminum salts activate the NALP3 inflammasome through phagosomal destabilization. Nat Immunol. 2008;9: 847–856.

141. Pétrilli V, Papin S, Dostert C, Mayor A, Martinon F, Tschopp J. Activation of the NALP3 inflammasome is triggered by low intracellular potassium concentration. Cell Death Differ. 2007;14: 1583–1589.

142. Chu J, Thomas LM, Watkins SC, Franchi L, Nunez G, Salter RD. Cholesterol-dependent cytolysins induce rapid release of mature IL-1β from murine macrophages in a NLRP3 inflammasome and cathepsin B-dependent manner. J Leukoc Biol. 2009;86: 1227–1238.

143. Casson CN, Copenhaver AM, Zwack EE, Nguyen HT, Strowig T, Javdan B, et al.

Caspase-11 activation in response to bacterial secretion systems that access the host cytosol. PLoS Pathog. 2013;9: 1–16.

144. Kayagaki N. Noncanonical inflammasome activation by intracellular LPS independent of TLR4. Science (80-). 2013;341: 1246–1249.

145. Gringhuis SI, Kaptein TM, Wevers BA, Theelen B, Van Der Vlist M, Boekhout T, et al. Dectin-1 is an extracellular pathogen sensor for the induction and processing of IL-1β via a noncanonical caspase-8 inflammasome. Nat Immunol. 2012;13: 246–254.

146. Philip NH, Dillon CP, Snyder AG, Fitzgerald P, Wynosky-Dolfi MA, Zwack EE, et al. Caspase-8 mediates caspase-1 processing and innate immune defense in response to bacterial blockade of NF-κB and MAPK signaling. Proc Natl Acad Sci. 2014;111: 7385–7390.

147. Yu JR, Leslie KS. Cryopyrin-associated periodic syndrome: An update on diagnosis and treatment response. Curr Allergy Asthma Rep. 2011;11: 12–20.

148. Verma D, Särndahl E, Andersson H, Eriksson P, Fredrikson M, Jönsson JI, et al. The Q705K polymorphism in NLRP3 is a gain-of-function alteration leading to excessive interleukin-1β and IL-18 production. PLoS One. 2012;7: 2–8.

149. Hoffman HM, Rosengren S, Boyle DL, Cho JY, Nayar J, Mueller JL, et al. Prevention of cold-associated acute inflammation in familial cold autoinflammatory syndrome by interleukin-1 receptor antagonist. Lancet. 2004;364: 1779–1785.

150. Goldbach-Mansky R, Dailey NJ, Canna SW, Gelabert A, Jones J, Rubin BI, et al. Neonatal-onset multisystem inflammatory disease responsive to interleukin-1β

inhibition. N Engl J Med. 2006;355: 581–592.

151. Masters SL, Latz E, Neill LAJO. The Inflammasome in atherosclerosis and type 2 diabetes. Perspective. 2011;3: 1–7.

152. Mortimer L, Moreau F, MacDonald JA, Chadee K. NLRP3 inflammasome inhibition is disrupted in a group of auto-inflammatory disease CAPS mutations. Nat Immunol. 2016;17: 1176–1186.

153. Petri WA, Smith RD, Schlesinger PH, Murphy CF, Ravdin JI. Isolation of the galactose-binding lectin that mediates the in vitro adherence of *Entamoeba histolytica*. J Clin Invest. 1987;80: 1238–1244.

154. Ravdin JI, John JE, Johnston LI, Innes DJ, Guerrant RL. Adherence of *Entamoeba histolytica* trophozoites to rat and human colonic mucosa. Infect Immun. 1985;48: 292–297.

155. Mortimer L, Moreau F, Cornick S, Chadee K. The NLRP3 inflammasome is a pathogen sensor for invasive *Entamoeba histolytica* via activation of α5β1 integrin at the macrophage-amebae intercellular junction. PLoS Pathog. 2015;11: e1004887.

156. Mortimer L, Moreau F, Cornick S, Chadee K. Gal-lectin-dependent contact activates the inflammasome by invasive *Entamoeba histolytica*. Mucosal Immunol. 2013;7: 829–841.

157. Kamada S, Funahashi Y, Tsujimoto Y. Caspase-4 and caspase-5, members of the ICE/CED-3 family of cysteine proteases, are CrmA-inhibitable proteases. Cell Death Differ. 1997;4: 473–478.

158. Munday NA, Vaillancourt JP, Ali A, Casano FJ, Miller DK, Molineaux SM, et al.

Molecular cloning and pro-apoptotic activity of ICErelII and ICErelIII, members of the ICE/CED-3 family of cysteine proteases. J Biol Chem. 1995;270: 15870–15876.

159. Casson CN, Yu J, Reyes VM, Taschuk FO, Yadav A, Copenhaver AM, et al. Human caspase-4 mediates noncanonical inflammasome activation against gram-negative bacterial pathogens. Proc Natl Acad Sci. 2015;112: 6688–6693.

160. Diamond LS, Harlow DANR, Cunnick CC. A new medium for the axenic cultivation of *Entamoeba* and other *Entamoeba histolytica*. Trans R Soc Trop Med Hyg. 1978;72: 431–432.

161. Angers S, Thorpe CJ, Biechele TL, Goldenberg SJ, Zheng N, MacCoss MJ, et al. The KLHL12-Cullin-3 ubiquitin ligase negatively regulates the Wnt-β-catenin pathway by targeting dishevelled for degradation. Nat Cell Biol. 2006;8: 348–357.

162. Mellacheruvu D, Wright Z, Couzens AL, Lambert JP, St-Denis NA, Li T, et al. The CRAPome: A contaminant repository for affinity purification-mass spectrometry data. Nat Methods. 2013;10: 730–736.

163. Keller A, Nesvizhskii AI, Kolker E, Aebersold R. Empirical statistical model to estimate the accuracy of peptide identifications made by MS/MS and database search. Anal Chem. 2002;74: 5383–5392. doi:10.1021/ac025747h

164. Nesvizhskii AI, Keller A, Kolker E, Aebersold R. A statistical model for identifying proteins by tandem mass spectrometry. Anal Chem. 2003;75: 4646–4658. doi:10.1021/ac0341261

165. Schmid-burgk JL, Gaidt MM, Schmidt T, Ebert TS, Bartok E, Hornung V. Caspase-4 mediates non-canonical activation of the NLRP3 inflammasome in

human myeloid cells. Eur J Immunol. 2015;45: 2911–2917.

166. Baker PJ, Boucher D, Bierschenk D, Tebartz C, Whitney PG, Silva DBD, et al. NLRP3 inflammasome activation downstream of cytoplasmic LPS recognition by both caspase-4 and caspase-5. Eur J Immunol. 2015;45: 2918–2926.

167. Broz P, Monack DM. Noncanonical inflammasomes: caspase-11 activation and effector mechanisms. PLoS Pathog. 2013;9: 9–12.

168. Pop C, Salvesen GS. Human caspases: Activation, specificity, and regulation. J Biol Chem. 2009;284: 21777–21781.

169. Kast J, Klockenbusch C. Optimization of formaldehyde cross-linking for protein interaction analysis of non-tagged integrinβ1. J Biomed Biotechnol. 2010;2010: 1–13.

170. Deshmane SL, Kremlev S, Amini S, Sawaya BE. Monocyte chemoattractant protein-1 (MCP-1): an overview. J Interf Cytokine Res. 2009;29: 313–326.

171. Kakurina GV, Kolegova ES, Kondakova IV. Adenylyl cyclase-associated protein 1: Structure, regulation, and participation in cellular processes. Biochem. 2018;83: 45–53.

172. Henning MS, Stiedl P, Barry DS, McMahon R, Morham SG, Walsh D, et al. PDZD8 is a novel moesin-interacting cytoskeletal regulatory protein that suppresses infection by herpes simplex virus type 1. Virology. Elsevier B.V.; 2011;415: 114–121.

173. Ravikumar B, Moreau K, Jahreiss L, Puri C, Rubinsztein DC. Plasma membrane contributes to the formation of pre-autophagosomal structures. Nat Cell Biol. 2010;12: 747–757.

174. El Eter E, Al-Masri AA. Peroxiredoxin isoforms are associated with cardiovascular risk factors in type 2 diabetes mellitus. Brazilian J Med Biol Res. 2015;48: 465–469.

175. Liu Y, Ross JF, Bodine PVN, Billiard J. Homodimerization of ror2 tyrosine kinase receptor induces 14-3-3β phosphorylation and promotes osteoblast differentiation and bone formation. Mol Endocrinol. 2007;21: 3050–3061.

176. Challa AA, Stefanovic B. A novel role of vimentin filaments: binding and stabilization of collagen mRNAs. Mol Cell Biol. 2011;31: 3773–3789.

177. Yan, L; Stanley SL. Blockade of caspases inhibits amebic liver abscess formation in a mouse model of disease. Infect Immun. 2001;69: 7911–7914.

178. Marie C, Verkerke HP, Theodorescu D, Petri WA. A whole-genome RNAi screen uncovers a novel role for human potassium channels in cell killing by the parasite *Entamoeba histolytica*. Sci Rep. 2015;5: 1–18.

179. Muñoz-Planillo R, Kuffa P, Martínez-Colón G, Smith B, Rajendiran T, Núñez G. K+ efflux is the common trigger of NLRP3 inflammasome activation by bacterial toxins and particulate matter. Immunity. 2013;38: 1142–1153.

180. Faucheu C, Diu A, Chan A, Blanchet A, Miossec C, Hervé F, et al. A novel human protease similar to the interleukin-1β converting enzyme induces apoptosis in transfected cells. EMBO J. 1995;14: 1914–1922.

181. Becker C, Watson AJ, Neurath MF. Complex roles of caspases in the pathogenesis of inflammatory bowel disease. Gastroenterology. 2013;144: 283–293.

182. Fleming R, Cooper CJ, Vega RR, Alardin AH, Boman D, Zuckerman MJ. Clinical manifestations and endoscopic findings of amebic colitis in a United States -

Mexico border city: a case series. BMC Res Notes. 2015;8: 1–9.

183. Kudelova J, Fleischmannova J, Adamova E, Matalova E. Pharmacological caspase inhibitors: research towards therapeutic perspectives. J Physiol Pharmacol. 2015;66: 473–482.

184. Lee H, Shin EA, Lee JH, Ahn D, Kim CG, Kim S, et al. Expert opinion on therapeutic patents caspase inhibitors: a review of recently patented compounds (2013-2015). Expert Opin Ther Pat. 2017;28: 47–59.

185. Dhimolea E. Canakinumab. MAbs. 2010;2: 3–13.

186. Tsuchiya S, Yamabe M, Yamaguchi Y, Kobayashi Y, Konno T, Tada K. Establishment and characterization of a human acute monocytic leukemia cell line (THP-1). Int J Cancer. 1980;26: 171–176.

187. Chanput W, Mes JJ, Wichers HJ. THP-1 cell line: An in vitro cell model for immune modulation approach. Int Immunopharmacol. 2014;23: 37–45.

188. Kalantari P, DeOliveira RB, Chan J, Corbett Y, Rathinam V, Stutz A, et al. Dual engagement of the NLRP3 and AIM2 inflammasomes by *Plasmodium*-derived hemozoin and DNA during malaria. Cell Rep. 2014;6: 196–210.

189. Gonçalves VM, Matteucci KC, Buzzo CL, Miollo BH, Ferrante D, Torrecilhas AC, et al. NLRP3 controls *Trypanosoma cruzi* infection through a caspase-1-dependent IL-1R-independent NO production. PLoS Negl Trop Dis. 2013;7: 1–11.

190. Cavailles P, Flori P, Papapietro O, Bisanz C, Lagrange D, Pilloux L, et al. A highly conserved Toxo1 haplotype directs resistance to toxoplasmosis and its associated caspase-1 dependent killing of parasite and host macrophage. PLoS Pathog. 2014;10: e1004005.

191. Wang H, Naghavi M, Allen C, Barber RM, Carter A, Casey DC, et al. Global, regional, and national life expectancy, all-cause mortality, and cause-specific mortality for 249 causes of death, 1980–2015: a systematic analysis for the Global Burden of Disease Study 2015. Lancet. 2016;388: 1459–1544.

192. Flood B, Oficjalska K, Laukens D, Fay J, O'Grady A, Caiazza F, et al. Altered expression of caspases-4 and -5 during inflammatory bowel disease and colorectal cancer: diagnostic and therapeutic potential. Clin Exp Immunol. 2015;181: 39–50.

193. Hattinger E, Wolf R. Caspase-5 rescues UVB-dependent IL-1β activity in ASC-deficient epidermal keratinocytes. Photodermatol Photoimmunol Photomed. 2016;32: 165–167.

4.5 Appendix

This appendix is composed of original blots from key experiments to illustrate cropped sections of blots for each of the figures. It also includes a list publications and book chapters that contain work completed during the course of this project, as well as permission obtained for excerpts used in Chapter 3.

4.5.1 *Original Blots*

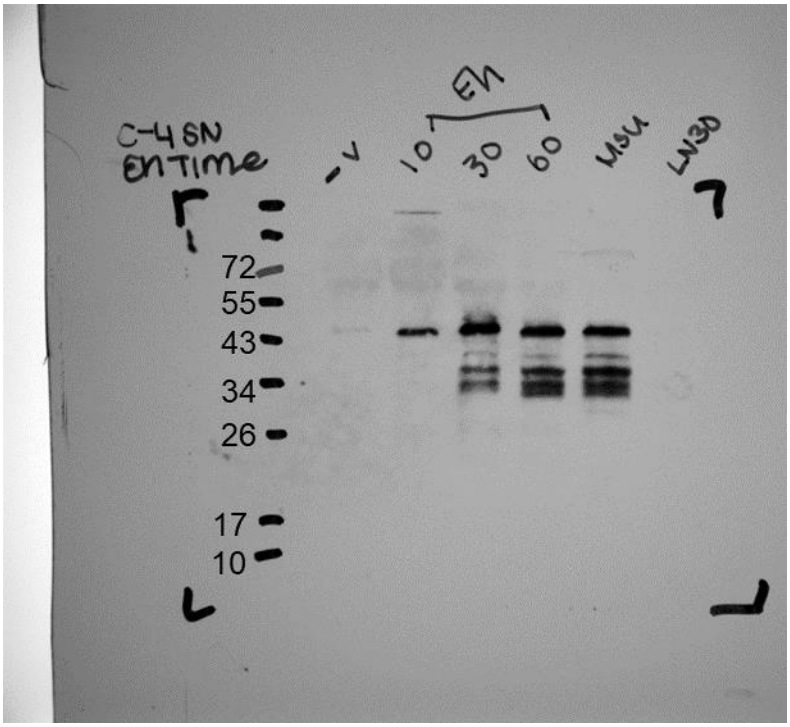

Figure 4.3 Original blot for caspase-4 detection in the supernatants of THP-1 macrophages stimulated with *Eh*.

Full blot scanned using ChemiDoc for Figure 3.1A *Eh* treatment for different timepoints and samples were run on a 10% SDS-PAGE gel and immunoblotted using caspase-4 M029-3 antibody followed by the anti-mouse IgG-HRP. The SuperSignal West Femto Chemiluminescence Reagent was added to detect proteins. The 43 kDa band is the pro-form of caspase-4, while the 32-36 kDa (triplet bands) are caspase-4 intermediate forms. The cropped image for final presentation of the western blot included the pro-form and the intermediate forms.

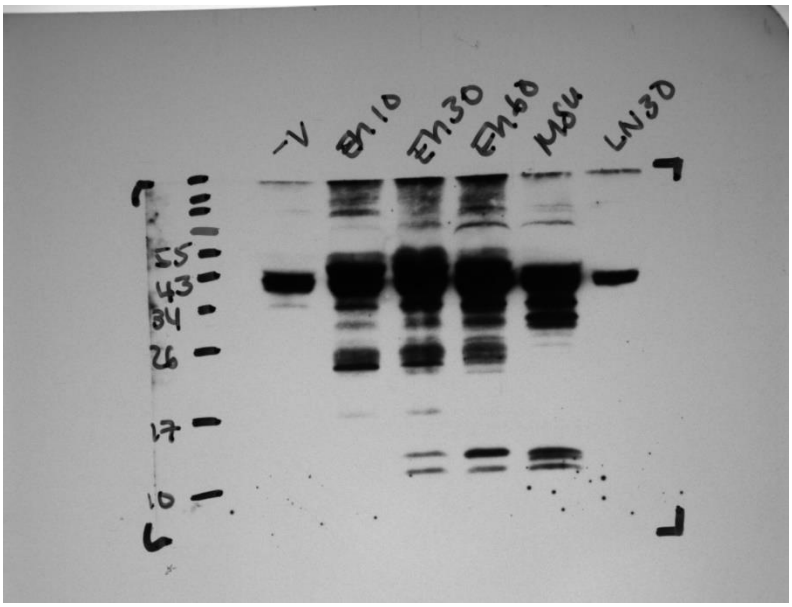

Figure 4.4 Original blot for caspase-1 CARD detection in the supernatants of THP-1 macrophages stimulated with *Eh*.

Full blot scanned using ChemiDoc for Figure 3.1A *Eh* treatment for different timepoints and samples were run on a 12% SDS-PAGE gel and immunoblotted using caspase-1 sc-622 antibody followed by the anti-rabbit IgG-HRP. The SuperSignal West Femto Chemiluminescence Reagent was added to detect proteins. The doublet band at around 11 kDa is the CARD domain of caspase-1 once it is cleaved from the pro-form. The pro-form (45 kDa) is over saturated due to the exposure time used. This doublet band was cropped from the western blots from all experiments performed to show the activation of caspase-1.

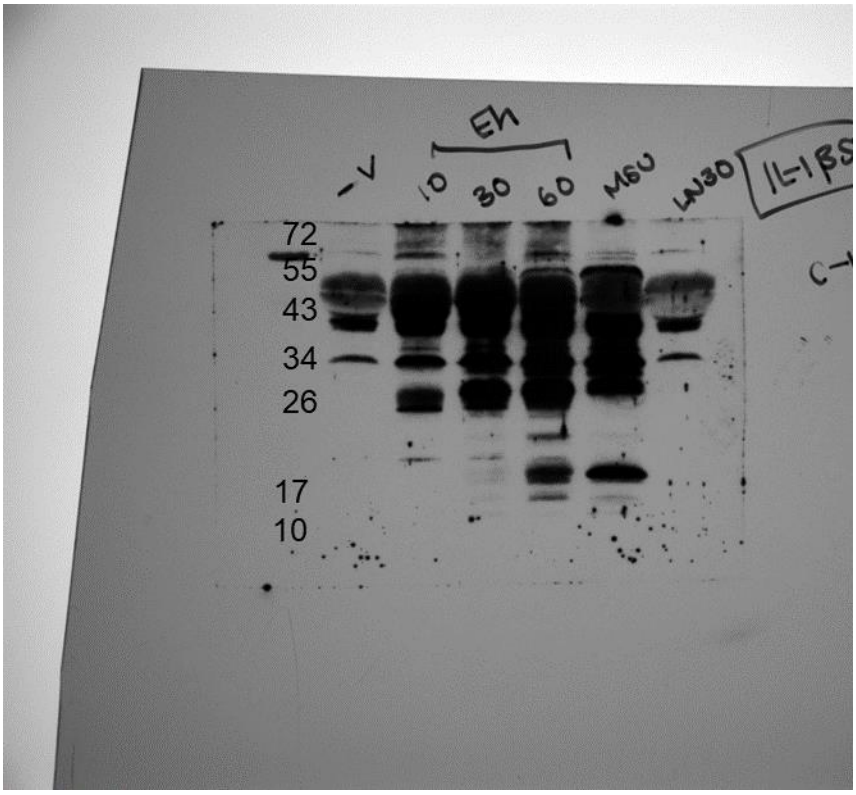

Figure 4.5 Original blot for IL-1β detection in the supernatants of THP-1 macrophages stimulated with *Eh*.

Full blot scanned using ChemiDoc for Figure 3.1A *Eh* treatment for different timepoints and samples were run on a 12% SDS-PAGE gel and immunoblotted using IL-1β sc-7884 antibody followed by the anti-rabbit IgG-HRP. The SuperSignal West Femto Chemiluminescence Reagent was added to detect proteins. The band at around 17 kDa is the cleaved (active) IL-1β. The pro-form (31 kDa) is over saturated due to the exposure time used. This band was cropped from the western blots from all experiments performed to show the cleavage of IL-1β.

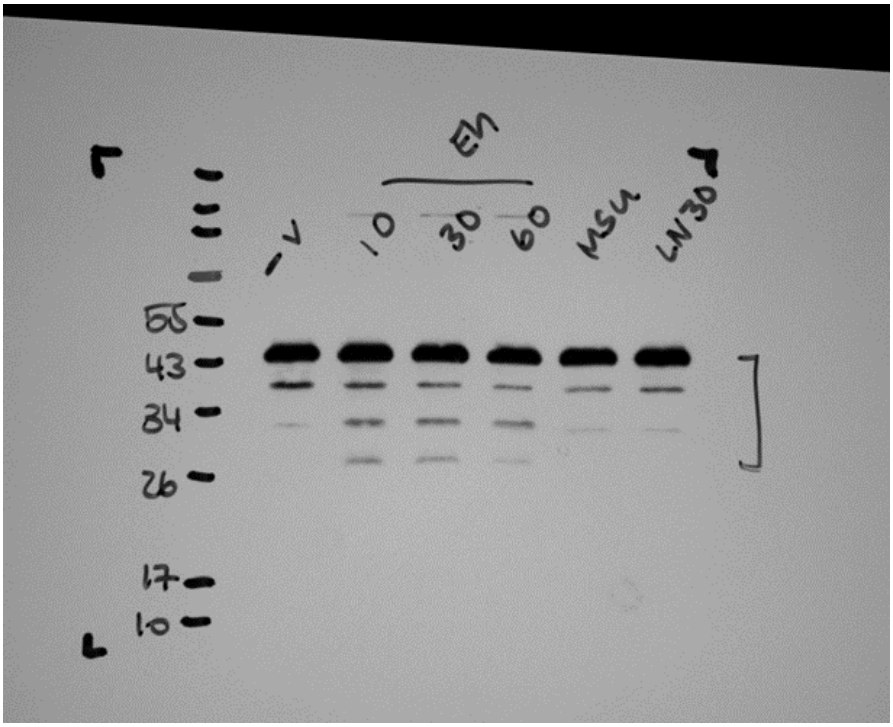

Figure 4.6 Original blot for pro-caspase-4 detection in the lysates of THP-1 macrophages stimulated with *Eh*.

Full blot scanned using ChemiDoc for Figure 3.1A *Eh* treatment for different timepoints and samples were run on a 10% SDS-PAGE gel and immunoblotted using caspase-4 M029-3 antibody followed by the anti-mouse IgG-HRP. The Western Chemiluminescent HRP Substrate was added to detect proteins. The 43 kDa band is the pro-form of caspase-4, while the 32-36 kDa (triplet bands) are caspase-4 intermediate forms. The cropped image for final presentation of the western blot data included the pro-form and the intermediate forms.

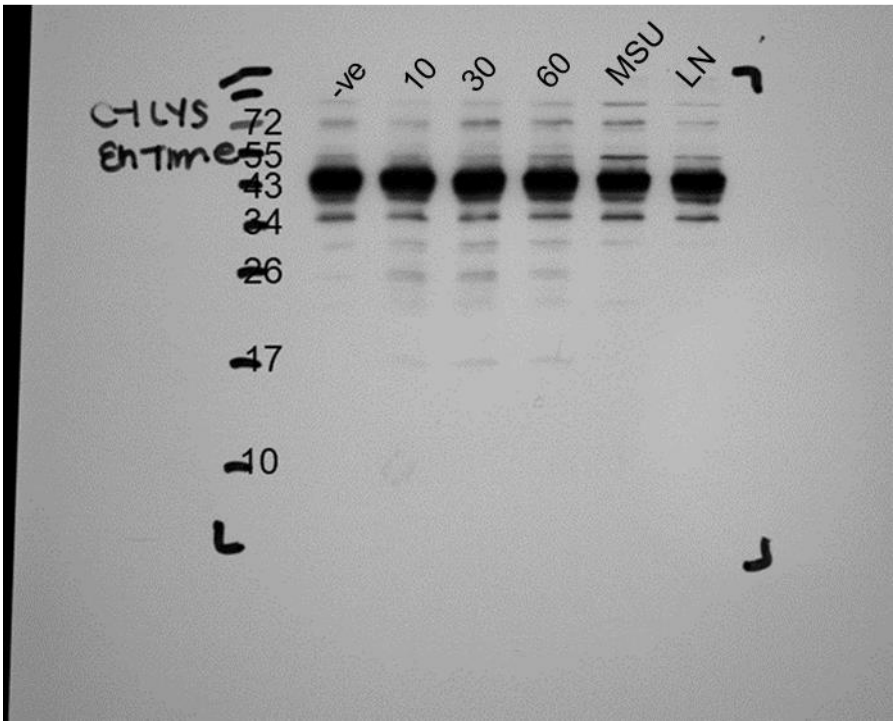

Figure 4.7 Original blot for pro-caspase-1 detection in the lysates of THP-1 macrophages stimulated with *Eh*.

Full blot scanned using ChemiDoc for Figure 3.1A *Eh* treatment for different timepoints and samples were run on a 12% SDS-PAGE gel and immunoblotted using caspase-1 sc-622 antibody followed by the anti-rabbit IgG-HRP. The Western Chemiluminescent HRP Substrate was added to detect proteins. The doublet band at around 11 kDa is the CARD domain of caspase-1 once it is cleaved from the pro-form. The pro-form (45 kDa) is over saturated due to the exposure time used. This single band was cropped from the western blots from all experiments performed to show pro-caspase-1.

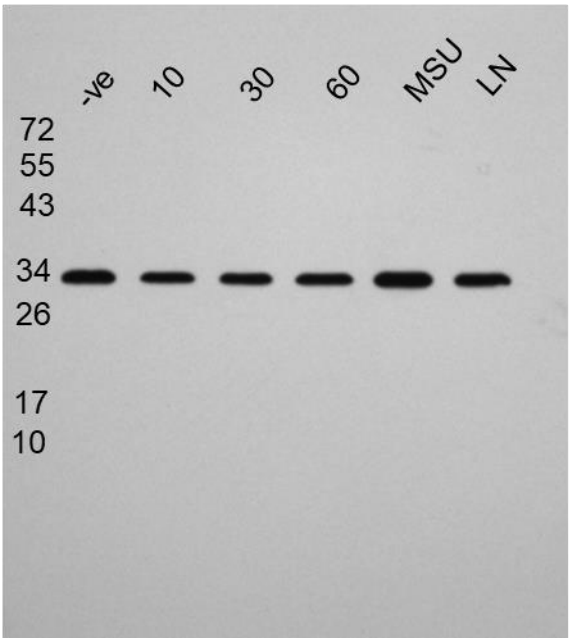

Figure 4.8 Original blot for pro-IL-1β detection in the lysates of THP-1 macrophages stimulated with *Eh*.

Full blot scanned using ChemiDoc for Figure 3.1A *Eh* treatment for different timepoints and samples were run on a 12% SDS-PAGE gel and immunoblotted using IL-1β sc-7884 antibody followed by the anti-rabbit IgG-HRP. The Western Chemiluminescent HRP Substrate was added to detect proteins. The band at around 31 kDa is the pro-IL-1β. This band was cropped from the western blots from all experiments performed to show the cleavage of IL-1β.

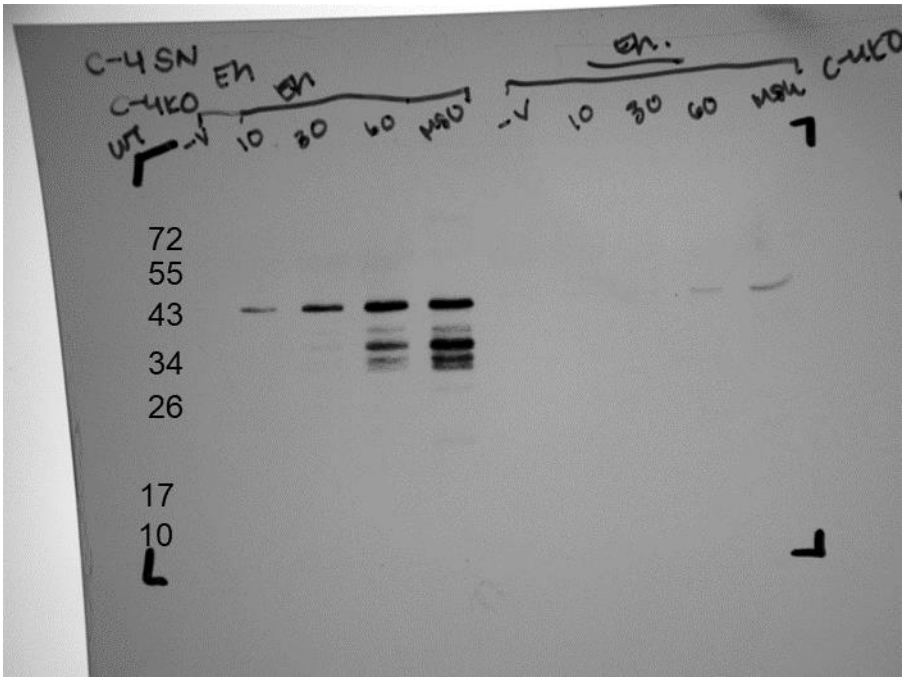

Figure 4.9 Original blot for caspase-4 detection in the supernatants of WT and Casp-4 KO THP-1 macrophages stimulated with *Eh*.

Full blot scanned using ChemiDoc for Figure 3.4A *Eh* treatment for different timepoints in WT as compared to Casp-4 CRISPR/Cas9 KO macrophages and samples were run on a 10% SDS-PAGE gel and immunoblotted using caspase-4 M029-3 antibody followed by the anti-mouse IgG-HRP. The SuperSignal West Femto Chemiluminescence Reagent was added to detect proteins. The 43 kDa band is the pro-form of caspase-4, while the 32-36 kDa (triplet bands) are caspase-4 intermediate forms. The cropped image for final presentation of the western blot data included the pro-form and the intermediate forms. There was no ladder run within the same gel, but a ladder was run on a separate gel to determine the molecular weight.

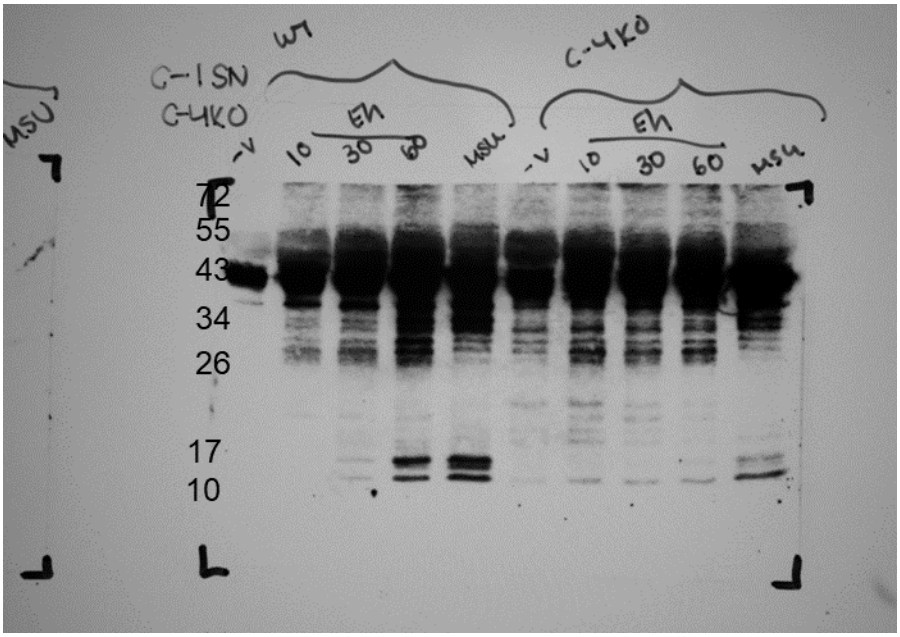

Figure 4.10 Original blot for caspase-1 CARD detection in the supernatants of WT and Casp-4 KO THP-1 macrophages stimulated with *Eh*.

Full blot scanned using ChemiDoc for Figure 3.4A *Eh* treatment for different timepoints in WT as compared to Casp-4 CRISPR/Cas9 KO macrophages and samples were run on a 12% SDS-PAGE gel and immunoblotted using caspase-1 sc-622 antibody followed by with the anti-rabbit IgG-HRP. The SuperSignal West Femto Chemiluminescence Reagent was added to detect proteins for the supernatants. The doublet band at around 11 kDa is the CARD domain of caspase-1 once it is cleaved from the pro-form. The pro-form is over saturated due to the exposure time used. This doublet band was cropped from the western blots from all experiments performed to show the activation of caspase-1. There was no ladder run within the same gel, but a ladder was run on a separate gel to determine the molecular weight.

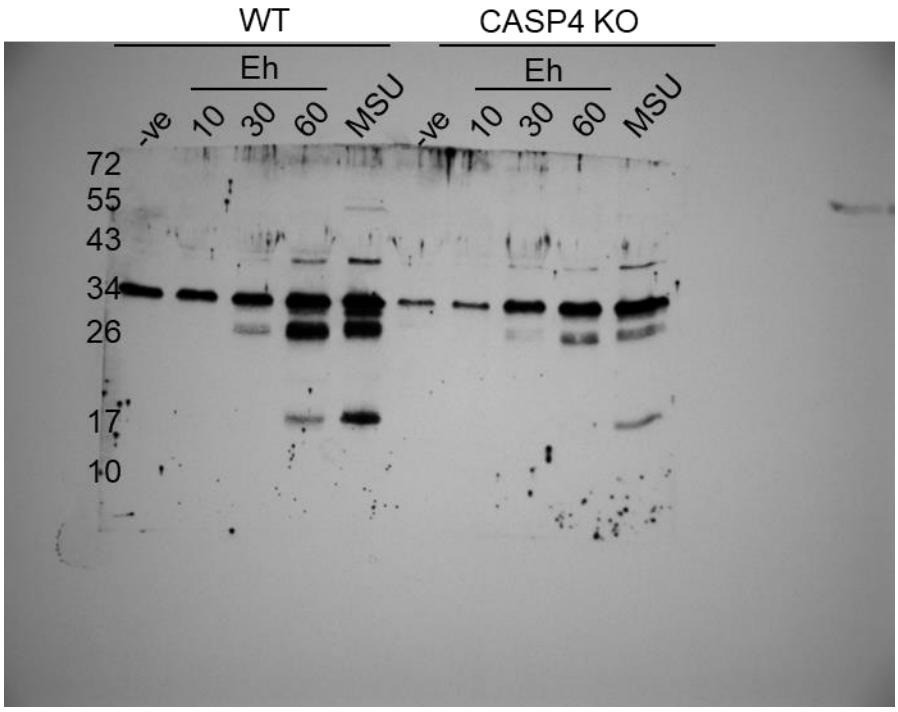

Figure 4.11 Original blot for IL-1β detection in the supernatants of WT and Casp-4 KO THP-1 macrophages stimulated with *Eh*.

Full blot scanned using ChemiDoc for Figure 3.4A *Eh* treatment for different timepoints in WT as compared to Casp-4 CRISPR/Cas9 KO macrophages and samples were run on a 12% SDS-PAGE gel and immunoblotted using IL-1β sc-7884 antibody followed by the anti-rabbit IgG-HRP. The SuperSignal West Femto Chemiluminescence Reagent was added to detect proteins. The band at around 17 kDa is the cleaved (active) IL-1β. The pro-form (31 kDa) is over saturated due to the exposure time used. This band was cropped from the western blots from all experiments performed to show the cleavage of IL-1β. There was no ladder run within the same gel, but a ladder was run on a separate gel to determine the molecular weight.

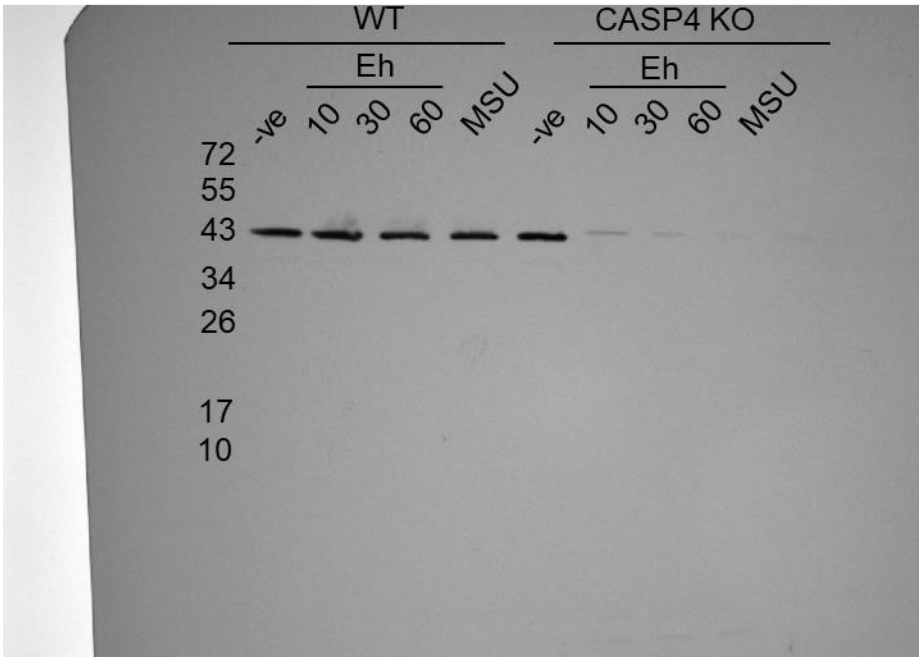

Figure 4.12 Original blot for caspase-4 detection in the lysates of WT and Casp-4 KO THP-1 macrophages stimulated with *Eh*.

Full blot scanned using ChemiDoc for Figure 3.4A *Eh* treatment for different timepoints in WT as compared to Casp-4 CRISPR/Cas9 KO macrophages and samples were run on a 10% SDS-PAGE gel and immunoblotted using caspase-4 M029-3 antibody followed by the anti-mouse IgG-HRP. The Western Chemiluminescent HRP Substrate was added to detect proteins. The 43 kDa band is the pro-form of caspase-4. The cropped image for final presentation of the western blot data only has the pro-form. There was the presence of a band slightly higher than 43 kDa in the Casp-4 CRISPR/Cas9 KO macrophages that may be a non-functional protein of caspase-4 that the antibody picked up or that it cross-reacted with other caspases. There was no ladder run within the same gel, but a ladder was run on a separate gel to determine the molecular weight.

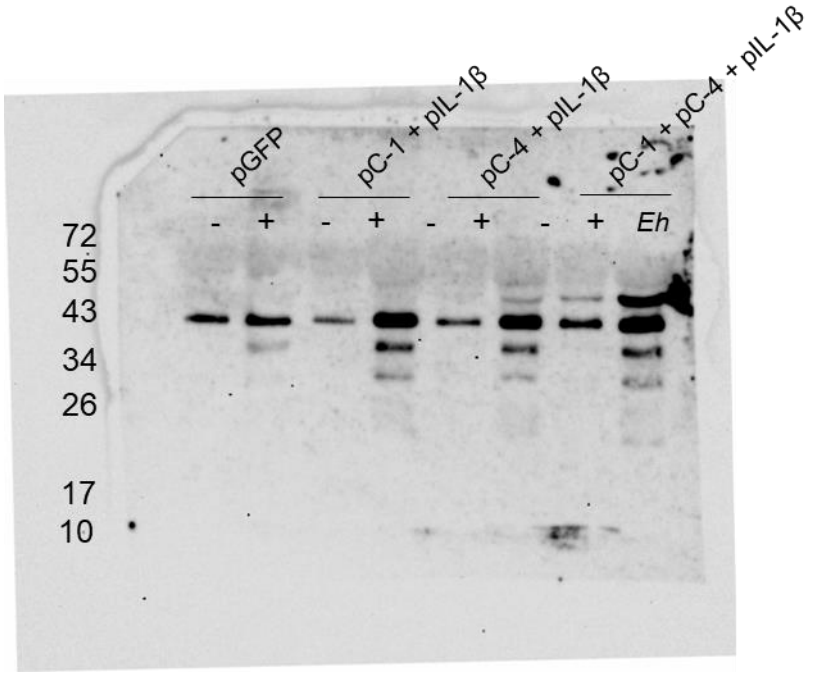

Figure 4.13 Original blot for caspase-4 detection in the supernatants of COS-7 cells stimulated with *Eh* following transfected plasmids.

Full blot scanned using ChemiDoc for Figure 3.8A *Eh* stimulated following different plasmid transfections and samples were run on a 10% SDS-PAGE gel and immunoblotted using caspase-4 M029-3 antibody followed by with the anti-mouse IgG-HRP. The SuperSignal West Femto Chemiluminescence Reagent was added to detect proteins for the supernatants. The 43 kDa band is he pro-form of caspase-4, while the 32-36 kDa (doublet bands) are caspase-4 intermediate forms. The cropped image for final presentation of the western blot data included the pro-form and the intermediate forms.

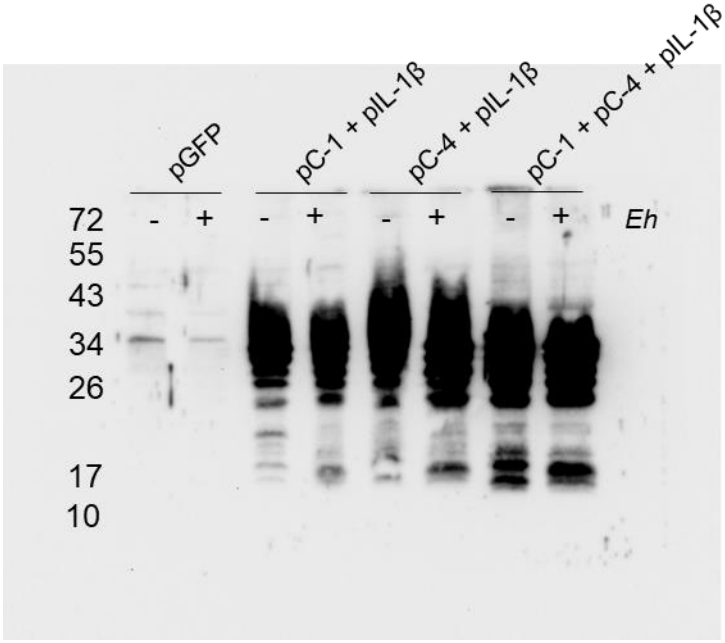

Figure 4.14 Original blot for IL-1β detection in the lysates in COS-7 cells stimulated with *Eh* following transfected plasmids.

Full blot scanned using ChemiDoc for Figure 3.8A *Eh* stimulated following different plasmid transfections and samples were run on a 12% SDS-PAGE gel and immunoblotted using IL-1β sc-7884 antibody followed by the anti-rabbit IgG-HRP. The SuperSignal West Femto Chemiluminescence Reagent was added to detect proteins for the supernatants. The band at around 17 kDa is the cleaved (active) IL-1β. The pro-form (31 kDa) is over saturated due to the exposure time used. This band was cropped from the western blots from all experiments performed to show the cleavage of IL-1β. There was no ladder run within the same gel, but a ladder was run on a separate gel to determine the molecular weight.

4.5.2 *Publications*

Manuscripts Submitted

Quach J, Moreau, F, Sandall C, Chadee K. 2018. *Entamoeba histolytica*-induced caspase-4 activation regulates IL-1β secretion through caspase-1. *PLOS Pathogens*. Manuscript in review for *PLoS Pathogens*.

Articles Published in Refereed Journals

St-Pierre J, Moreau F, Cornick S, **Quach J**, Begum S, Fernandez LA, Gorman H, Chadee K. 2017. The macrophage cytoskeleton acts as a contact sensor upon interaction with *Entamoeba histolytica* to trigger IL-1β secretion. *PLOS Pathogens*. 13(8):e1006592.

Begum S, **Quach J**, Chadee K. 2015. Immune evasion mechanism of *Entamoeba histolytica*: progression to disease. *Frontiers in Microbiology*. 6:1394. doi:10.3389/fmicb.2015.01394.

Quach J, St-Pierre J, Chadee K. 2014. The future for vaccine development against *Entamoeba histolytica*. *Human Vaccines & Immunotherapeutics*. 10: 1514-1521.

Book Chapters

Quach J, Chadee K. 2016. The emerging role of inflammasomes in protozoan infections. In: Inflammasomes: mechanism of action, regulation and role in disease. A Mason Editor. Chapter 3, pages 55-74. Nova Science Publishers, NY, USA.

Quach J, Chadee K. 2016. *Entamoeba histolytica*: pathogenesis and innate host defense – Immunity to Intestinal Protozoa. In: Encyclopedia of Immunobiology, Edited by Michael JH Ratcliffe. Academic Press. Pages 133 -141.

4.5.3 *Copyright*

ELSEVIER LICENSE
TERMS AND CONDITIONS

Apr 16, 2018

This Agreement between Jeanie Quach ("You") and Elsevier ("Elsevier") consists of your license details and the terms and conditions provided by Elsevier and Copyright Clearance Center.

License Number	4330920059956
License date	Apr 16, 2018
Licensed Content Publisher	Elsevier
Licensed Content Publication	Elsevier Books
Licensed Content Title	Encyclopedia of Immunobiology
Licensed Content Author	Jeanie Quach,Kris Chadee,Jan R. Mead,Steven M. Singer
Licensed Content Date	Jan 1, 2016
Licensed Content Pages	9
Start Page	133
End Page	141
Type of Use	reuse in a thesis/dissertation
Portion	excerpt
Number of excerpts	7
Format	both print and electronic
Are you the author of this Elsevier chapter?	Yes
Will you be translating?	No
Order reference number	1
Title of your thesis/dissertation	Entamoeba histolytica-Induced Caspase-4 Activation Regulates IL-1β Secretion Through Caspase-1
Expected completion date	Apr 2018
Estimated size (number of pages)	200
Requestor Location	Jeanie Quach

INTRODUCTION

1. The publisher for this copyrighted material is Elsevier. By clicking "accept" in connection with completing this licensing transaction, you agree that the following terms and conditions apply to this transaction (along with the Billing and Payment terms and conditions established by Copyright Clearance Center, Inc. ("CCC"), at the time that you opened your Rightslink account and that are available at any time at http://myaccount.copyright.com).

GENERAL TERMS

2. Elsevier hereby grants you permission to reproduce the aforementioned material subject to the terms and conditions indicated.

3. Acknowledgement: If any part of the material to be used (for example, figures) has appeared in our publication with credit or acknowledgement to another source, permission must also be sought from that source. If such permission is not obtained then that material may not be included in your publication/copies. Suitable acknowledgement to the source must be made, either as a footnote or in a reference list at the end of your publication, as follows:

"Reprinted from Publication title, Vol /edition number, Author(s), Title of article / title of chapter, Pages No., Copyright (Year), with permission from Elsevier [OR APPLICABLE SOCIETY COPYRIGHT OWNER]." Also Lancet special credit - "Reprinted from The Lancet, Vol. number, Author(s), Title of article, Pages No., Copyright (Year), with permission from Elsevier."

4. Reproduction of this material is confined to the purpose and/or media for which permission is hereby given.

5. Altering/Modifying Material: Not Permitted. However figures and illustrations may be altered/adapted minimally to serve your work. Any other abbreviations, additions, deletions and/or any other alterations shall be made only with prior written authorization of Elsevier Ltd. (Please contact Elsevier at permissions@elsevier.com). No modifications can be made to any Lancet figures/tables and they must be reproduced in full.

6. If the permission fee for the requested use of our material is waived in this instance, please be advised that your future requests for Elsevier materials may attract a fee.

7. Reservation of Rights: Publisher reserves all rights not specifically granted in the combination of (i) the license details provided by you and accepted in the course of this licensing transaction, (ii) these terms and conditions and (iii) CCC's Billing and Payment terms and conditions.

8. License Contingent Upon Payment: While you may exercise the rights licensed immediately upon issuance of the license at the end of the licensing process for the transaction, provided that you have disclosed complete and accurate details of your proposed use, no license is finally effective unless and until full payment is received from you (either by publisher or by CCC) as provided in CCC's Billing and Payment terms and conditions. If full payment is not received on a timely basis, then any license preliminarily granted shall be deemed automatically revoked and shall be void as if never granted. Further, in the event that you breach any of these terms and conditions or any of CCC's Billing and Payment terms and conditions, the license is automatically revoked and shall be void as if never granted. Use of materials as described in a revoked license, as well as any use of the materials beyond the scope of an unrevoked license, may constitute copyright infringement and publisher reserves the right to take any and all action to protect its copyright in the materials.

9. Warranties: Publisher makes no representations or warranties with respect to the licensed material.

10. Indemnity: You hereby indemnify and agree to hold harmless publisher and CCC, and their respective officers, directors, employees and agents, from and against any and all

claims arising out of your use of the licensed material other than as specifically authorized pursuant to this license.
11. No Transfer of License: This license is personal to you and may not be sublicensed, assigned, or transferred by you to any other person without publisher's written permission.
12. No Amendment Except in Writing: This license may not be amended except in a writing signed by both parties (or, in the case of publisher, by CCC on publisher's behalf).
13. Objection to Contrary Terms: Publisher hereby objects to any terms contained in any purchase order, acknowledgment, check endorsement or other writing prepared by you, which terms are inconsistent with these terms and conditions or CCC's Billing and Payment terms and conditions. These terms and conditions, together with CCC's Billing and Payment terms and conditions (which are incorporated herein), comprise the entire agreement between you and publisher (and CCC) concerning this licensing transaction. In the event of any conflict between your obligations established by these terms and conditions and those established by CCC's Billing and Payment terms and conditions, these terms and conditions shall control.
14. Revocation: Elsevier or Copyright Clearance Center may deny the permissions described in this License at their sole discretion, for any reason or no reason, with a full refund payable to you. Notice of such denial will be made using the contact information provided by you. Failure to receive such notice will not alter or invalidate the denial. In no event will Elsevier or Copyright Clearance Center be responsible or liable for any costs, expenses or damage incurred by you as a result of a denial of your permission request, other than a refund of the amount(s) paid by you to Elsevier and/or Copyright Clearance Center for denied permissions.

LIMITED LICENSE

The following terms and conditions apply only to specific license types:
15. **Translation**: This permission is granted for non-exclusive world **English** rights only unless your license was granted for translation rights. If you licensed translation rights you may only translate this content into the languages you requested. A professional translator must perform all translations and reproduce the content word for word preserving the integrity of the article.
16. **Posting licensed content on any Website**: The following terms and conditions apply as follows: Licensing material from an Elsevier journal: All content posted to the web site must maintain the copyright information line on the bottom of each image; A hyper-text must be included to the Homepage of the journal from which you are licensing at http://www.sciencedirect.com/science/journal/xxxxx or the Elsevier homepage for books at http://www.elsevier.com; Central Storage: This license does not include permission for a scanned version of the material to be stored in a central repository such as that provided by Heron/XanEdu.
Licensing material from an Elsevier book: A hyper-text link must be included to the Elsevier homepage at http://www.elsevier.com . All content posted to the web site must maintain the copyright information line on the bottom of each image.

Posting licensed content on Electronic reserve: In addition to the above the following clauses are applicable: The web site must be password-protected and made available only to bona fide students registered on a relevant course. This permission is granted for 1 year only. You may obtain a new license for future website posting.
17. **For journal authors:** the following clauses are applicable in addition to the above:
Preprints:
A preprint is an author's own write-up of research results and analysis, it has not been peer-reviewed, nor has it had any other value added to it by a publisher (such as formatting, copyright, technical enhancement etc.).
Authors can share their preprints anywhere at any time. Preprints should not be added to or enhanced in any way in order to appear more like, or to substitute for, the final versions of

articles however authors can update their preprints on arXiv or RePEc with their Accepted Author Manuscript (see below).
If accepted for publication, we encourage authors to link from the preprint to their formal publication via its DOI. Millions of researchers have access to the formal publications on ScienceDirect, and so links will help users to find, access, cite and use the best available version. Please note that Cell Press, The Lancet and some society-owned have different preprint policies. Information on these policies is available on the journal homepage.
Accepted Author Manuscripts: An accepted author manuscript is the manuscript of an article that has been accepted for publication and which typically includes author-incorporated changes suggested during submission, peer review and editor-author communications.
Authors can share their accepted author manuscript:

- immediately
  - via their non-commercial person homepage or blog
  - by updating a preprint in arXiv or RePEc with the accepted manuscript
  - via their research institute or institutional repository for internal institutional uses or as part of an invitation-only research collaboration work-group
  - directly by providing copies to their students or to research collaborators for their personal use
  - for private scholarly sharing as part of an invitation-only work group on commercial sites with which Elsevier has an agreement
- After the embargo period
  - via non-commercial hosting platforms such as their institutional repository
  - via commercial sites with which Elsevier has an agreement

In all cases accepted manuscripts should:

- link to the formal publication via its DOI
- bear a CC-BY-NC-ND license - this is easy to do
- if aggregated with other manuscripts, for example in a repository or other site, be shared in alignment with our hosting policy not be added to or enhanced in any way to appear more like, or to substitute for, the published journal article.

Published journal article (JPA): A published journal article (PJA) is the definitive final record of published research that appears or will appear in the journal and embodies all value-adding publishing activities including peer review co-ordination, copy-editing, formatting, (if relevant) pagination and online enrichment.
Policies for sharing publishing journal articles differ for subscription and gold open access articles:
Subscription Articles: If you are an author, please share a link to your article rather than the full-text. Millions of researchers have access to the formal publications on ScienceDirect, and so links will help your users to find, access, cite, and use the best available version.
Theses and dissertations which contain embedded PJAs as part of the formal submission can be posted publicly by the awarding institution with DOI links back to the formal publications on ScienceDirect.
If you are affiliated with a library that subscribes to ScienceDirect you have additional private sharing rights for others' research accessed under that agreement. This includes use for classroom teaching and internal training at the institution (including use in course packs and courseware programs), and inclusion of the article for grant funding purposes.
Gold Open Access Articles: May be shared according to the author-selected end-user license and should contain a CrossMark logo, the end user license, and a DOI link to the formal publication on ScienceDirect.
Please refer to Elsevier's posting policy for further information.

Taylor & Francis
Taylor & Francis Group

Our Ref: P011218-03

12 January 2018

Dear Jeanie Quach on Behalf of the University of Calgary,

We are in receipt of your request to reproduce your Open Access article

Material requested: Jeanie Quach, Joëlle St-Pierre & Kris Chadee (2014)
The Future for Vaccine Development against *Entamoeba histolytica*
Human Vaccines & Immunotherapeutics 10 (6): 1514–1521.
DOI: 10.4161/hv.27796

for use in your dissertation. You may use your published version of article.

This permission is all for print and electronic editions.

We will be pleased to grant you permission free of charge on the condition that:

This permission is for non-exclusive English world rights. This permission does not cover any third party copyrighted work which may appear in the material requested.

Full acknowledgment must be included showing authors, year published, article title, and full Journal title, reprinted by permission of Taylor & Francis LLC (http://www.tandfonline.com).

Thank you very much for your interest in Taylor & Francis publications. Should you have any questions or require further assistance, please feel free to contact me directly.

Sincerely,

Mary Ann Muller

Permissions Coordinator

E-mail: maryann.muller@taylorandfrancis.com

Telephone: 215.606.4334